Macromolecules for drug delivery

A thesis submitted in partial fulfilment of the requirements of
the University of Sheffield for the degree of Doctor of
Philosophy

by

Enas Bshena

Department of Chemistry

The University of Sheffield

November 2022

Acknowledgments

Alhamdulillah, praise be to Allah the Most Gracious and Most Merciful. First and foremost, I would like to acknowledge and give my warmest thanks to my supervisor (Dr Lance Twyman) who made this work possible. His guidance and advice carried me through all the stages of writing my thesis. I would also like to thank all my group member Chen, Abdullah, Reyad, Khalid, and Abdelfattah. Special thanks to Lucy Hamson, who has worked and shirred the ideas. Also, a particular thank you to Amal, who has always been very encouraging.

Additionally, I would also like to express sincere gratitude for my husband (Abdulrahim) as well as both my beloved children (Ahmed and Anas) for their support, love, and patience as I conducted my research and wrote my thesis. Your prayer for me has kept me going until this point.

I am especially grateful to my parents, who supported me emotionally and financially. Your belief in me and desire for the best have always been clear to me. Thank you, mam, and dad, and to my sisters and brother for supporting me spiritually throughout writing this thesis and my life in general.

I also wish to thank my sponsor (The Libyan Ministry of Higher Education and Scientific Research) for granting me this opportunity.

.

List of Abbreviations

^{1}H NMR	Proton Nuclear Magnetic Resonance Spectrometry
^{13}C NMR	Carbon-13 Nuclear Magnetic Resonance Spectrometry
DLS	Dynamic light scattering
DMSO	Dimethylsulphoxide
ε	Extinction coefficient
GPC	Gel Permeation Chromatography
HBP	Hyperbranched Polymer
HBPAMAM	Hyperbranched PAMAM
MA	Methyl acrylate
PAMAM	Poly (amido amine)
PAMAM-OH	Neutral Hydroxyl Terminated PAMAM
PDT	Photodynamic therapy
PS	Photosensitizers
TDHPP	Tetrakis (3.5-dihydroxyphenyl) -porphyrin
TDMPP	Tetrakis (3,5-dimethoxyphenyl) -porphyrin
THF	Tetrahydrofuran
UV/Vis	Ultraviolet/Visible Spectrometry
ZnTDHPP	Zinc tetrakis (3,5-dihydroxy phenyl)- porphyrin
DDSs	Drug delivery systems

Table of Contents

Abstract

The optimization of drug delivery systems (DDSs) is essential for improving drug therapy effectiveness and solving people's health problems. There has been a growing interest in dendrimers in academia and industry in recent years. The most prominent feature of their application is that they are capable of delivering hydrophobic, poorly soluble molecules to specific sites. The internal space of dendrimers can be used to host small guest molecules, and able to host small guest molecules through secondary interactions in cases of high generational dendrimers. However, the high cost and time required to synthesize dendrimers limit their use. A simple and cheaper solution may be available through the use of hyperbranched polymers (HBP) if they can achieve the same results as dendrimers. In this research, we compare the encapsulation ability of two different HBPs with dendrimers for applications in drug delivery.

The first area studied involved dendrimers that were synthesised to obtain neutral PAMAM dendrimers. The encapsulation studies using co-precipitation technique have been carried out for three dendrimer generations. The ability of G3.0-OH was the most generation to increase the concentration of encapsulated drug compared to G2.0 8OH and G4.0 32OH. These studies showed that ibuprofen loading was not linear and plateaued after 2.50E-04 M. The DLS showed formation of a big species around 250 nm at dendrimer concentration of 3.0E-04 M. A similar encapsulation study was also undertaken to investigate the effect of metal coordination on the encapsulation ability of porphyrin molecules with potential application in photodynamic therapy (PDT). The results revealed encapsulated porphyrins were increased with increased dendrimer generation. Dendrimers were able to improve solubility and encapsulate both porphyrins, however the encapsulated and solubility for metal porphyrin was improved more than 3-fold compared to free base porphyrin.

The second part of this project involves synthesizing hyperbranched polymers similar to PAMAM dendrimer in functionality. However, HBPAMAM could not be converted to hydroxyl terminal groups. The encapsulation studies were conducted for both HBPs. Amine ended hyperbranched (HBPAMAM-NH$_2$) was able to improve the solubility of Ibuprofen at low and high concentrations. However, the concentration of encapsulated drug was decreased with increased polymer concentrations. According to the DLS, the hydrodynamic radius increased with increased polymer concentration, the polymers aggregated at concentration above 0.04 mg/mL. In spite of this, when encapsulating bigger molecules of Zn THDPP, the concentration of encapsulated Zn THDPP increased along with the concentration of polymer. Also, the encapsulated concentrations of Ar-HBPAMAM-OH were enhanced at 0.32 mg/mL and reduced at high concentration of 0.75 mg/mL, because of aggregation as seen with dendrimer-OH and HBPAMAM-NH$_2$.

The final part of this project is the comparison between dendrimers and HBPs. The findings indicate that although dendrimers increased the solution concentration of both guest molecules (Ibuprofen and Zn TDHPP) significantly, the ability of HBPs to encapsulate these compounds was not significantly inferior. In comparisons between amine terminated PAMAM dendrimer G2/G3 and the amine ended HBPAMAM, there was no significant difference in the encapsulation ability between the two systems. For example, the G2 PAMAM dendrimer could encapsulate ibuprofen with maximum concentration of 7.5E-03 and 7.0E-03, respectively.

The comparison between G3.0-OH and Ar-HBPAMAM, the G 3.0-OH dendrimer and the Ar-HBPAMAM-OH 23 were able to encapsulate similar amounts of drug. Overall, the OH ended macromolecules appeared to encapsulate significantly more than the amine ended systems.

Keywords: Drug delivery systems, Dendrimers, Hyperbranched polymers, Encapsulation, Photodynamic therapy.

Chapter 1: Introduction

1.1. Overview

Drug delivery systems are technological systems that formulate and store drug molecules into suitable forms like tablets or solutions for administration. Drugs can be introduced into the body through several routes, to maximize therapeutic efficacy and minimize off-target accumulation. [1,2] They accelerate the delivery of drugs to specific targeted sites. These include oral administration, buccal and sublingual administration, nasal and ophthalmic administration, [5, 6] transdermal and subcutaneous administration, [7, 8] anal and transvaginal administration, and intravesical administration. [1] The components of the drug determine its physiochemical properties and how it affects the body system after consumption.

Before the modern era, people depended on medicinal plants. Although they were beneficial, they lacked consistency, homogeneity, and specificity in drug delivery.[10] Prior to controlled drug delivery, all pharmaceuticals were produced and stored in pill or capsule formulations. It is dissolved when it comes into contact with gastrointestinal fluids. It permeates the gut wall, then passes into the bloodstream through blood capillaries. There was no ability to control drug release kinetics. In order to mask the bitter taste of drugs, Rhazes and Avicenna introduced coating technology. This coating method altered the drug release rate. It was adopted in the 10th century however in the form of gold, silver, and pearl-coated tablets.

The 20th century brought advanced coating technology with keratin, shellac, sugar, enteric coating, and pearl coating was also introduced. However, keratin and shellac were ineffective due to storage instability and high pH for adequate dissolution in the small intestine. Malm et al. [11] introduced an enteric-coated material with polymeric cellulose acetate phthalate that is dissolved at a very weak alkaline pH, like that of the small intestine. This makes it highly suitable for enteric controlled release. The first generation was extremely productive. It focused

on the development of numerous oral and transdermal controlled-release formulations for clinical use and the establishment of controlled drug-release mechanisms.

Lipowski developed the first sustained-release oral formulation in 1951, by coating pills with enteric polymers (like beads) such that the drug and coat were layered alternatively, resulting in slow release of the drug, regularly, and periodically.[12] This was further developed by Smith, Klein Beecham, and French (SKF) in 1952. The scientists developed Spansule technology, an oral predetermined-release formulation that sustains and controls drug kinetic release gradually.[13] This formula is made of hundreds of micro pellets drug loaded beads with variable layers of natural water-soluble wax with dissimilar thicknesses on individual pellets. As the beads transit down the GI tract, the outer capsule rapidly disintegrates, and the waxy coating around the beads gradually dissolves as they transit down the GI tract. This liberates the drug-loaded beads. This improved patient compliance and convenience by reducing the dosing schedule, resulting in great popularity.[14] This technology was further developed by replacing the wax with more reproducible synthetic polymers.[15]

The first nanoparticle therapeutic was reported by Jatzkewitz when he prepared the first polymer-drug conjugate In 1955. the first nanotechnology known as liposome (lipid vesicles) was discovered.[2,3] In the early sixties. Polymer-drug conjugates and liposomes mark the birth of nanocarriers. In this decade, the ALZA Corporation did not create drugs they specialized in targeting and controlling the release of drugs at the right place and time.[4] In 1972, Scheffel and his colleague prepared the first protein-based microspheres. In 1976, "micelle" and "emulsion" polymerization techniques were used to prepare drug-loaded nanoparticles and microcapsules by Peter Paul Speiser's research group.[5] In 1977, Couvreur et al.[6] reported the lysosomotropic effects of the nanoparticles, and T.C. Ezike et al. Heliyon they produced the first rapidly biodegradable acrylic nanoparticles. The drug delivery formulations developed during the second generation (2G) were impressive, but they did not produce the expected

clinical results. [7] The researchers were interested in developing drug delivery systems with constant drug release rates, self-regulating, long-term depot formulations, and nanotechnology-based formulations, particularly nanoparticle formulations. In this era, long-term depot-sustained drug-release formulations of peptide/protein drugs were developed.[8] In addition, smart polymers and hydrogels were developed to stabilise drug delivery systems that are affected by physiological changes such as pH, temperature, electric field, and glucose. Furthermore, efforts were made to develop targeted nanotechnology DDS for tumors and gene delivery using biodegradable polymers in nanoparticle structures such as polymeric micelles, chitosan, lipids, and dendrimers. The idea was to modify the nanoparticles so that they could be administered directly into the body for increased drug accumulation at the site of action. Although this nanotechnology-based DDS demonstrated high efficacy in controlling tumor growth in animal models, the FDA only approved a few drugs. [9]

Drug delivery systems are integral to providing new systems of drug administration, vaccines and finding diagnoses. Drug delivery that is controlled prolongs the concentration of the drug for the intended time frame by controlling the rate at which the drug is administered. By controlling the drug delivery, it focuses on the disease site and targeted cells which then reduces the risk of side effects across the body. Thus, the system intercepts premature degradation which elevates uptake so as to improve bioavailability. Additionally, biodegradable polymers used within implants allow for a consistent, gradual release of the drug. This system is advantageous for upholding a sustained and controlled drug delivery. [10]

The achievable efficacy of any drug is a vital element as this indicates the maximum capability of the drug. This means that if the drug fails to reach specific cells or targeted tissues the efficacy is limited. [11] The body has obstructions that can decrease the concentration of the drug before it reaches the target, this is particular in some drugs that only remain active for a restricted timeframe. Drug administration must therefore be precise as if the concentration is

too low then the drug will fail to show effect, however if the concentration is too strong it may be toxic to the patient.

There has been notable research into drug delivery systems over the past two decades as the stability and solvability properties are often limited within the drug itself. The delivery system must incorporate these elements to improve the drug's effects. The research has focused on developing consistent drug levels, side effect reductions, the range of the drug and advancement in tissue or organ specificity. [12]

The aim of a drug delivery system is to improve the efficacy to the highest degree. This is conducted by carrying and discharging the drug to the targeted area. The drug delivery can be active or passive but it must aim to decrease off-target accumulation or effect. [13] A drug delivery system that is able to preserve the drug and release it in the intended area while simultaneously being biochemically inert and innocuous is the ultimate formulation. [14] However, there are constraints to the existing systems such as limited availability, high dosage, first pass effect syndrome, intolerance, and fragility. They are not reliable in obtaining the desired effects and are inconsistent in plasma drug outputs. These constraints have resulted in new delivery systems being researched. [15]

One route of research is nanoscale delivery systems which incorporate liposomes, polymeric micelles, nanogels, nanocapsules, dendrimers, carbon nanotubes, nanocrystals, and solid lipid nanoparticles.[16] This type of delivery has the capability to carry minute molecule drugs alongside therapeutic macromolecules such as proteins, peptides, single strain DNA and small-scale RNA (siRNA). [17, 18] Furthermore, nanomedicines do not exhibit the limitations of other options such as low biodistribution and pharmacokinetics, limited solvability, multidrug resistance, lack of suppression of unwanted outcomes and dosage reliant on the toxicity . [18,19]

It is important when designing nanocarriers, to consider the factors which may lead to potential safety concerns. Factors such as the material used for construction of the nanocarriers, the dose or concentration of the nanocarriers, their dimension size, shape, surface charge, reactivity and the solubility. [17,20,21] It may potentially help with reducing the dose-limiting cytotoxicity of the drug and also enabling the drug to overcome drug resistance associated with cancer treatment. [22]

However, they do offer positive characteristics such as drug reliability and stability, improved PK and biodistribution alongside their ability to improve the solubility of hydrophobic agents. The payload is altered by the nanocarriers being able to control the payload and modifying their surface chemistry. [23] The payload is specifically designed to target diseased cells and tissues. Nanocarriers are also able to reach temporal and spatial control over the release of therapeutic payloads.[17,24 ,25] This is achieved because the nanocarriers react to a wide range of internal and external stimuli to trigger release. This delivery system could decrease the dosage constraints and drug toxicity often associated with cancer treatments. [22]

1.2. Nanoparticles for drug delivery

Nanoparticles refer to the dissemination of particles that are on the nanoscale which can vary between a single nanometre (nm) to multiple hundred nanometres, this is dependent on how they are being applied [26] . They were established over ten years ago and as a modern medicine they have proven to be vital due to their advantageous characteristics in comparison to conventional drug delivery methods (Oral, Buccal, Rectal ,Intravenous ,Subcutaneous and Intramuscular delivery. [23,27] An area where nanoparticles are proving effective is in cancer treatment. This is because they are able to expose, diagnose and remedy the disease as they are able to perforate the tissues at a molecular level. There are some nanocarrier drug delivery

systems on the market and others are still being developed. The different types of ligands based nanocarriers for their drug delivery is shown in Figure1.1.

The beginning of controlled drug release is regarded as the first generation as it developed most of the initial drug delivery systems through oral and transdermal methods. There was limitations to this method however, as they were fragile and did not always give the desired effect. The introduction of nanotechnology was established over a century ago by Michael Faraday who composed gold particles on a nanometric scale. [28] He used the gold particles to combine with antibodies to target a specific strain, the method was deem the immune-gold straining. This began the colloidal gold as a drug delivery system.
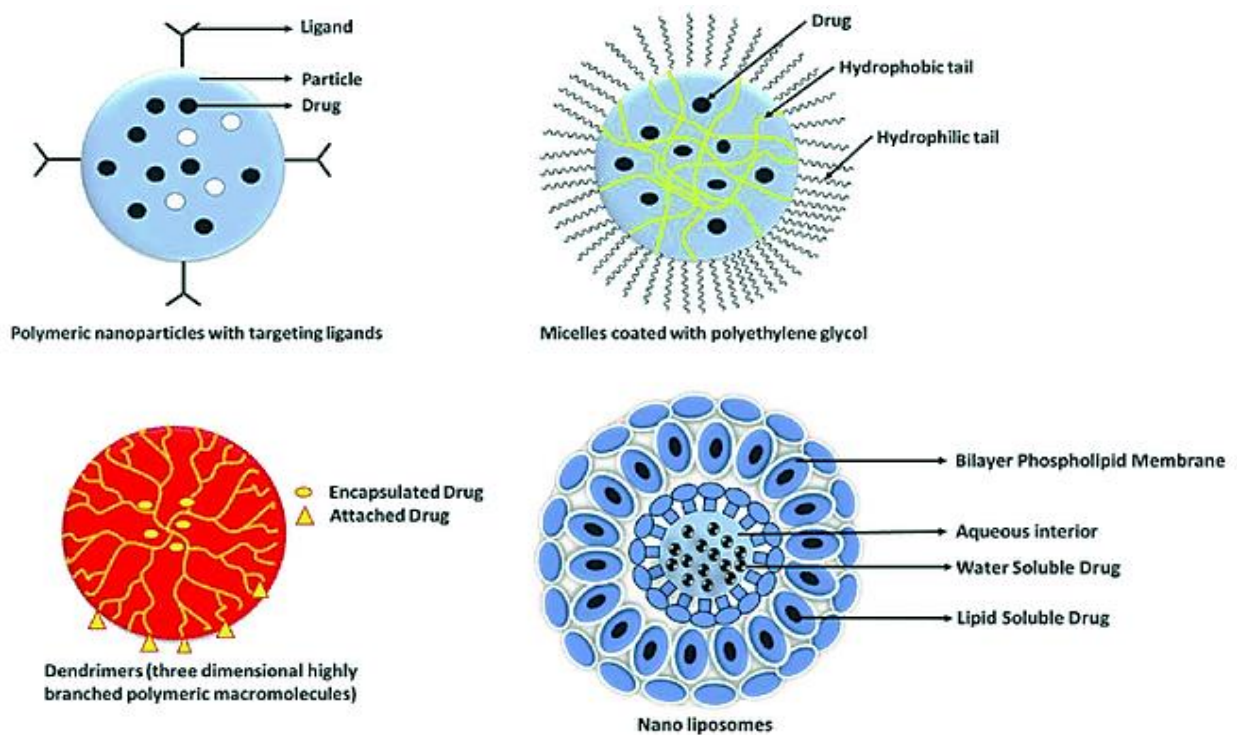
Figure 1. 1: Types of nanocarriers used for biomedical application. Adopted with permission from (1 P. Chaubey, M. Momin and S. Sawarkar, Front. Pharmacol. 2020, 10, 1–1). [29]

The focal intentions of developing nanoparticles for drug delivery are to establish control over particle dimensions, surface area and release pharmacologically active agents that reach the targeted cells while maintaining the optimal rate and dosage. This means the drug reaches the target cells and tissues with the accurate concentration to carry out the desired results. Liposomes and polymer micelles were recognised in the 1960s however they were not distinguished as nanoparticles until 40 years later. [30] Liposomes have attributes as carriers such as navigating the target site, low level toxicity and prevention of drug degradation so they stay as their intended form. Despite this, they are difficult to store correctly and have low encapsulation efficiency. When they are introduced to a blood component the water-soluble drug may seep uncontrollably. The polymeric nanoparticles therefore present distinct attributes over liposomes. These are increased stability of drugs and proteins and provide commendable controlled release properties. [31,32]

Micelles are a notable drug delivery approaches for poorly soluble cytotoxic drugs that are used for controlled drug release. They are too able to remain stable and navigate the drug release, however they are unstable in an aqueous environment. Moreover, early drug release can reduce its credibility as a nanocarrier. [33] Furthermore, they have a large surface area while remaining small which may cause particle to particle aggregation. This will make them laborious to handle in liquid and dry states. Its dimensions can produce limited drug loading and a burst release. [31] The limitations of micelles therefore need to be researched further before nanoparticles can be applied clinically or on the clinical market.

1.3. Dendrimers

Dendrimers have multiple arms forming from the central core showing a highly branched and globular macromolecular structure. They can be identified by their optimal, symmetrical formulation and monodispersed nature. [34,35] Their diameter can range from 1nm to 10nm which makes them adaptable for passing through biological barriers. [36] They are comprised of three main elements the core, dendritic and terminal units. The dendritic units are connected to the core to establish a repetitive branch unit. The repeated unit creates a new generation and as it synthesizes the increases by a half. The growth of the generations develops the terminal groups numerically from the periphery. Dendrimers can be utilised for both active and passive targeting because they have a structure dissimilar to other systems. Their peripheral function groups are a concentrated at a higher degree than linear polymers. The dimensions of the dendrimer can be changed when the generation size differs. This means that dendrimers are flat when the generations are low however as the generations develop, they transform into globular structures.
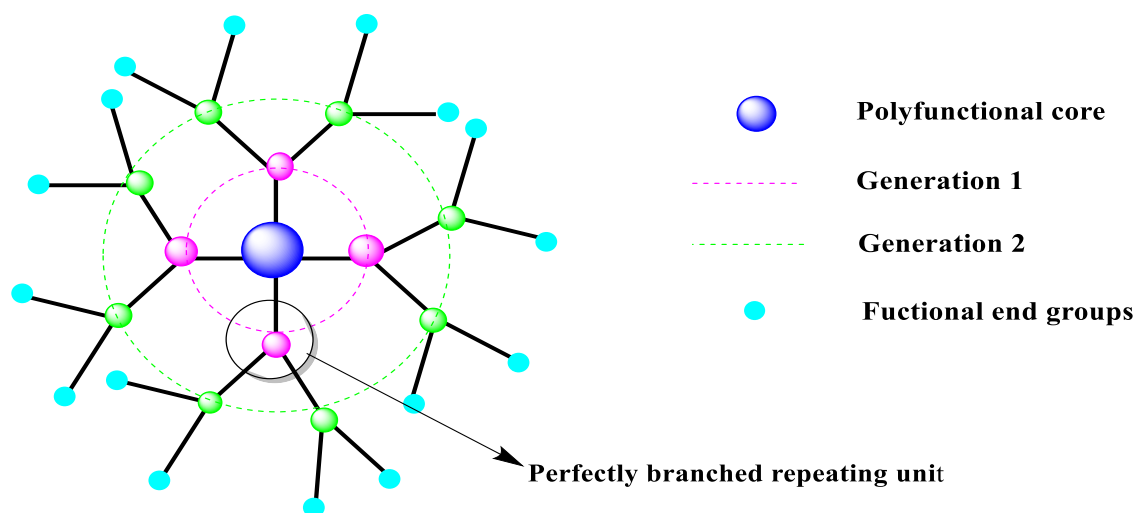
Figure 1. 2: General representation of the model structure of a dendrimer

The globular structures then encapsulate small host molecules. [37,38] Despite this, the dendrimers are not to behave perfectly. When the generations grow into a high number the PAMAM dendrimers can self-terminate due to the steric overcrowding within the terminal group. [39] This limitation may cause dendrimer degradation which will have a negative effect on the drug's payload. Additionally, they are not time effective and require high financial backing to synthesize. Researchers have therefore began investigating other drug delivery approaches with less limitations for example hyperbranched polymers.

1.3.1. Synthetic routes for dendrimers

The ability to formulate dendritic structures following the controllability of dendrimer synthesis generated structures with varying backbones and surface functional groups. Dendrimers are synthesized using two dominant methods, examples are displayed in Figure 1.3. There is divergent synthesis established by Donald Tomalia, which is carried out by the dendrimer being activated and cured so that it develops radially from a polyfunctional core to the surface[40]. The second approach by Craig Hawker and Jean Fréchet of convergent synthesis assigns dendrimers radially from the surface to focal areas. [41] There are advantages and limitations to both approaches despite each final structure being of equivalent value.

A

Initiator core

Surfuce

B

Surfuce   focal point
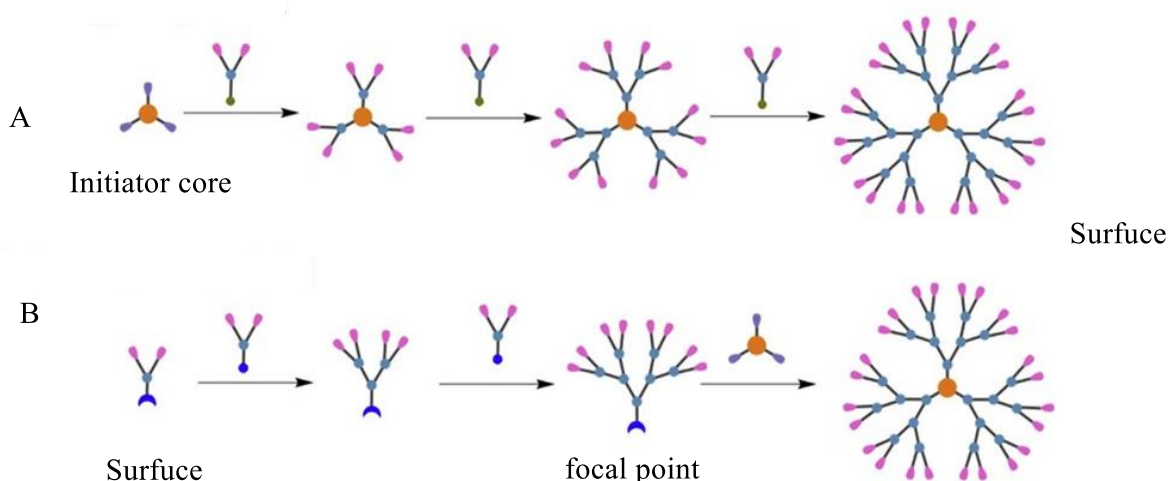
Figure 1. 3: Synthesis routs for dendrimers. (A) Divergent method. (B) Convergent method. This figure is adapted from reference.[42]

When the dendrimer is produced on a large scale the divergent synthesis approach is applied.[43] The limitation of large-scale production and high generation dendrimers results in defects such as absent arms, dimers or trimers. This arises because the growth of iterative reaction sequences paired with each generation and developing steric strain at the periphery. Furthermore, there is strenuous purification needed after each process. The convergent method does not have this difficulty as instead of synthesising the whole dendrimer from an initial point it develops independent dendrons. The individual dendrons are then purified and integrated with the polyfunctional core to form the dendrimer. [35] Yet, this method is limited because it has steric overcrowding around the core making it difficult to formulate high generation dendrimers. [44] Thus, each method of synthesising dendrimers has limitations as the dimensions, surface area and backbone structure fundamentally influence the dendrimer's biological interactivity. This research will use the divergent synthesis of PAMAM dendrimers as this method is adaptable to produce modified, functionalised dendrimers.

1.3. 2. Interactions between dendrimers and drug molecules

The research into dendrimers has grown since their establishment over a century ago. They have been studied due to their individual density distribution such as their malleable internal space surrounding the focal core and densely formed peripheral functions. They were applied to the drug industry over around 30 years ago as they are able to combine a drug molecule to the periphery either covalently or non-covalently to assist delivery.[45] This is displayed in Figure 1.4.
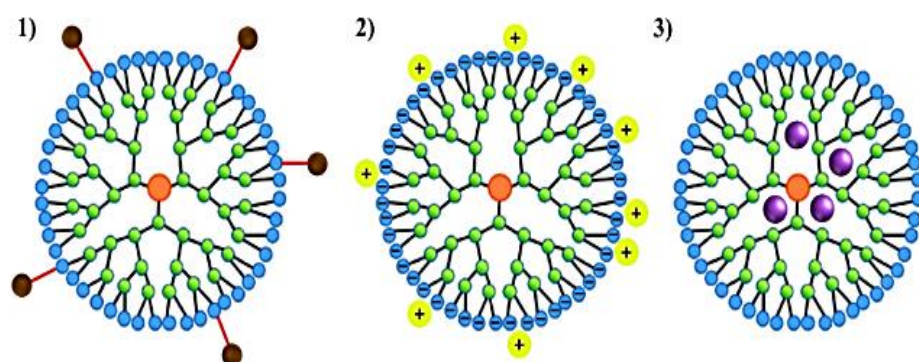
*Figure 1. 4: A schematic representation of the three mechanisms used to bind drugs in dendrimers: (**1**) by covalent interaction between the drug and the periphery of the dendrimer; (**2**) by coordination of the drug to the outer functional groups of the dendrimer via ionic interactions; (**3**) by simple encapsulation of the drugs into the dendrimer cavities. Reprinted from The Reference. [46]*

1.3.2.1 Noncovalent encapsulation of drugs

Dendrimers have been examined as drug delivery systems because they have an open structure inside. They are able to encapsulate gust molecules by non-bonding interactions. [47] The internal structure of a dendrimer is comprised of hydrophobic elements which allows them to engage with poorly soluble drugs. They are able to combine with drug molecules by a hydrogen bond formation as nitrogen and oxygen lie within these internal cavities. This suggests that the dendrimer's encapsulation ability is reliant on the hydrophobic interactions, hydrogen bonding and electrostatic engagement such as acid/base interaction.

Initial research found that hydrophilic hard peripheries and soft cores of unimolecular micelles were adaptable for globular proteins. This discovery by Meijer and colleagues allowed for the development of amino acid-protected dendritic box on the 64-amine terminal of PPI dendrimers. [48] The research understood that the dendrimer could combine four large guest molecules (Rose Bengal) with to ten small guest molecules (p-nitrobenzoic acid). Further study was conducted by Fréchet in regard to hydrophobic interactivity with the carboxylic acid surface on a poly (benzyl either) dendrimer and a hydrophobic chromophore. [49] This concluded that the dendrimer was capable of improving the solubility of hydrophobic guest molecules such as pyrene in water as an assistance for interactivity. The assistance was between benzyl ether building blocks and aromatic guest molecules. This establishment has proven to be promising as many drugs have hydrophobic properties.

According to available literature, dendrimers exert their solubilizing effect through ionic interaction, hydrogen bonding, and hydrophobic interactions. Kojima et al also studied the anticancer drugs methotrexate (MTX) and Adriamycin (ADR), both practically water-insoluble .[50] It has been successfully demonstrated that hydrophobic drugs can be encapsulated in the hydrophobic interior of MPEG-PAMAM dendrimers. The results showed that the ADR was complexed and solubilized on the surface of MPEG chains. However, in the case of the MTX, the number of encapsulated molecules increased due to electrostatic interaction that resulted from an acid base reaction between dendrimer and MTX.

Other approaches to forming host-guest complexes include acid–base interactions and hydrogen bonding. The authors of the report revealed the ability of adamantyl urea- and adamantyl thiourea-modified PPI dendrimers as potential carriers for (BOC)-protected peptides. It was found that the peptide was also bound by ionic interactions, as well as hydrogen bonding to the dendrimer, and was easily released under mild acidic conditions. [51]

1.3.2.2. Drug Coordination – covalent conjugate

As dendrimers consist of a high number of surface groups they are applicable for covalent conjugation for a wide range of drugs that have the relevant functional groups. [52] In terms of PAMAM dendrimers the conjugation approach can be tested using ionisable interactions. This has been documented showing multiple examples of drugs forming stable complexes, including ibuprofen [12] and piroxicam. [53] The drug can be covalently conjugated to dendrimers by utilising spacers, some of which are PEG, p-amino benzoic acid, p-amino hippuric acid and lauryl chains. This promotes a positive drug stance that improves drug release and stability. There have been instances where research has advanced using conjugated penicillin V, venlafaxine, 5-aminosalicylic acid, naproxen, and propranolol with PANAM dendrimers. Furthermore, dendrimers have been specialised to cooperate with anticancer drugs such as cisplatin, [54] doxorubicin, [55] epirubicin, [56] , methotrexate [57] and paclitaxel. [58] The complexes have exhibited a higher degree of solubility and control release in comparison to conventional drugs.

1.3.3. Surface Modification

The external layer of cationic dendrimers is often comprised of amine groups that exhibit a positive charge in a physiological environment. This is related to the potential toxicity alongside the nonspecific accumulation occurred after administration. The toxicity of polymers is a complex concern that incorporates the molecular function and physiochemical nature of polymers. The navigation of the dendrimer, dosage, biodistribution characteristics and physiological interactivity are further concerns of the polymer toxicity.

Research was undertaken by Malik et al to investigate the results of varying dendrimer categories (PAMAM, PPI) with a diamino butane (DAB) and diamino ethane (DAE) core, carbosilane-polyethyleneoxide (CSi-PEO), surface molecules (amine, carboxylate) and

disparate generations (G1-4). [59] The catatonic dendrimers were found to be cytotoxic to B16F10 cells producing hemolysis in the generation which depended on the influence of the lysine dendrimers. It was unexpected that the cationic PAMAM dendrimers had lower toxicity levels compared to cationic DAB and DAE PPI dendrimers that had an identical amount of surface amine groups. To compare, anionic and neutral dendrimers induced a lower level of hemolysis but had increased toxicity which was uncovered by the lower generation of CSi-PEO dendrimers. This highlighted a potential concern of accessibility of toxins to the central core of the cells. [60] The explanation for the cytotoxicity of cationic dendrimers is exhibited from the interaction between negatively charged cell membranes and the positively charged dendrimer surface. This interaction forms nanopores in the cell membrane causing destruction that forces leakage of the cellular content, thus the cell will perish. To resolve the structure-induced cytotoxicity there have been many theories established that rely on the suppression of the cationic surface by PEGylation, acetylation and modification with anionic, neutral and ligand molecules. [60]

1.3.4. Dendrimer-based drug delivery systems

Nanoscale drug design has advanced beyond other options due to its substantial research projects. The advancement in technology has revealed that the nanoscale advantages encompass its possibility to modify properties like solubility, drug release profiles, diffusivity, bioavailability, and immunogenicity. This can impact the development of convenient administration routes and refine toxicity, side effects, biodistribution and extend drug life cycle. [61] Because dendrimers have nanometric dimensions and other protein-like properties, they can be recognized as biomimetic artificial proteins. [62] Their nanoscale size allows them to interact with biological targets and act like proteins, and they are able to recognize and bind to certain

molecules with high specificity. This makes them suitable for a wide range of applications, from drug delivery to tissue engineering.

Despite the fact that dendrimers are suitable as pharmaceutical excipients due to their properties, they also exhibit less advantageous properties, which may hinder their use, particularly because of their cytotoxicity, the difficulty of incorporating drugs into dendrimers, and the difficulty in controlling drug release rates. [63]

Size limitation is a primary concern. PAMAM dendrimers of generation 5 or lower can be sufficiently eliminated via glomerular filtration in the renal excretion pathway, while the clearance of PAMAM generation 6 and higher rely more on the hepatic clearance pathway.[64] Dendrimers with sizes ranging from 4–10 nm have the ability to interact with nanometric cellular components and have the capacity to overcome the cellular endocytosis barrier.[65] However, PAMAM dendrimers of generation 6 and higher have high costs and severe toxicity, [64] therefore the higher generation of PAMAM dendrimers are rarely used.

Numerous chemical modifications have been proposed to dendrimers in order to reduce their cytotoxicity and increase their cavity space. Several studies have shown that cytotoxicity of dendrimers could be significantly reduced by surface modifications with inert particles such as PEG [66] and fatty acids. [63] Moreover, covalent conjugation of the drug to the dendrimer surface can circumvent the lack of control over the release rate of the drug from the dendrimer. This then controls the drug release from the dendrimer. [63]

Dendrimers can be used as building blocks for bigger nanoparticles through the development of certain strategies. For instance, dendrimer cluster-derived size-switchable or adaptable nanoparticles exhibit desirable properties. [67] Most of these particles are hundreds of nanometres in size, and they remain stable around while blood circulates.[68,67] When

nanoparticles enter their target tissues, they break apart and release individual dendrimers, which they use to exert their remarkable tissue penetration and cell internalisation properties. [69] However, the higher generation dendrimers of 6 and higher have high costs and severe toxicity. [64] thus dendrimers with high generation are rarely used.

Size- and charge-adaptive clustered nanoparticles were created by Gao et al. [68] The outside layer of the clustered nanoparticle is made up of PEG chains, and the inner core is made up of complexes of PLy chains with PAMAM. When the clustered nanoparticles were somewhat larger than 100 nm (112 nm) and contained peripheral PEG chains, they were shown to have prolonged blood circulation and a slightly negatively charged surface (-2.2 mV).

It is suggested by Gupta that the half-life of drugs can be increased by conjugating using dendrimers. This evidence for this statement was given by the half-life of methotrexate being increased considerably when conjugated with a PAMAM dendrimer. The increased half-life can escalate the drug efficacy and lower the frequency of drug administration which coordinates higher patient compliancy.[44]

Zhang established the innovation of the tryptophan-rich peptide dendrimer (TRPD) in an antineoplastic therapy, [70] this is exhibited in Figure 1.5. TRPD can generate efficient supramolecular aggregates by engaging with intracellular DNA. This dendrimer can easily penetrate through the tumour cell membrane to exert a high degree of cytotoxic effect on the cell. Thus, the tryptophan-rich peptide dendrimer can restrict the tumour cell proliferation in vivo and cause to tumour cell apoptosis. This indicates that the treatment of cancer cells is being researched effectively with the discovery of this dendrimer and its abilities.
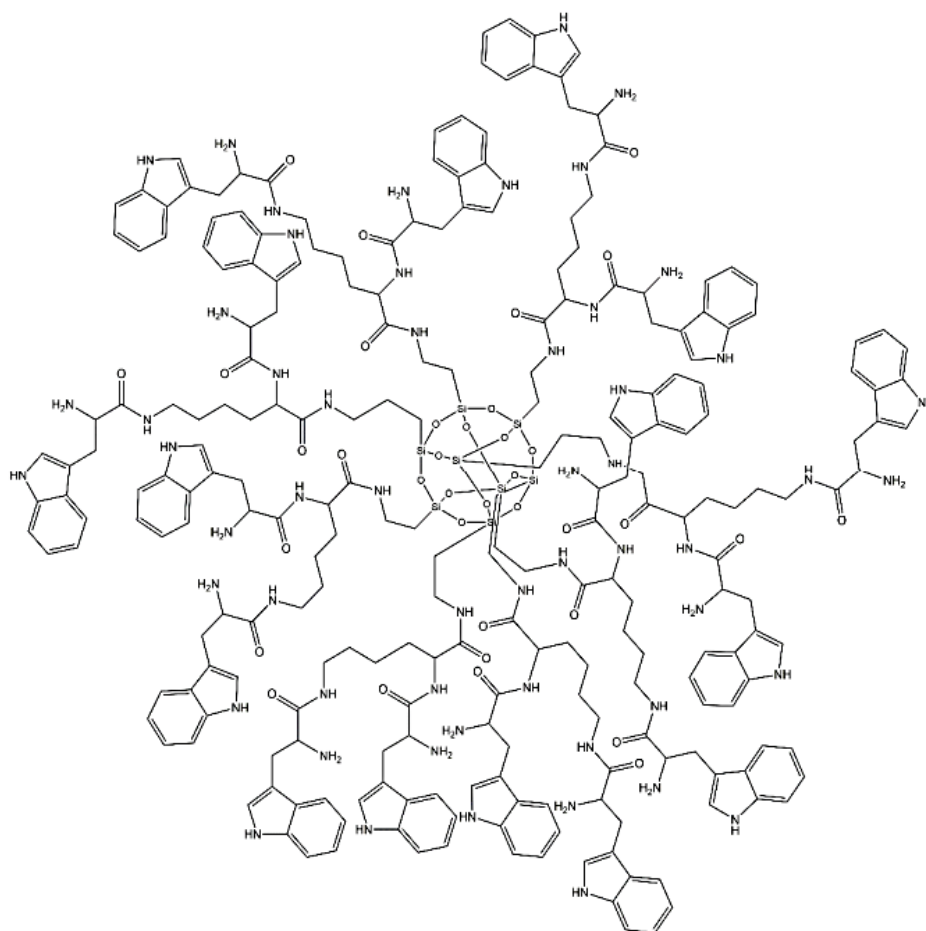
Figure 1. 5: Structural representation of the TRPD dendrimer .Adapted form. [70]

Enhanced permeability and retention (EPR) effect is used in passive targeting while active targeting is achieved by conjugating with antibodies, peptides, aptamers, and small molecules. Compared with free drugs, targeted delivery helps reduce toxicity in normal cells, protect drugs from degradation, increase half-life, loading capacity, solubility. [71,72]

To achieve optimal passive targeting, polymeric delivery systems take advantage of a drug's pharmacokinetic properties, such as its solubility, half-life, and prolongation of plasma circulation time. In this way, passively transported drugs are delivered to solid tumours.[73] Additionally, passive targeting certainly depends strongly on two parameters: The tumour endothelial permeability to macromolecules and the presence of reduced lymphatic outflow.

These two factors determine how well passive targeting works. When these factors are improved, the likelihood of passive targeting would increase. PAMAM dendrimers with semitelechelic Hydroxypropyl Methyl Cellulose (HPMA) polymers embedded with doxorubicin were developed for passive tumor treatment by researchers.[74] According to the results, dendronized nanoparticles with diameters ranging from 10 to several hundred nanometres are capable of passive targeting through the EPR approach. It is generally agreed that dendrimers of 10 nm–20 nm in diameter are most suitable for passive tumor targeting. [75]

Active targeting is a strategy that can decrease the absorption of a drug in normal tissue and increase its concentration in cancerous tissue. [76] The passive targeting and the EPR can only deliver drugs to solid tumours, not to cancer cells internally, and delivering a low dose of drugs to certain cancer cells can make chemotherapy ineffective.[77] Active targeting overcomes some of these limitations by attaching precisely targeted ligands to the outside of nanostructures that exert an attractive force on specific receptors on cancer cells. [78] Poly (2-methacryloyloxyethyl phosphorylcholine) modified G3- PAMAM dendrimer enhanced tumor targeting in U-87 tumor mouse model with significantly reduce the cytotoxicity of PAMAM dendrimers, while efficiently target the brain tumor. [79]
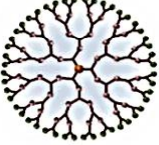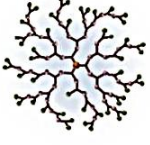
1.4. Hyperbranched polymers

Polymers have been studied the most among the materials used in drug delivery systems. In particular, graft, star, and branched polymer systems appear very promising. This is because it has been reported to be low in toxicity and high in transfection efficiency.[80] hyperbranched polymers offer the potential for multivalent ligand binding as well as opportunities for covalent and non-covalent, [81] drug interactions due to its multifunctionality.[82] The multifunctionality of branched and dendritic architectures also offers a new opportunities for theranostic applications combined diagnostic as well as therapeutic, [83, 82] In order to accomplish certain properties, polymeric tailoring could be carried out directly on biopolymers by chemical derivatization. [84]

Hyperbranched polymers (HBPs) are polydisperse structures, three dimensional and present a high number of terminal groups and internal spaces. They are categorised as dendritic macromolecules, but they do not withhold the perfect structure of a dendrimer. A comparison is displayed in Table 1. They are constructed with a highly branched formulation and chemical stability resulting in them being efficient drug carrier system.

HBPs have like dendrimers a three-dimensional globular structure that have attracted the attention from both academia and industry. When compared to dendrimers, their structures are irregular with dendritic, linear, and terminal units randomly distributed, and their synthesis leads to macromolecules with broad molecular weight distributions. However, HBPs can be easily synthesized in a one-pot reaction and thus are more cost efficient as compared to the multi-step approach for the dendrimers requiring a purification step after each coupling reaction. Also, due to their higher steric hindrance, dendrimers may be more challenging to functionalize than HBPs.

Table 1: Comparison of a hyper-branched polymer with a dendrimer

Polymer	Dendrimer	Hyperbranched
Structure		
Topology	3D Globular	3D Ellipsoidal
synthesis	One step, cost effective	Multi steps, laborious
Purification	Easy purification by precipitation	Difficult to purify and time consuming
Functional groups	At peripheral units	At linear and peripheral units
MW PDI Scaling up	Same MWs PDI 1.0 Difficult	Mixed MWs PDI 0.4-0.6 Already easy
Solubility	Very high	high
Viscosity	Very low	low

HBPs, similar to dendrimers, form cavities that encapsulate molecules of different sizes. For instance, DOX, [85] 5-fluorouracil (5-FU). [86] A further study was conducted on the encapsulation property of high molecular weight hyperbranched polyglycerol (HBPGs) as drug nanocarriers. It was found that Rhodamine B (RB) molecules are bound to the formed cavities within HBPGs through hydrogen bonds and electrostatic interactions.

Generally, HBPs of high molecular weight can be relatively easily synthesized reaching a reasonable size (> 10 nm) to passively target tumors by EPR effect, while dendrimers with a number of generation higher than five are difficult to prepare due to steric hindrance affording nanostructures with a hydrodynamic diameter lower than 10 nm that are thus not suitable for passive targeting. However, unimolecular HBPs of low molecular weight have a small size and cannot be used for size-related passive targeting at the tumor via EPR effect as they can be easily removed by renal excretion or through bypassing filtration by the spleen. [87]

Additionally, The self-assembly of HBPs into multimolecular nanostructures has been considered to increase the size of the nanocarriers. [88,89]

Commonly, HBPs encapsulate drugs by physical encapsulation and covalent binding. They are dependent on their own molecular weight to perform effectively as they modulate the cavity and terminal groups. Polyglycerol and hyperbranched polyol were examined to be drug delivery systems by Kolhe. [90] The conclusions stated that ester linkages that occur between the two polymers and ibuprofen can form conjugate with high numbers of the drug's molecules. This suggests that both hyperbranched polymers can initiate considerable therapeutic effect in vivo studies.

Additionally, research has uncovered that hyperbranched polyglycerol (HPG) can be modified with varying functional groups, Figure 1.6. This highlights its ability to effectively attach anticancer drugs such as docetaxel [91] and cisplatin. [92] It is soluble in water at high concentrations without any notable increase in its viscosity which is beneficial for enhancing the solubility of hydrophobic drugs in biological fluids. [93] The studies of hyperbranched polymers therefore infer that they may be effective drug delivery agents, which could be competitive with dendrimer.
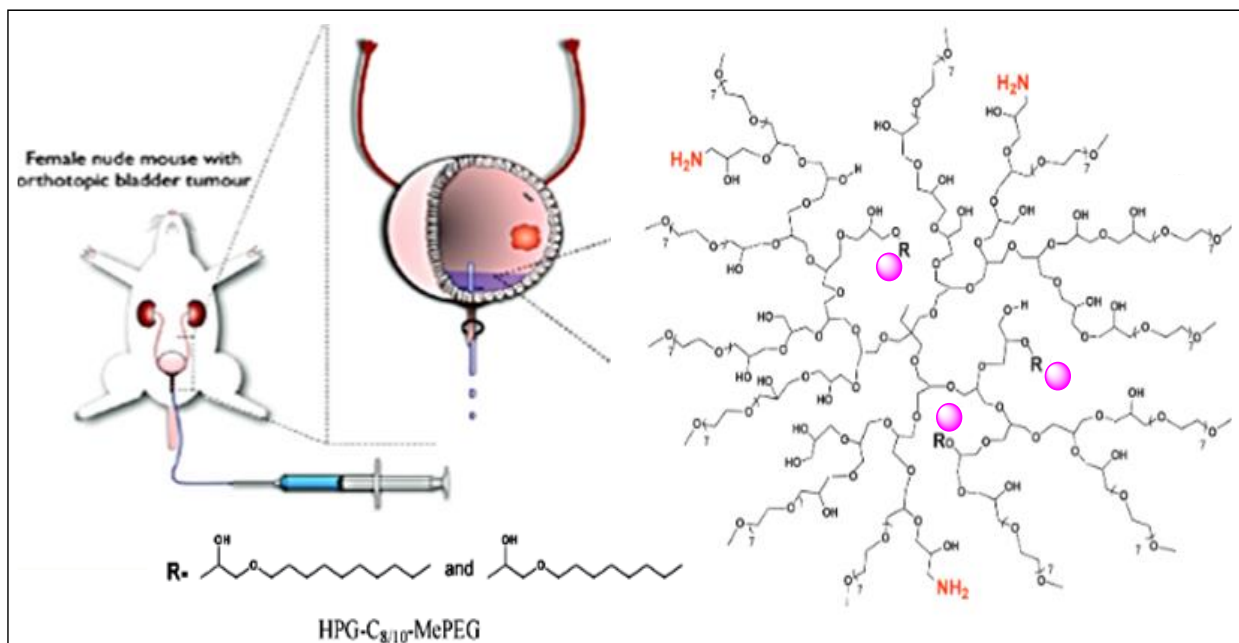
Figure 1. 6: Diagram showing how docetaxel (DTX) is loaded hydrophobically into derivatized hyperbranched polyglycerols to treat bladder cancer. Adopted from.[91]

1.4.1. Synthetic strategies

There are two approaches to compose hyperbranched polymers, the first is by introducing a single monomer. This can be by step growth or chain growth polymerisation such as using an AB_x monomer. The second approach uses a double monomer by direct polymerisation of two complementary monomers, for example $A_2 + B_n)$ n > 2. [94] The variability between AB_2 monomers and multifunctional $A_2 + B_3$ is illustrated in Figure 1.7. The first approach formulates a polymer with a single A-group and multiple B groups. No cyclisation is assumed. The polymer with multiple A and B functional groups are assembled in the second approach.
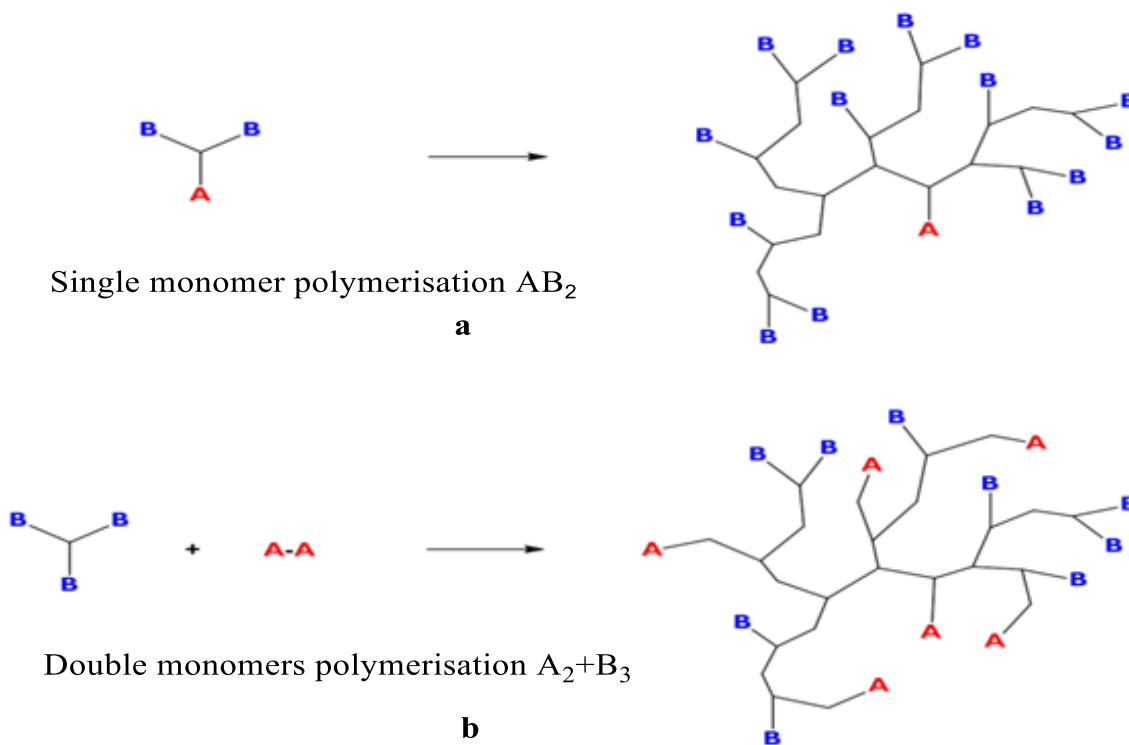
*Figure 1. 7: Schematic representation of the polymerization of strategies for synthesising hyperbranched polymers (**a**) AB$_2$ monomer (**b**) A$_2$ + B$_3$ monomer mixture*

The efficient monetary value of starting monomers is an influencing factor in the synthesis of hyperbranched polymers. There are advantages of utilising functional symmetric monomer pairs compared to AB$_n$ monomers such as its reachable availablity and versitily. The AB$_n$ monomers are not commercially obtainable thus limiting their use for industrial applications. The reachability and relatively effortless synthesis of A$_2$ and B$_n$ presents a flexible platform for modifying polymer properties and structures. The commercial availability of multifunctional monomers authorises the preparation of hyperbranched polymers to be conducted swiftly while maintaining a low expense to the project.

1.5. Photodynamic therapy

PDT is a clinically validated therapeutic procedure consisting of three components: photosensitizers, light, and oxygen. Two types of chemical reactions can be initiated by photosensitizers (PS) once they are activated by lights of the appropriate wavelength and intensity as shown in Figure 1.8. [95] In type I reactions, free radicals and radical ions are formed when electrons or hydrogens are transferred between photosensitizers and substrates. [96] In type II mechanism of PDT (the dominant process), singlet oxygen species ($^1O_2$) are produced via the energy transfer process between PS and molecular oxygen. [97] As the $^1O_2$ has a high reactivity, it has an optimal action radius in 20 nanometres, making the PDT a highly localized treatment. [96] Dual selectivity is available in the PDT for accumulating PSs preferentially in cancerous lesions and precise spatiotemporal control of the light. Due to these advantages, PDT can destroy the primary tumor rapidly and avoid unnecessary side effects on healthy tissues. [98]

One of the major drawbacks of the hydrophobic photosensitizers PSs is that they cannot be injected intravenously as they form aggregates in solution, limiting their medical applications. Moreover, although not being toxic individually, photosensitizers can be activated by light of a certain wavelength. This leads to energy transfer to nearby oxygen molecules that causes cytotoxicity. Therefore, hydrophobic photosensitizers require complex formulations for systematic delivery.[99]
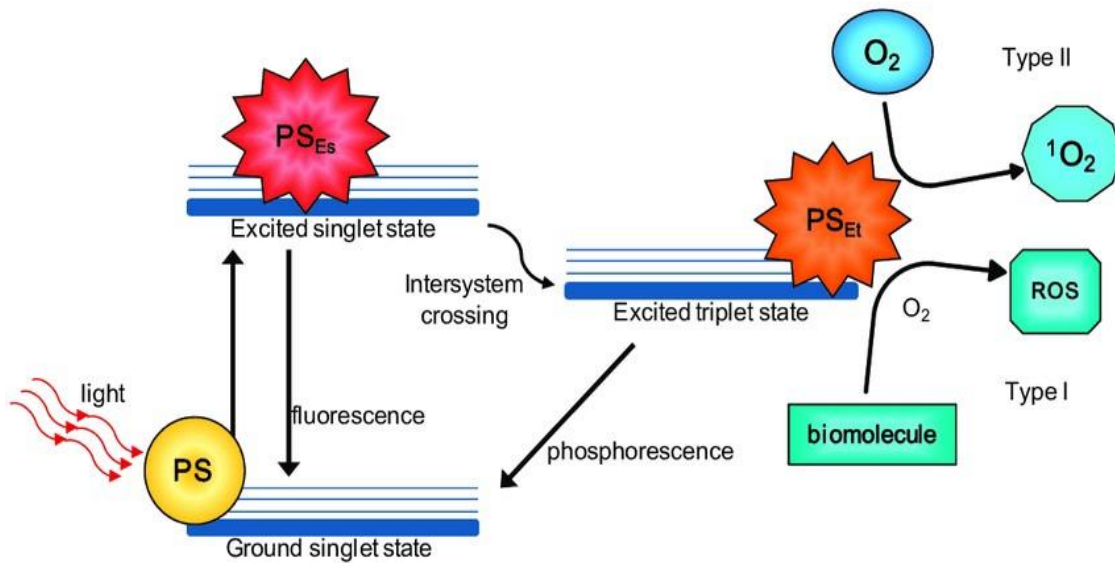
Figure 1. 8: A schematic Jablonski's diagram illustrates Type I and Type II reactions in PDT (photodynamic therapy) adopted from.[100] After absorption, the PS is in a singlet state. Following an intersystem cross, the PS, which is now in a singlet excited state, reacts with biomolecules in two ways: The PS undergoes a hydrogen atom transfer (electron transfer) to form radicals. These radicals react with molecular oxygen, generating ROS type I reaction. Alternatively, the PS in a triplet state reacts directly with oxygen, resulting in the formation of singlet oxygen (type II reaction). (PSEs): PS excited singlet state. (PSEt): PS excited triplet state. (ROS): reactive oxygen species. ($^1O_2$): singlet oxygen.

The treatment depth is determined by the wavelength of light at which a PS can be activated to produce Reactive Oxygen Species (ROS). Light at wavelengths below 650 nm has a low tissue penetration depth, while light over 850 nm is not sufficient for a PS to be activated to produce excited singlet oxygen. Therefore, the optimal phototherapy window index wavelength for PDT is between 650–850 nm .[101]

There are several generations of Porphyrin PSs on the market today, but most research seems to be focused on developing or investigating different types of porphyrins. Porphyrins PSs and their derivatives are heterocyclic organic macrocycles with high phototoxicity and can be used for a variety of diagnostic and therapeutic applications. [101] on the other hand, they have poor water solubility and self-aggregation characteristics, which lead to significant difficulties in the

localization and uptake of PS subcellular, thus impacting the overall treatment results in PDT cancer therapy.[102] They absorb light in the therapeutic window wavelength region and so produce ROS through intersystem crossing, allowing them to perform very well within PDT and PTT cancer treatment applications.

Porphyrins containing metal ions in the inner cavity, such as Zn and Al, have also been used in photodynamic therapy (PPT). [103] Cationic Porphyrins (for example, zinc(II) meso-tetricity porphyrin, N-n-hexylpyridinyl-3-yl porphyrin or 5-trifluoro-phenyl-10,15-20-tris-4-tris-mono-porphyrin) are the most promising porphyrins (PPs) for cancer treatment because of their amphiphilic characteristics . [104] Anionic Porphyrins and their derivatives, like tetrakis-porphyrin, tend to self-accumulate and are self-limiting in total ROS generation . [105] The chemical structures of some porphyrins and their derivatives are shown in Figure 1.9.

 Kubat et al found that dendrimers G5 and G4.5 with 128 surface binding sites are used as templates for porphyrin self-assembly. This was due to that porphyrin are bound to PAMAM dendrimers primarily by electrostatic interactions with amines or their carboxyl groups. The pH value of a solution and the peripheral functionalization of porphyrins play a role in this reaction. [106] Since porphyrins absorb in the red-light part of the spectrum, light can penetrate deep tissues to treat deep tumours.
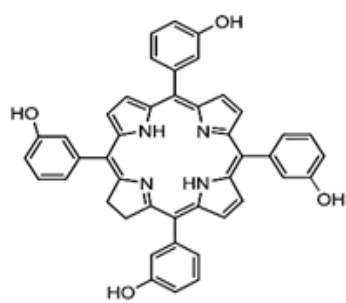
Meta-tetra(hydroxyphyenyl chlorin
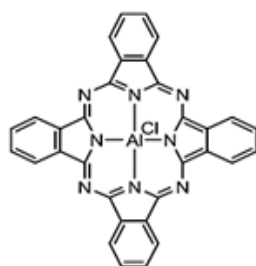
Aluminum phthalocyanine chloride
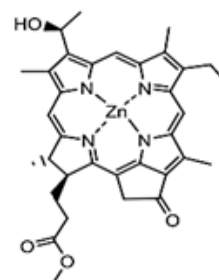
Methyl zinc bacteriopheophobide
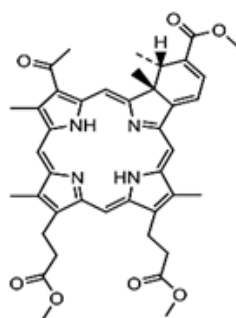
3-Acetylbenzoporphyrin Derivative
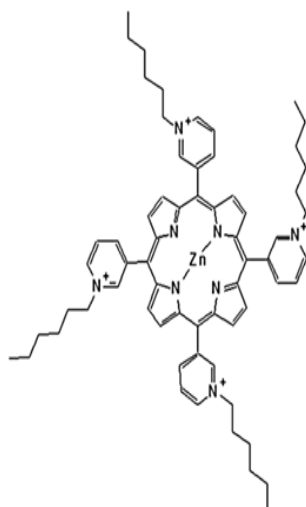
ZnTnHex-3-PyP
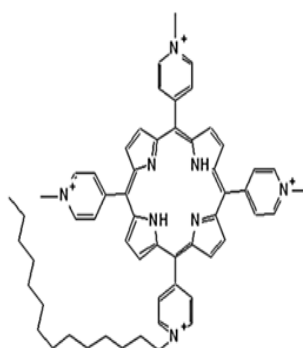
TMPyP4-C14
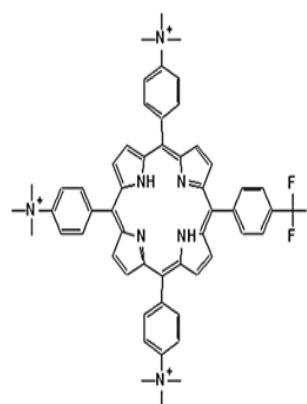
TFAP(3+)

Figure 1. 9: Structures of porphyrins and their derivatives used extensively in photodynamic therapy

Chapter 2: Aims and objectives

2.1. Aims and objectives

Humans have been tried to develop effective treatments for diseases over many decades. This includes extensive research on the development of drug delivery systems. Researchers have investigated the delivery of drugs using a variety of materials, such as nanoparticles and lipids, however their application is often limited because of high cytotoxicity and low drug loading and/or poor drug release.[107] The ability to tune a polymer's composition, topology, and functionality makes them more attractive and versatile than alternative systems. Dendritic polymers, including dendrimers and hyperbranched polymers are a relatively new class of polymers that may be able to offer improved properties with respect to drug delivery.[82] As such, these new dendritic polymers could play a critical role in future clinical application of drug delivery systems.

Dendrimers have attracted much attention since being introduced by Newkome and Frechet . [108] Dendrimers are well defined, monodisperse, and highly organized structures. Their multifunctional terminal surface makes them an ideal delivery agent, Having the capability to modify surface chemistry to make them water soluble, and the ability to bind aqueously insoluble drugs within their hydrophobic cavities . [109] Figure 2.1 illustrates dendrimer as a delivery system. Dendrimers and drugs can interact either by encapsulating the drug inside the cavity of the dendrimer and/or conjugating with the functional groups on the surface. Despite this, synthesising dendrimers is difficult, time-consuming, and expensive.
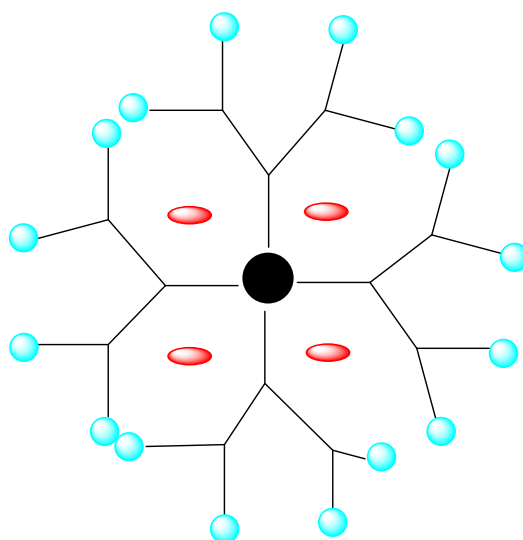
◇ encapsulation of drug in dendrimer via electrostatic and hudrogen bonding

◯ solubilizing group

Figure 2. 1: A cartoon illustration of dendrimer being used as a delivery agent.

One of the main reasons for using a delivery system is to overcome the poor solubility of many therapeutically active molecules. This lack of solubility can often be the limiting factor preventing an otherwise effective molecule being used clinically. For this application, it is essential that any delivery system be water soluble, as this enables it to transport drugs through the bloodstream and deliver them to the specific site of action. [110] The research proposed in this thesis is focused primarily on neutral water-soluble dendritic polymers, as they multiple charges on the surface of large globular molecules can be toxic. [76]

The main aim of this project is to study the drug delivery potential of dendrimers and HBPs, and to explore whether HBPs are as efficient as dendrimers with regards to encapsulation of guest molecules for drug delivery. Initially, the project will focus on dendrimers, before studying some related HBPs for comparison. The other part of the project to synthesis HBPs that are similar in structure to PAMAM dendrimer in terms of internal groups as well as peripheral groups. Also, the molecular weights and functionality will be controlled to ensure

each variable has a complete examination and a valid comparison, the molecular weights and functionality will be controlled to ensure each variable has a complete examination and a valid comparison.

The studies often compare systems (dendrimers and HBPs) with completely different structures and internal functionality. Due to their globular shape, multiple branches, and empty interior spaces, PAMAM dendrimers allow the direct encapsulation of drug molecules into their macromolecule interior. Hydrophobic properties of these hollow interior cavities make it possible to interact with poorly soluble drugs via hydrophobic interactions. Consequently, this interaction increases the drug's aqueous solubility, it affects the drug's bioavailability and release profile. A variety of factors affect the encapsulation, including dendrimer generation, internal composition, and the degree of functionalization of surface groups. In early studies, Jean Haensler et al reported that DNA can be complexed with PAMAM dendrimers for gen delivery application. A study suggested that positively charged dendrimers bind electrostatically and sterically to anionic DNA and form a complex. [111] The PAMAM dendrimer possesses internal amin groups (tertiary amins and amide groups), which allow it to interact with drug molecules through hydrogen bonding and electrostatic interactions. Devarakonda et al revealed that, Nifedipine, which has partially water solubility, could interact with the nitrogen atoms of the dendrimer amines through hydrogen bond formation. PAMAM dendrimers possess all the characteristics (including, internal and external groups) that make them suitable for drug delivery.

Previously, our group studied comparison between dendrimer and hyperbranched polyglycerol, [112] which are different in terms of structures and internal functionality. However, this neutral PAMAM dendrimers consisting of an ethylenediamine core and a hydroxyl group at the surface will be prepared by the divergent approach. The OH groups at the periphery contribute to the water-solubility of dendrimer. The size of the dendrimer increases with increasing generation.

Higher generation dendrimers have more space and therefore capability to encapsulate more hydrophobic molecules. However, as dendrimer size increases, so does the internal steric hindrance. [15] This is caused by steric congestion between the internal branches or steric interaction at the surface. This phenomenon is known as dense packing. [113]

In this research, G2.0, G3.0 and G4.0 OH-ended dendrimers with a molecular weight of 1437 Da, 3272 Da and 6941 Da respectively will be synthesized to investigate the effect of dendrimer size and dendrimer concentration on the ability of dendrimers to improve solubility and bind hydrophobic drug molecules. These OH terminated dendrimers will be synthesised from ester terminated dendrimers after reaction with ethanolamine.

Additionally, investigate ibuprofen interactions within three generations of hydroxyl ended PAMAM dendrimers. Once synthesised we will try and identify any interactions between encapsulated drug to dendrimer size. Once an optimum dendrimer has been identified we will go on to examine any effect of concentration and drug encapsulation (at concentrations ranging between 10^{-4} and 10^{-3} M). Ibuprofen was chosen, due to it is widely available and extensively used in similar research. [114] Ibuprofen belongs to the propionic acid class of non-steroidal anti-inflammatory drugs and is used to reduce pain, fever, and inflammation. In addition, this common drug is a weakly acidic pharmaceutical molecule bearing carboxylic groups that can bond hydrophobically via hydrogen bonding with dendrimer internal amines (amide groups), as well as that can bond through acid/base interactions with the internal basic amines.

Another objective is to explore the encapsulation of porphyrins for PDT by non-covalent methods. Our research group has previously focused on improving poorly soluble anticancer therapies for PDT using dendrimers. [115]

Therefore, it will perform encapsulation studies on porphyrin photosensitizers. Porphyrins are extremely hydrophobic. However, the hydrophobicity of porphyrins can be enhanced through strong metal to ligand coordination using the amine functionality within the interior of the dendrimers. Studies can be carried out with metalated and non-metalated porphyrins to identify how these secondary interactions influence encapsulation efficacy. It was found that simple tetraphenyl porphyrin (TPP) and metal porphyrins (ZnTP) were successfully encapsulated within dendritic molecules, however the loadings were incredibly low. [115,61] This was due to the extreme hydrophobicity of the TPP and ZnTPP which limits the ability to encapsulate drugs and to synthesis dendrimer-drug complexes (more explanation on this will be provided later in the thesis). Therefore, to improve drug loading we proposed using phenolic porphyrins, as these have some limited water solubility. Also, the phenolic group is acidic and can in principle bind electrostatically to the amines within the dendrimer Figure 2.2.
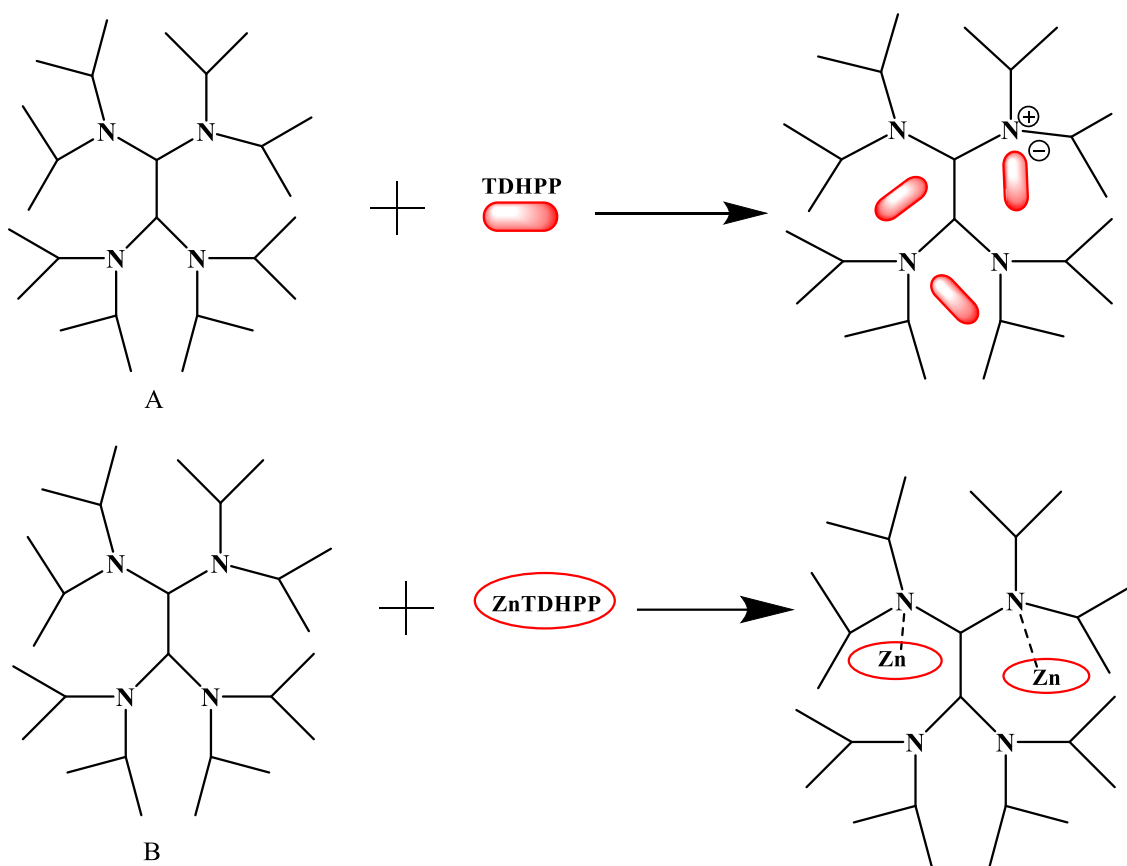
*Figure 2. 2: The encapsulation of porphyrin PSs. **A**: free base porphyrin TDHPP (hydrogen bonding and hydrophobic interactions) **B**: The additional interaction of Zinc porphyrin ZnTDHPP provided by coordination.*

Tetra-Dihydroxyphenyl-porphyrin (TDHPP) has 8 hydroxyl groups and some water solubility. This and related porphyrins are also known to be effective PDT sensitizers. As such we intend to synthesis TDHPP in metalated and non-metalated forms and test the encapsulation and release properties within dendrimers and HBPs.

Dendrimers are exceptionally functional molecules. However, larger generation dendrimers exhibit from high steric hindrance, which makes it difficult to encapsulate large numbers of drugs as confirmed by Perumal. O et al, which studied G4 dendrimers with ethylenediamine (EDA) cores and sized terminations. [116] In addition, the lengthy stepwise synthesis of dendrimers makes them extremely expensive to make and use. This is primarily the reasons why scientists wanted to develop alternative systems that possessed the same structural properties as dendrimers but were much easier and cheaper to synthesise. This resulted in the

development of a new dendritic system known as hyperbranched polymers (HBPs). These can be easily synthesized using a one-step polymerization synthesis. Although simpler, these methods lead to imperfections in branching, resulting in a less ordered structure. As such, the problem of dense packing and steric hindrance is reduced. Overall, these simpler macromolecules may be better and cheaper alternatives to dendrimers, if they can encapsulate and release drug molecules with similar encapsulation ability. This is one of the important aspects that will be investigated during this project and thesis.

PAMAM dendriemr   hyperbranched PAMAM polymer
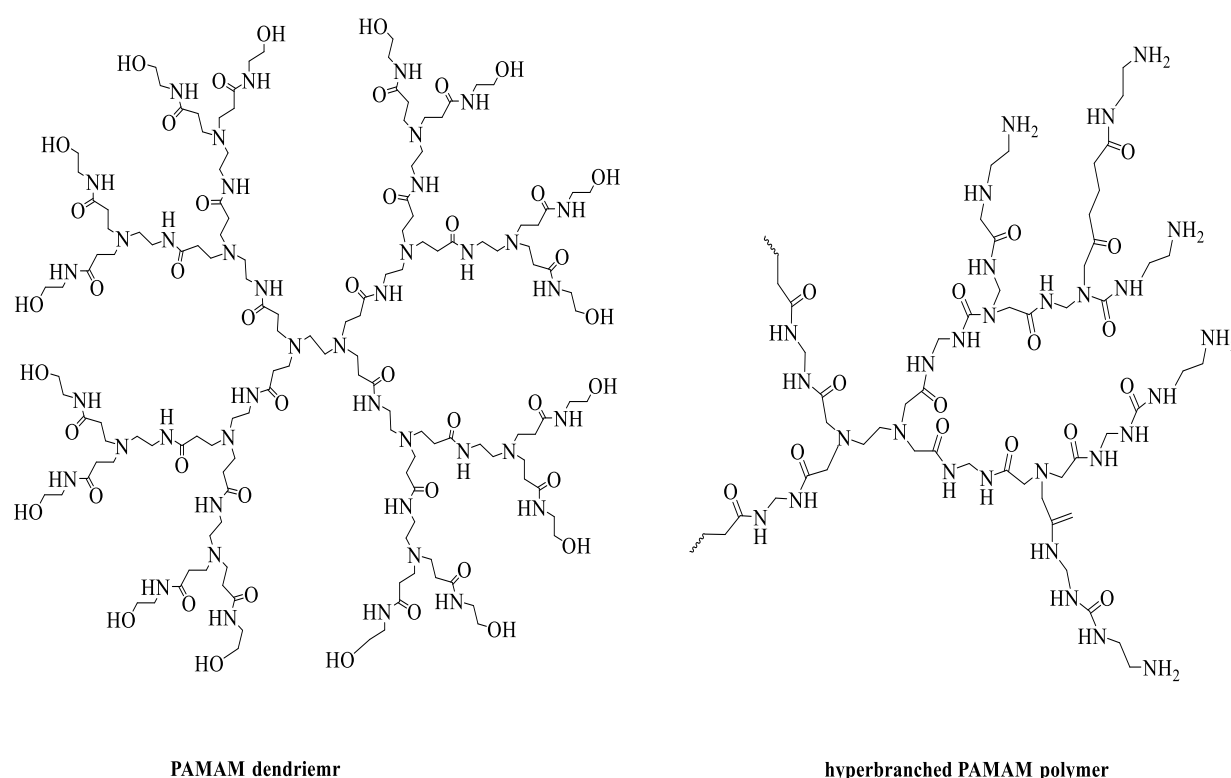
Figure 2. 3: Structures of PAMAM dendrimer and Hyperbranched PAMAM polymer

To investigate whether or not HBPs can be effective alternatives to dendrimers, we must compare like for like (where possible). That is, we must compare systems with similar (or ideally identical) internal functionality. There, a suitable HBP to compare with a PAMAM dendrimer would need to be a hyperbranched PAMAM (HBPAMAM) that possessed the same dendritic units and functional groups as the PAMAM dendrimers. One example, along with a PAMAM dendrimer, is shown in Figure 2.3. The interior of the HBPAMAM is made up of

similar repeating units of ethylenediamine (EDA) and amide units. After completing our studies on PAMAM dendrimer, we intend to investigate the encapsulation properties of some hyperbranched PAMAMs using the same set of experiments used when studying the PAMAM dendrimers.

Chapter 3: The synthesis of Hydroxyl Terminated PAMAM Dendrimers And

Encapsulation of Ibuprofen and Tetrahydroxy porphyrin

3.1. Introduction

The therapeutic efficacy of any drug is often diminished by its inability to reach its target in an appropriate dose. This is caused by the poorly solubilized nature of the drug in the body's aqueous environment also lack targeting. In the initial stages of drug development, medicinal chemists synthesize water-soluble derivatives of the drug moiety. However, even small structural changes can dramatically decrease the performance of the drug. To address this problem, scientists are trying to develop a system that will deliver a drug efficiently and minimize the need for structure modifications. [89, 117]

Since the early 1990s, dendrimers have emerged as promising agents to deliver drugs in the pharmaceutical industry. They were introduced for the first time by Newkome and Tomalia in 1985. These polymers are characterized as well as defined structure, hyperbranched macromolecules possessing a large number of terminal groups. [118] Due to their nanostructure and chemical versatility, dendrimers have become attractive candidates for nanodrug delivery. [119] The advantages of dendrimers over polymeric drug delivery vehicles include: 1) stable architecture; 2) high density and well-defined surface functionalities, which can be used to target, image, and kill cells; and 3) are monodispersed polymers, enabling reproducible pharmacokinetics; 4) Easy to penetrate through the cell membrane, enabling cellular uptake of the drug complex or conjugation, and 5) controllable shapes, making them suitable for diverse medical applications. [120, 121, 13] As a result of their unique assembly structure, dendrimers of high generation have a large concentration of functional groups on their periphery. Due to their high functionality, they are highly useful for both active and passive targeting. This could be achieved by surface modification of dendrimers utilizing a variety of targeting moieties, including folic acid (FA), peptides, monoclonal antibodies and sugar groups.[110] Several successful active and passive targeting attempts have been made by modifying the surface groups and branching units of dendrimers. Gupta et al explored the successful conjugation of

FA to G5 PPI dendrimers and its feasibility in targeted delivery of an anticancer drug (doxorubicin). It was found that FA conjugated dendrimers exhibited higher cell uptake in MCF-7 cancer cell lines and reduced toxicity significantly. [122]

In addition to generational size, dendrimer shape is affected by its 3D geometry. When dendrimers are synthesised at low generations, for example G1 and G2, they are flat, but when they are constructed at higher generations, they become globular, which makes them better suited for encapsulating small host molecules. However, dendrimers are difficult to synthesize and suffer from steric crowding at high generation, resulting in self-termination. [39] Drug delivery systems based on dendrimers must be water-soluble in order to be administered systemically. Furthermore, dendrimer structures with hydrophobic regions allow for better encapsulation and efficient solubilization of hydrophobic drug molecules inside dendrimer voids.[123,109,14] Because poor solubility is usually associated with a low bioavailability, preparing drugs can be a major challenge. Hydrophobic drugs can interact with the internal amines of dendrimers to improve their solubility. Duncan et al developed conjugates of PAMAM dendrimers with Cisplatin, an anticancer drug with nonspecific toxicity and poor water solubility. [124] The conjugates exhibit increased solubility and reduce systemic toxicity. Another study conducted by Patel et al reported that PAMAM dendrimers were able to significantly enhance the solubility of poor water-soluble drugs such as aceclofenac. [124] This was due to interaction of the internal amines with drug molecules by hydrogen bond formation.

The aim of this part of the project was to investigate the ability of the PAMAM dendrimer to enhance solubility via hydrogen bonding ion pairing reactions and amine-metal coordination. PAMAM Dendrimers have shown that they can enhance the solubility of poorly soluble drugs [125] and increase their bioavailability. [126] Yiyun et al reported an increase in solubility of poor soluble non-steroidal anti-inflammatory drug (ketoprofen) when encapsulated in PAMAM-NH_2 dendrimers. [125] A study by Duncan and colleagues found that PAMAM-NH2 dendrimers were cytotoxic to three cancer cell lines with damaged membranes. [34] The damage was caused by the cationic nature of amine terminated PAMAM dendrimer, and it was directly associated with the generation number, the concentration, and the duration of its incubation time. [34, 123] NH_2 dendrimers toxic as they cause cell aggregation via charge-charge interactions (cells are negative and NH_2 dendrimers are protonated and its positive in aqueous environments). Ester-terminated dendrimers are nontoxic, but insoluble in water. Further, in physiological environments, these systems are hydrolysed rapidly, releasing carboxylic acids that enable their solubility. [127]

Eester-terminated PAMAM dendrimers were converted to hydroxyl-terminated dendrimers following the method originally developed by Newkome et al. [128] Similar conversion results were also achieved by the Twyman group.[129] Using TRIS (hydroxymethyl)aminomethane, an ester-terminated PAMAM dendrimer can be converted to a hydroxyl-terminated dendrimer. Using this method, each ester terminated with three hydroxyl groups. [129] The De Gennes density packing effect has been reported in several reports to result in defective branching architectures in large dendrimers with crowded branches. [113, 123] De Gennes hypothesizes that in the early generations, starburst structures would be quite flexible, whereas surface branch cells would become rigid and restricted as one approaches the dense-packed limit of the starburst. [113]

As such, dendrimers with TRIS terminal groups can become gennes packed at low generations. To minimize this problem, we propose a modified PAMAM dendrimer using ethanolamine, where each ester has been converted to a single hydroxyl in each branch.

3.2. Synthetic method of PAMAM dendrimers

The initial aim of our study was to synthesize different PAMAM dendrimers with different sizes in order to obtain the best dendrimer. These made using a divergent approach which can minimize side reactions and steric issues. Essentially, this synthesis technique involves synthesising the smallest generation (G0.5), then proceeding on to successively synthesize higher generations. PAMAM dendrimers were synthesised sequentially by two reactions. Michael addition of PAMAM dendrimers to form ester-terminated dendrimers, followed by an amination reaction to form amine-terminated dendrimers. The Michael addition step uses methyl acrylate, which is an α-β unsaturated carbonyl compound. Due to the high electronegativity of oxygen and conjugation a δ positive charge on the terminal carbon is formed. As a result, the β carbon becomes electropositive, making it susceptible to nucleophilic attack by the EDA. The Michael addition mechanism is illustrated in Scheme 3.1.
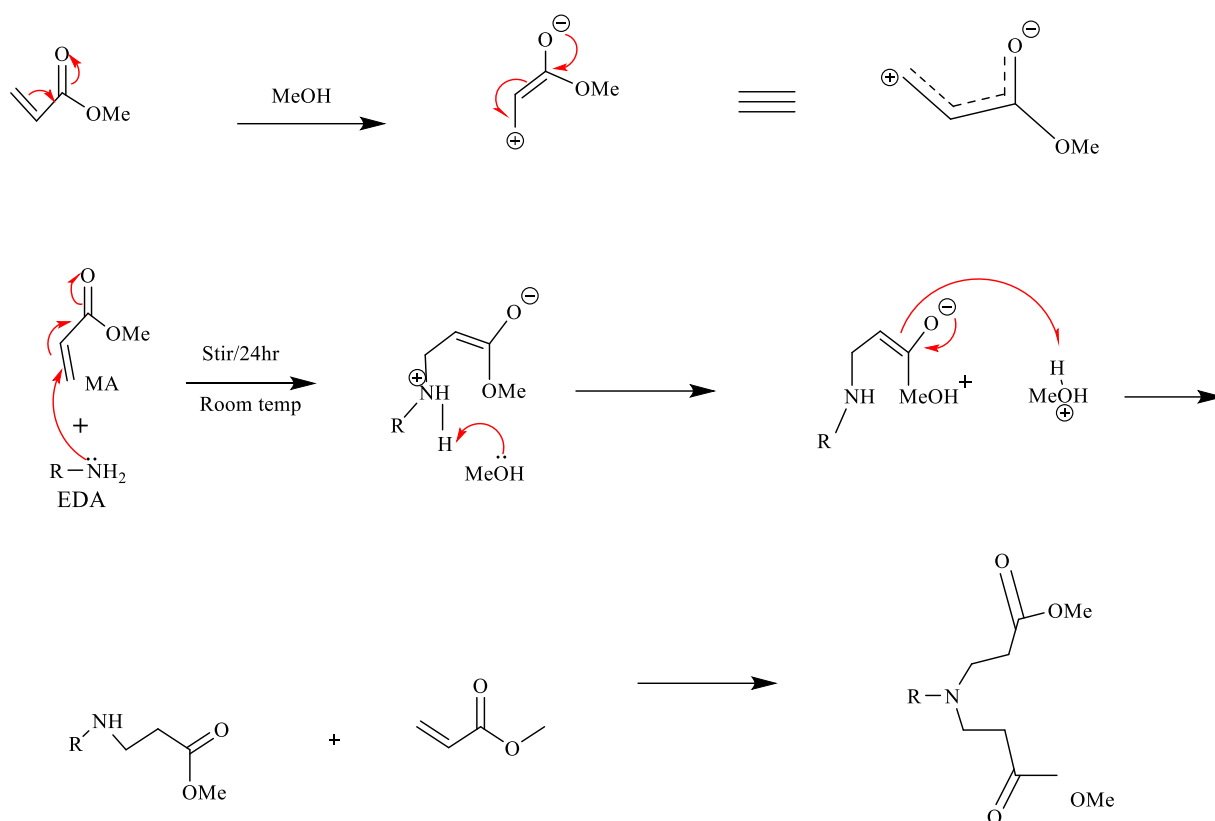
Scheme 3. 1: The Michael addition mechanism used to synthesise half generations PAMAM dendrimer

The Michael addition mechanism used to synthesise half generations PAMAM dendrimer. After the Michael addition step is completed, the amination step follows, shown in Scheme 3.2. The reaction involves the nucleophilic lone pair of nitrogen from EDA attacking the electropositive carbonyl carbon and forming a tetrahedral intermediate. During the intermediate state, the secondary amine is deprotonated intramolecularly. Carbonyl is then formed by releasing the methoxy group from the tetrahedral intermediate. This results in the release of the product and the formation of a methanol molecule. To build dendrimers, the Michael addition and amination steps are repeated sequentially. Detailed information about each synthesis will be provided in the next section.
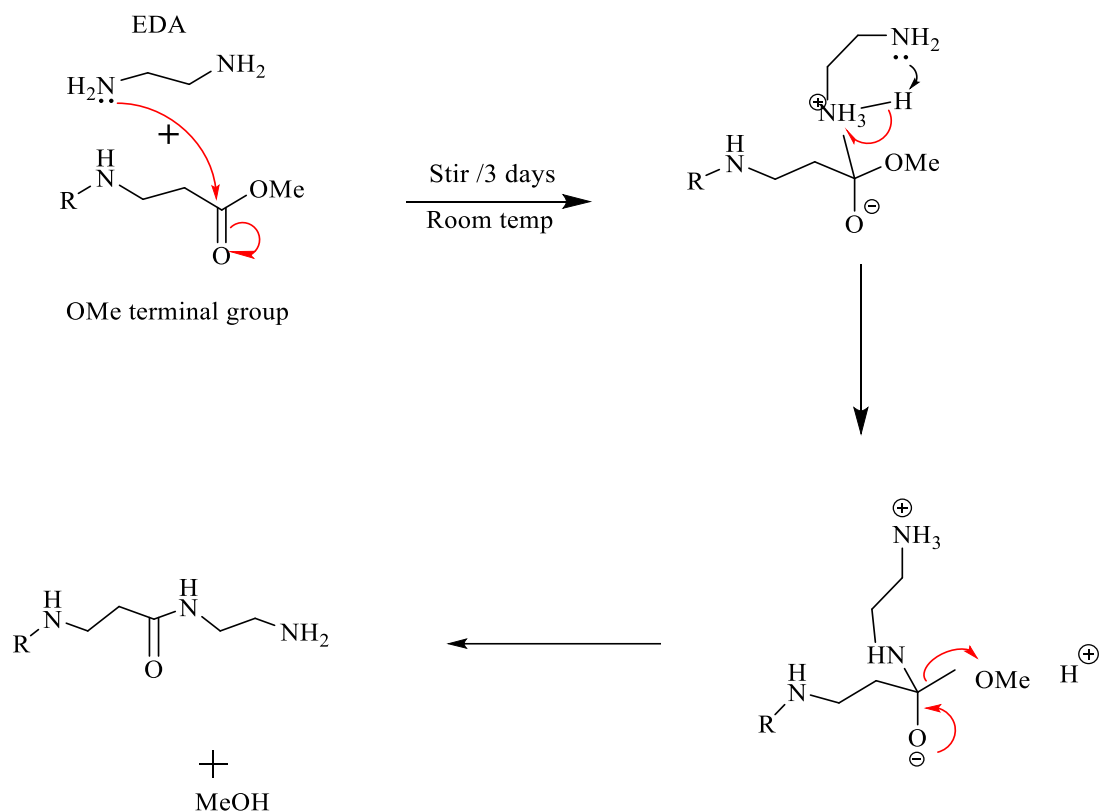
Scheme 3. 2: The mechanism of amination step used to synthesis full generations dendrimers

3.2.1. Synthesis of half generation PAMAM dendrimers

Half generation dendrimers were synthesized by adding two equivalents of methylarylate (MA) per amine either the core ethylenediamine EDA or the amine terminated dendrimers. The reaction solution was stirred at room temperature and then the solvent and excess reagents removed using a rotary evaporator. No further purification was required. This procedure is shown in Scheme 3.3 using G 0.5 as an example.
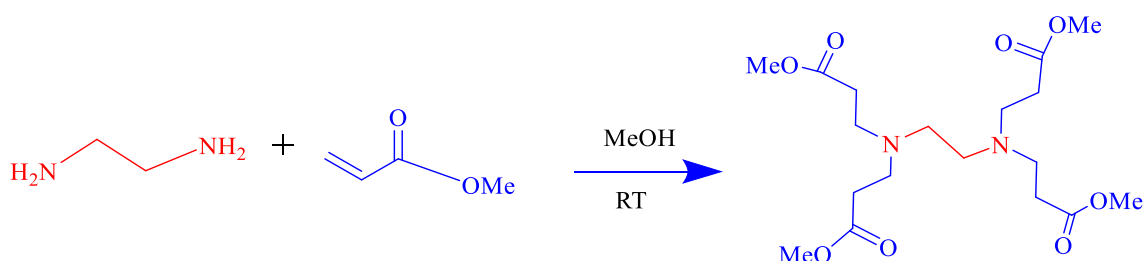
Scheme 3. 3: The synthesis of G 0.5 PAMAM dendrimer

Larger generations were generally taking more time to synthesize. In order to check how each reaction was progressing and ensure they were complete, small volumes were analysed using ^{1}H NMR. To confirm that all MA had been successfully removed, ^{1}H NMR spectroscopy was used to observe any remaining alkene peaks at 4.5-6 ppm. Generally, all PAMAM dendrimers were obtained as a honey-coloured oil that became more viscous at higher generation.

3.2.2. Synthesis of full generation PAMAM dendrimers

Full generation PAMAM dendrimers were synthesised by adding an excess of EDA to the ester terminated PAMAM dendrimers. These were dissolved in methanol at room temperature. The procedure is illustrated using the G1 synthesise as an example, Scheme 3.4.
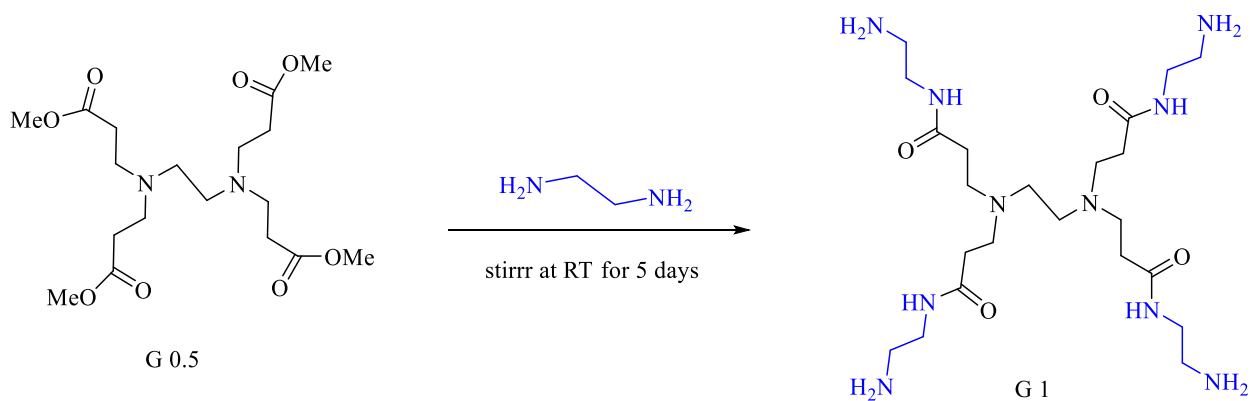
Scheme 3. 4: The synthesis of full generations PAMAM dendrimer

To achieve monodisperse dendrimers without causing any side reactions, excessive amounts of starting material were used, 20 equivalents of EDA per ester. To remove the excess EDA, a mixture of toluene and methanol (9:1) was used. After washing several times, the EDA peak

~2.7 ppm was no longer visible in the ^{1}H NMR spectrum. The subsequent section provides a detailed description of the purification process.

3.3. Purification of PAMAM dendrimers

The purification stage is arguably the most crucial step in the synthesis of PAMAM dendrimers. An excess of starting materials must be removed from the resulting products to prevent structural defects. It was not difficult to purify all half-generation dendrimers, as several methanol washes were used to remove excess MA. However, amine terminated PAMAM dendrimers were more difficult to purify. The excess EDA was removed by multiple washings using toluene/methanol in a 9:1 ratio. It was required to use excess EDA in order to synthesize the dendrimer that was desired. However, if it is not completely removed, it may lead to the formation of new dendritic centres through separate Michael addition reactions. These new dendritic centres are tough to purify out, because the difference in size between perfectly formed and imperfect dendrimers is very small. Therefore, dendrimers easily lose their monodispersed, and a high polydispersity will result.

During purification of dendrimers, it was necessary to ensure all EDA was removed. The excess EDA was primarily removed by rotary evaporation under pressure. However, there was still a trace of ethylenediamine detected in the ^{1}H NMR at 2.7 ppm. For complete removal of EDA, multiple washes were performed with a 9:1 azeotropic mixture of toluene and methanol.

Then was followed by a rotary evaporator to remove all solvent traces. Figure 3.1 shows ^{1}H NMR spectra obtained during purification.
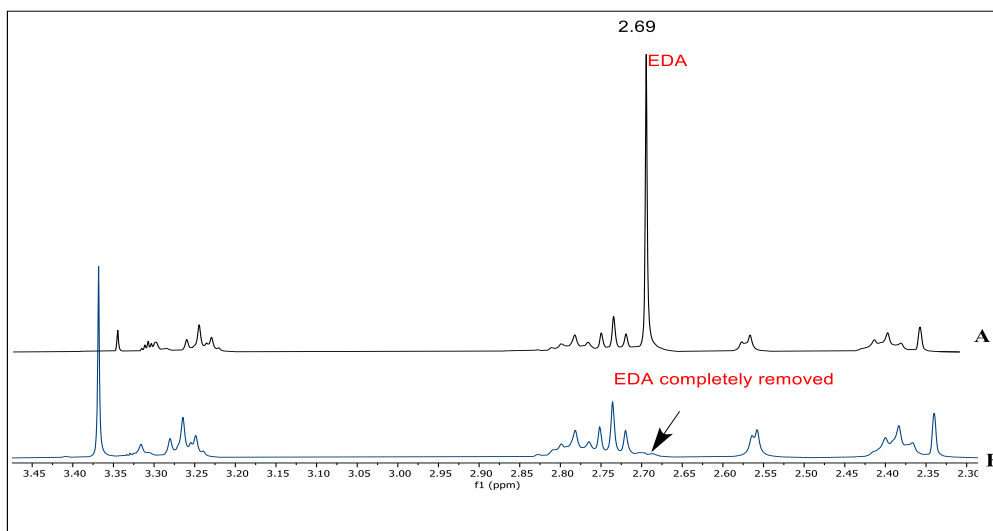
*Figure 3. 1: The ^1H NMR spectra taken during purification process of the G 1 PAMAM dendrimer in CD_3OD. **A**. spectrum before washing with Toluene: Methanol. **B**. spectrum after several washes with Toluene: Methanol.*

The azeotropic mixture is used because there are strong hydrogen bonds between the dendrimer and ethylenediamine (EDA). The hydrogen bond is usually competitively attacked by methanol. However, during evaporation, methanol is removed more quickly than EDA, which rebind to the H bonding sites. The use of toluene generates a higher boiling azeotrope that can compete with EDA and has higher boiling point than EDA. The new peak appeared in spectrum B at 3.37 ppm as a result of traces amount of methanol.

EDA hydrogen bonds to the dendrimer's interior
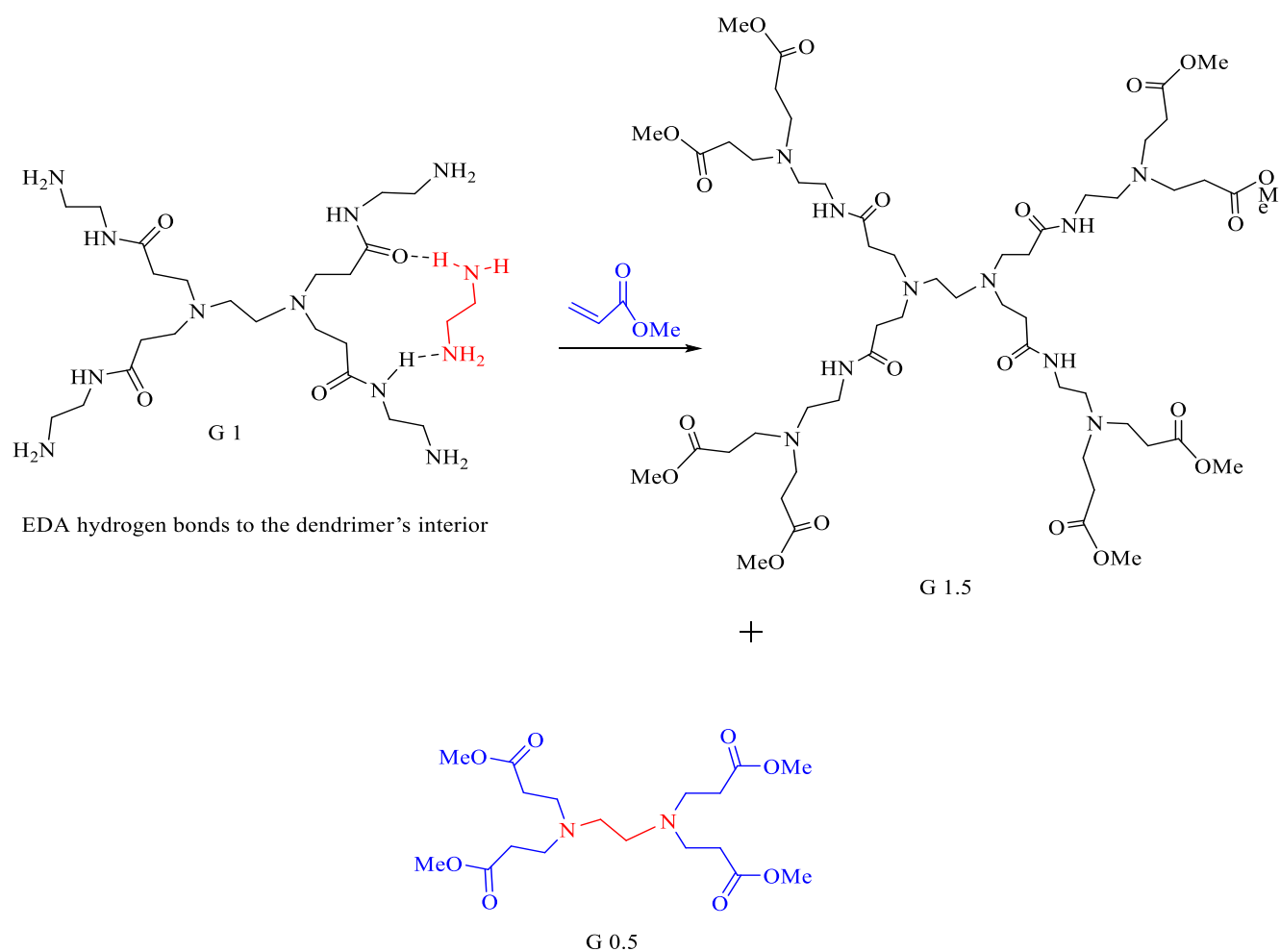
Scheme 3. 5: The incomplete removal of EDA and the by products

However, if the EDA is not completely removed, it will behave as a new initiator core, forming

undesired by-products as shown in Scheme 3.5. For example, in the case of generating G1.5

and G0.5 together, the two dendrimers are very difficult to separate because they are

structurally and physically similar. They are also hard to differentiate by ^{1}H ^{13}C NMR for this

reason, dendrimers will have a broad molecular weight distribution. An excess of EDA also

prevents other unwanted side reactions which lead to structural imperfections.[130] Possible

structural defects shown in Scheme 3.6.
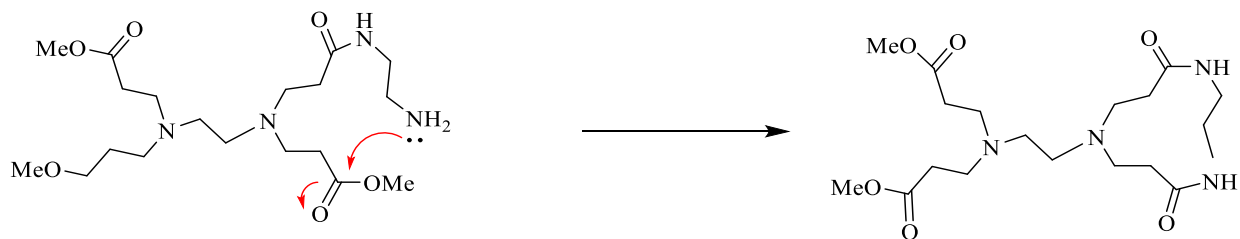
Intramolecular reaction(cyclazation)
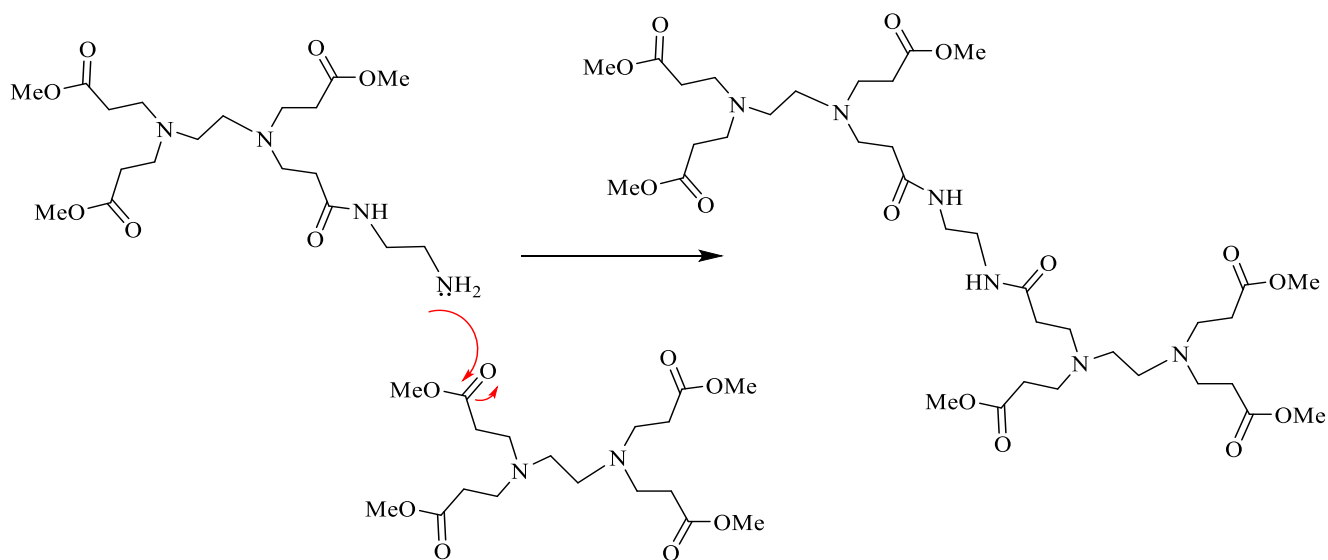
Intermolecular reaction(Dimer formation)

Scheme 3.6: Possible structural defects produced by the different side-reactions in PAMAM dendrimer synthesis

3.4. Characterisation of PAMAM dendrimers

The characterization of PAMAM dendrimers can be achieved in a variety of ways. One of the most useful methods is NMR spectroscopy, including ^{1}H and ^{13}C NMR spectroscopy as well as IR and MS spectroscopy. For ^{1}H NMR using the G 0.5 dendrimer as an example, there are four clearly defined proton environments Figure 3.2. It is believed that the singlet peak at 3.69 ppm represents methoxy protons. In addition, the two triplet peaks at 2.79 ppm and 2.43 ppm indicate the presence of two methylene proton groups in the dendrimer, while the core protons (EDA) peak at 2.54 ppm.
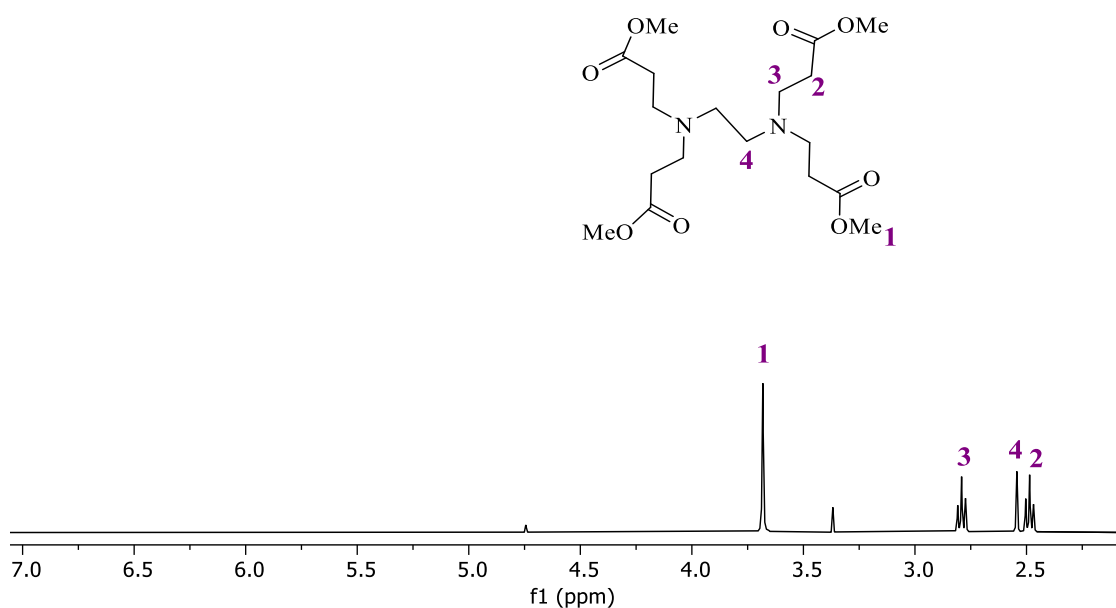
Figure 3. 2: ^{1}H NMR spectra for G 0.5 PAMAM dendrimer in CD₃OD. No remaining MA at alkene region

^{1}H NMR can also be used to distinguish full-generation dendrimers from half-generation dendrimers. All half-generation dendrimers possess a methoxy peak owing to ester groups at their periphery. In the spectra of dendrimers of full generation, this should no longer be observed since the esters have been converted into amide groups as shown in Figure 3.3.
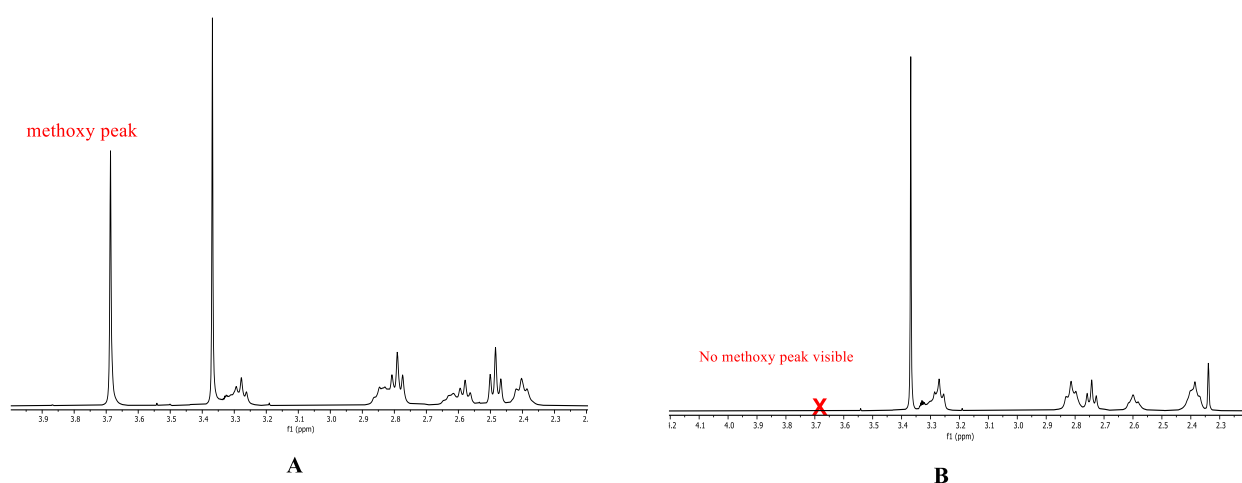
*Figure 3. 3: ^{1}H NMR spectrums show the distinguish between half (**A**) and full generation dendrimers (**B**)*

The dendrimers were also characterized by ^{13}C NMR. The spectrum of G 0.5 **1** indicated the ester carbonyl at 173.3 ppm, while at 174.3 ppm, the spectrum of G1.0 **2** corresponded to the amide carbonyl. Also, the carbonyl region showed two peaks in higher generations, corresponding to exterior and interior carbonyl environments. In all PAMAM dendrimers, they showed peaks between 52.4 and 32.2 ppm, indicating the presence of many C-N, C-C, and CH$_2$ proton environments.

Mass spectrometry can be particularly beneficial for analysing dendrimers and observing any structural defects. Structural defects of PAMAM dendrimer could develop due to the side reaction during the synthesis. [131,132] The defects could be the result of a retro-Michael reaction, which leads to an asymmetrical structure caused by the absence of arms. Additionally, it may be caused by dimer formation in the amidation step. An intramolecular cyclization could also occur due to EDA acting as a bifunctional reactant in the same step, and EDA residual may also act as a new core and make up a half-generation. A mass-related analysis obtained in mass spectroscopy shows that specific structural defects resulting from imperfect molecules differ from the ideal expected structures by a known amount of mass.

Electrospray ionisation mass spectrometry (ESI-MS) was used to analyse smaller generations (G0.5 – G2), where the molecular weight is less than 2500 g mol^{-1}. Whereas for large generation dendrimers (G 2.5 - G 4.5), matrix-assisted laser desorption ionisation (MALDI) was applied. Table 2 show mass spectrometry analysis data. Researchers have reported an increasing complexity of ESI mass spectra with increasing generations due to multiple charging phenomena produced during the electrospray process. [133] This is due to multiple charging phenomena induced by the electrospray process. The electrospray method induces multiple charging phenomena. In the case of PAMAM dendrimers of the third or higher generation, the ESI-MS is unable to detect multiple charging of molecules due to the unit resolution mass analysis.

Table 2: The molecular weight of PAMAM dendrimers (G 0.5-G3.5)

Dendrimer Generation	Molecular Formula	Terminal Groups	Calculated M_r (g mol^{-1})	Molecular Ion Peak (m/z)
G 0.5 **1**	$C_{18}H_{32}N_2O_8$	4	404	427
G1.0 **2**	$C_{22}H_{48}N_{10}O_4$	4	516	539
G1.5 **3**	$C_{54}H_{96}N_{10}O_{20}$	8	1205	1227
G 2.0 **4**	$C_{62}H_{128}N_{26}O_{12}$	8	1429	1428
G2.5 **5**	$C_{126}H_{224}N_{26}O_{44}$	16	2804	2809
G 3.0 **6**	$C_{142}H_{288}N_{58}O_{92}$	16	3256	3257
G 3.5 **7**	$C_{270}H_{480}N_{58}O_{92}$	32	6011	6054

The use of IR spectroscopy enables the determination of any changes to the structure of the PAMAM dendrimer based on its functional groups. For example, it is clear that half-generation dendrimers have been converted to full generation dendrimers, as the half generation dendrimers have an ester C=O stretch and an amide stretch for G 1.5 **3** and higher. However full generation dendrimers have a single amide stretches, IR data are shown in Table 3.

Table 3: IR PAMAM dendrimer data for all generations

Dendrimer Generation (G)	IR Stretch (cm^{-1})	
	C=O (ester)	C=O (amide)
G0.5 **1**	(1731)	-
G1.0 **2**	-	(1639)
G1.5 **3**	(1731)	(1645)
G2.0 **4**	-	(1637)
G2.5 **5**	(1732)	(1643)
G3.0 **6**	-	(1635)
G3.5 **7**	(1732)	(1642)

3.5. Synthesis of hydroxyl terminated PAMAM dendrimers

PAMAM dendrimers have been neutralized by converting the amine end groups into hydroxyl groups to make them less toxic. The DMSO solution of half generation PAMAM dendrimers was treated with ethanolamine and potassium carbonate. This reaction is similar to the EDA reaction, although, the reaction conditions were different from those for EDA substitution. The ester groups were converted into amides via an amination reaction, which resulted in hydroxyl-containing carbon chains (Scheme 3.6). Potassium carbonate was required because the tetrahedral intermediate needs to be deprotonated. Previously, for the EDA reaction, the terminal amine was basic enough to deprotonate the intermediate via favourable cyclic transition state. For ethanolamine, the terminal group is OH, and the oxygen is not as basic as nitrogen, which is why we added the base. All solid reagents were removed by filtering the crude product. A thick product was obtained, which was purified by multiple washings with acetone. It was then dissolved in a small amount of distilled water and precipitated in acetone to yield natural PAMAM dendrimer.
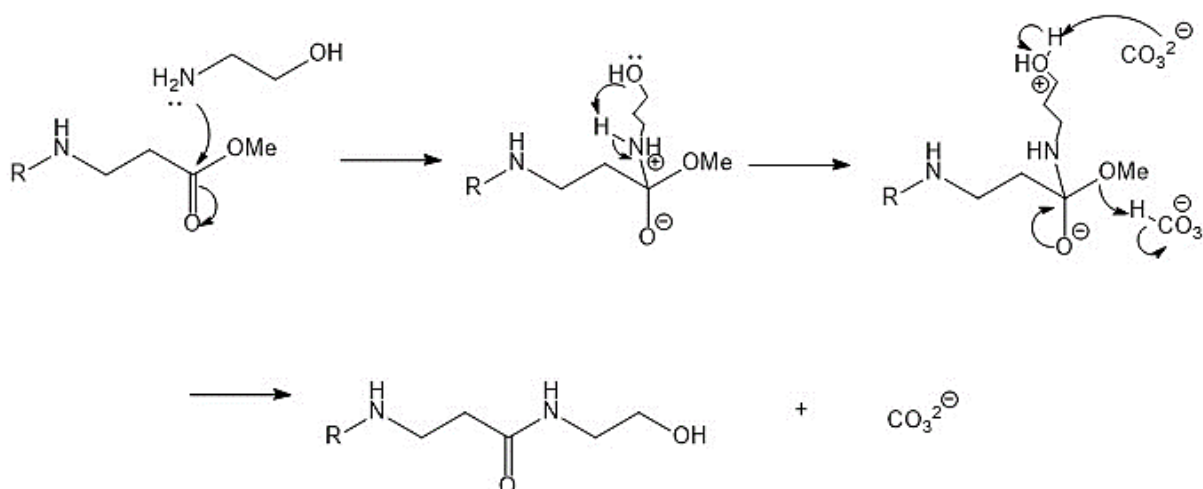
Scheme 3. 6: Mechanism of the Addition of Ethanolamine to obtain the hydroxyl terminated PAMAM dendrimers.

3.5.1. Characterisation of hydroxyl-terminated PAMAM dendrimers

Characterizing the hydroxyl-terminated PAMAM dendrimers was achieved using a variety of spectroscopic techniques. The ^{1}H NMR technique was most informative since the singlet corresponding to the methoxy protons in the esters no longer appear in the esters spectra after conversion as shown in Figure 3.4. Also, A new triplet peak for the methylene protons of ethanolamine was observed at 3.62 ppm. Compared to other methylene groups, these protons show higher chemical shifts due to their deshielding by the more electronegative oxygen atoms. The absence of peaks for ester groups on the ^{1}H and ^{13}C NMR spectra of PAMAM-OH indicates the reaction is complete.
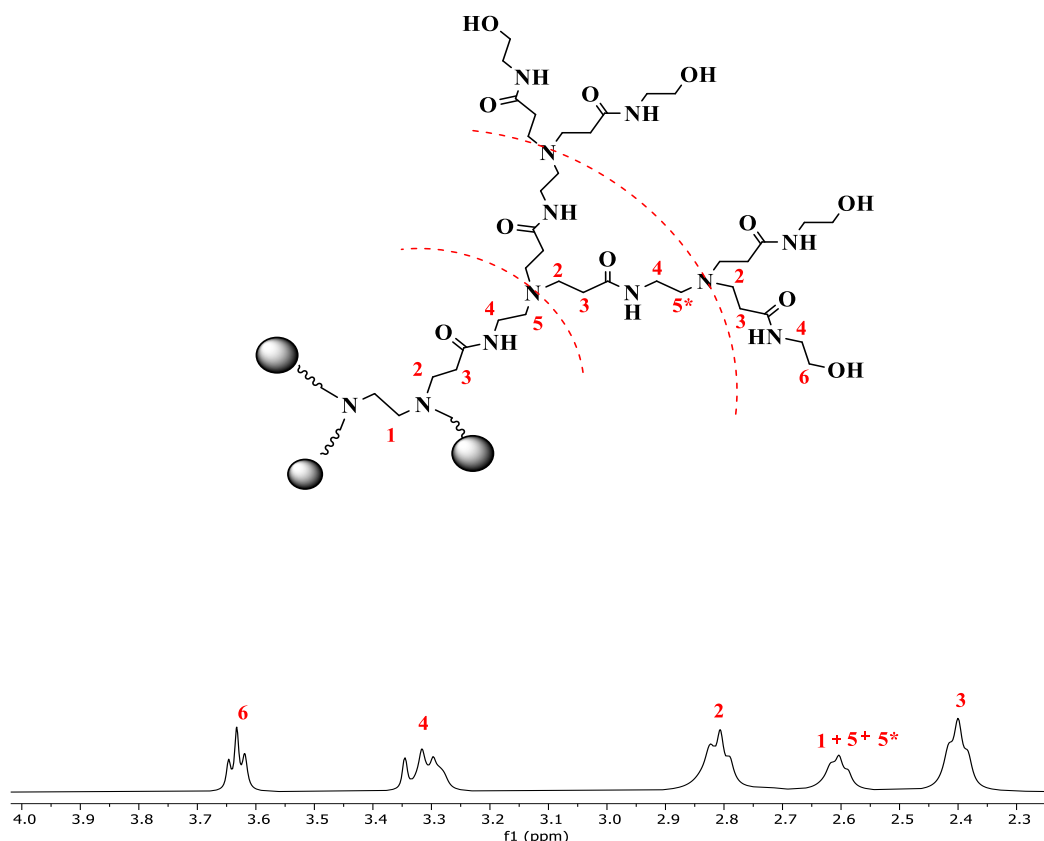
*Figure 3. 4: ^{1}H NMR spectra showing one arm of G3.0-OH **3***

Dendrimer Generation	Molecular Formula	Calculated Mr (g mol^{-1})	Number of OH ending groups	Molecular Ion Peak (m/z)
G1.0-OH **8**	$C_{22}H_{44}N_6O_8$	520	4	520
G2.0-OH 9	$C_{62}H_{120}N_{18}O_{20}$	1438	8	1438
G3.0-OH **10**	$C_{142}H_{272}N_{42}O_{44}$	3273	16	3272
G4.0-OH **11**	$C_{302}H_{576}N_{90}O_{92}$	6914	32	6940

In the ^{13}C NMR spectrum, we expected to observe additional peaks for new C-O environments. When compared with the ^{13}C NMR spectrum of G2.5 and G3.5, the neutral dendrimers possess additional peaks between 63.7 -52.34 ppm which are evidence of hydroxyl environments (C-O). It is evident from the IR spectra that the dendrimers with hydroxyl termini have a broad peak at 3272 cm^{-1}, indicating hydroxyl periphery groups, while an intense peak at 1640 cm-1 corresponds to amide carbonyl groups. It would be expected that no C=O stretch would occur at 1730 cm^{-1} if carbonyl to amide conversion is successful. For these neutralised molecules, we expect an amide stretch (~1600 cm^{-1}) and a broad OH stretch (~3000 cm^{-1}). The mass spectrometry was also used to analyse neutral dendrimers up to 32-OH. The mass spectrometry data are summarized in Table 4.

G2-8OH 9

G3-16OH 10

G4-32OH 11
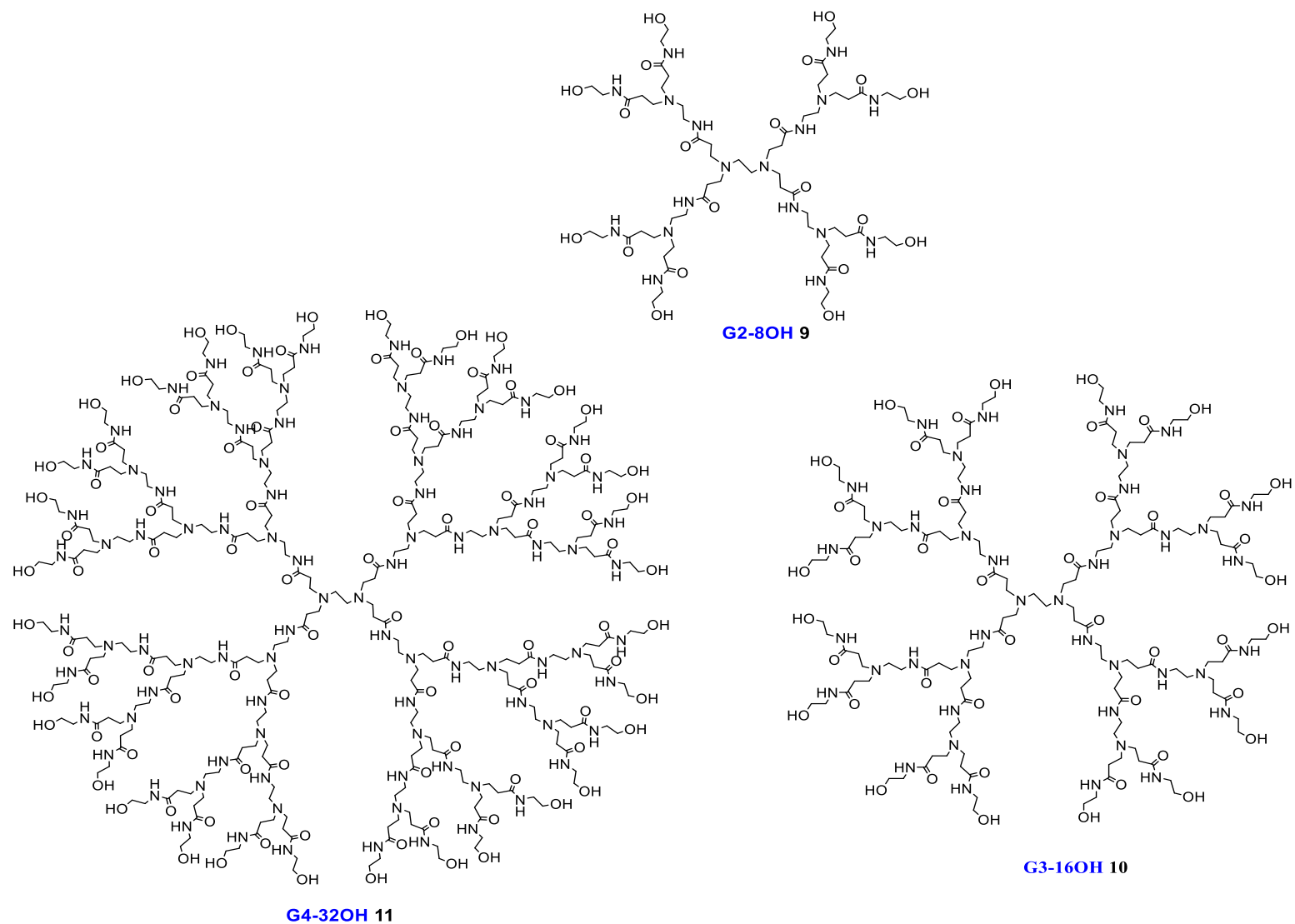
Figure 3. 5: Structure of neutral PAMAM dendrimer generations

3.6. Encapsulation of hydrophobic molecules with water soluble PAMAM Dendrimer

The primary aim of this project was to compare dendrimers and HBPs for drug delivery potential. Furthermore, we wanted to determine if HBPs can encapsulate and deliver drugs as effective as dendrimers. Our initial method simply involved calculating the amount of drug concentration in solution when dendrimers/HBPs were present versus when they were not. As the chosen drug must be at least partially water soluble, we can measure any improvement in solubility within a dendrimer or hyperbranched polymer, thus assessing the effectiveness of the polymer. According to previous work by the Twyman group,[118] acidic gust molecules are effectively encapsulated due to pH-dependent binding. Also, gusts with H-bonding groups could also be encapsulated. However, the best encapsulation involved guests with acidic and H-bonding groups. Neutral hydrophobic gusts were encapsulated less well. [129] In this study we chose Ibuprofen due to of its commercial availability and its structure. It has an acid group that can form salts or/and H-bonding with the dendrimers. Moreover, Ibuprofen is also UV-active, making it easy to calculate its solution concentration. The absorption peaks of ibuprofen are shown in Figure 3.6. As a first step in this analysis, a Beer Lambert plot was used to determine the extinction coefficient of Ibuprofen using the peak at 273 nm. As Ibuprofen is poorly soluble in water, methanol was initially used as the solvent. `
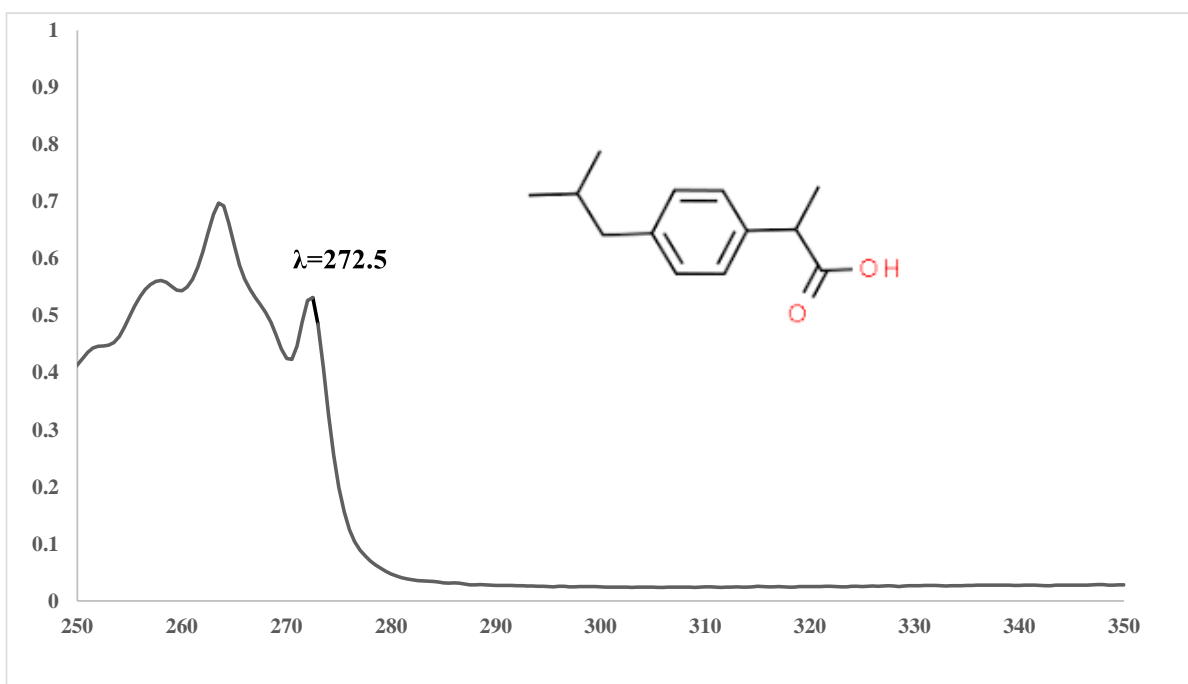
Figure 3. 6: The structure of ibuprofen and the λ max that will be monitored in encapsulation studies

The first experiment was designed to determine the maximum concentration of Ibuprofen in phosphate buffer (pH 7.4, 0.01M) without dendrimer. For all future dendrimer measurements, we subtracted this value to make sure we were only considering encapsulated Ibuprofen. This was achieved by dissolving excess Ibuprofen in buffer and removing solid residues by vacuum filtration. The absorption was measured using UV-vis absorption. Using this method and our Beer Lambert plot, the maximum saturated concentration of Ibuprofen was to be 7.72E-4 mol dm^{-3} . The characterisation of ibuprofen shown in Table 5.

Table 5: The characterisation of ibuprofen

Parameter	Ibuprofen
λ max (nm)	272.5
Extrintion cofficient	290 dm^3 mol^{-1} cm^{-1}
Solubility of ibuprofen in phosphate buffer	7.72x10^{-4} M

A co-precipitation technique was used to prepare the host/guest complex for the encapsulation experiments. Methanol was used to dissolve ibuprofen and dendrimer, and then methanol was removed using a rotary evaporator to give a coprecipitated complex. Then, buffer was added and any non-encapsulated or insoluble Ibu was filtered out. As the dendrimers are soluble in phosphate buffer, they are kept in solution alongside any encapsulated Ibuprofen molecules. A measurement of absorbance was taken for each complex. To compensate for any baseline drift, we calculated absorption values between 274 and 276 nm. This required us to re do the Beer lambert analysis using the same Δ Abs values. The results indicated that PAMAM dendrimer significantly improved the solubility of ibuprofen as shown in Figure 3.7 The final encapsulated ibuprofen concentration values were determined via equations (A and B) below.

A $\qquad [concentration \ of \ Ibuprofen] = \frac{Absorbance}{\varepsilon_{Ibuprofen}}$

B $\qquad [encapsulated \ Ibuprofen] = [\ Ibuprofen \ concentration\ ] - [Free \ Ibuprofen]$
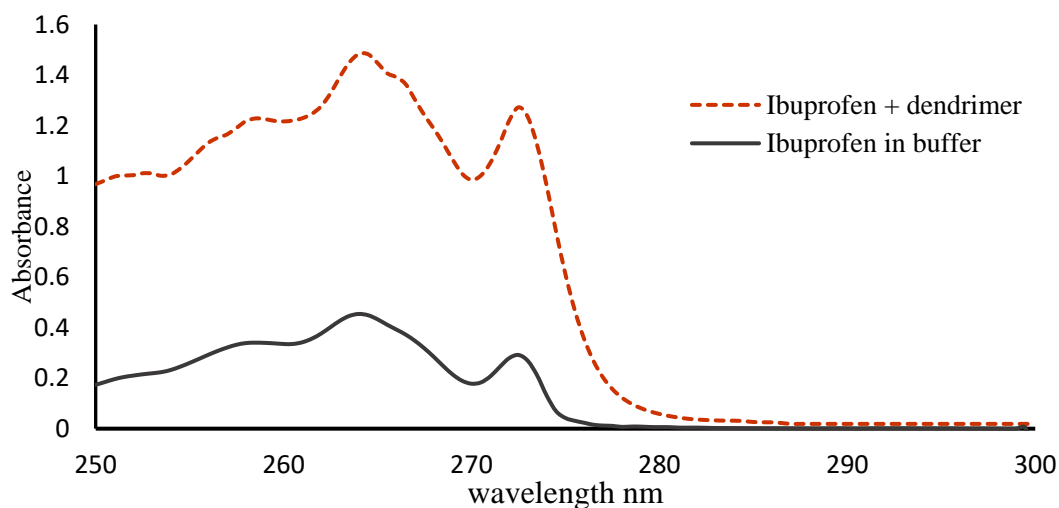
Figure 3. 7: UV-vis spectra show an improvement in solubility of ibuprofen after encapsulation in PAMAM dendrimer 1.0E-04 M using excess amount of ibuprofen (two-fold).

In order to assess the potential of the encapsulation methodology using neutral PAMAM-OH dendrimers, different generations of neutral PAMAM dendrimers were investigated specifically G2.0-8OH **9**, G3.0-16OH **10** and G4.0-32OH **11**. In the encapsulation experiment, PAMAM dendrimers at a concentration of 1.0E-04 M were used to encapsulate excess amounts of ibuprofen (two-fold). Then, by using Beer lambert analysis and the calculations described above, we determined the amount of ibuprofen encapsulated within each PAMAM dendrimer. The peaks observed were initially too strong indicating high levels of encapsulation and needed to be diluted by 10 times. The resulting UV spectrum can be seen in Figure 3.8. Using equation c, loading per dendrimer was calculated by dividing encapsulated Ibuprofen concentration by dendrimer concentration.

(C) $\qquad The\ loading\ per\ dendrimer\ =$

$[concentration\ of\ encapsulated\ Ibuprofen]\ /\ [Dendrimer\ concentration]$
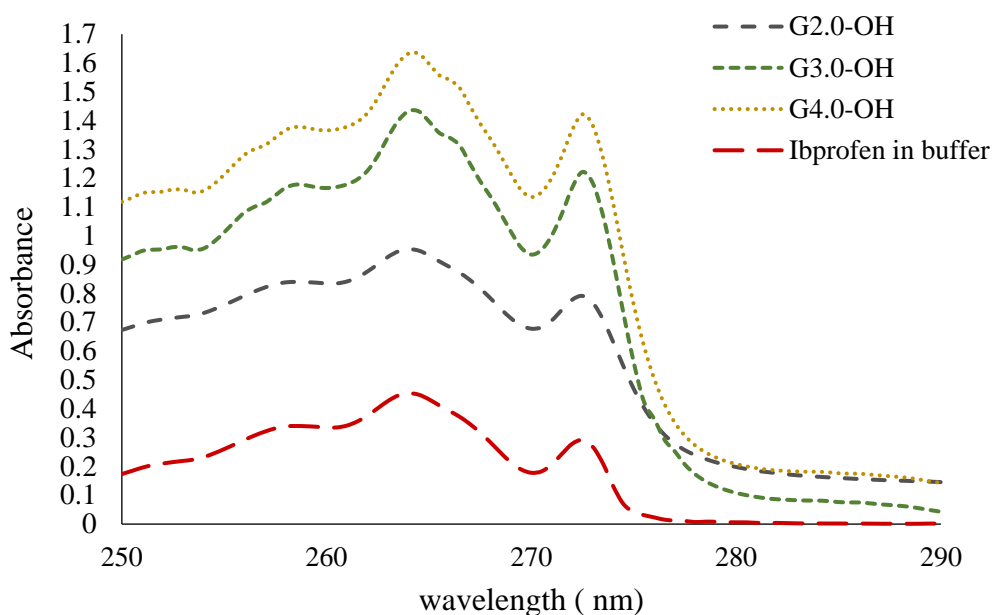
Figure 3. 8: UV absorbance data before and after encapsulation of ibuprofen in different generation of neutral dendrimer. Dilution by 10 times (control spectrum the red line shown in Not diluted)

Table 6: Analysis data of encapsulation of ibuprofen within PAMAM-OH (G 2.0-OH, G 3.0-OH and G4.0-OH).

PAMAM-0H generation	Δ Absorbance	[D] x10⁻⁴ M	[Total Ibuprofen] M	[Encapsulated Ibu] M	Loading per dendrimer
G2.0 **9**	0.037		1.25E-04	4.78E-04	5.0±0.37
G3.0 **10**	0.056	1.0E-04	1.96E-03	1.19E-03	12 ±0.53
G4.0 **11**	0.048		1.62E-04	8.51E-04	9.0±0.35
Maximum free ibuprofen concentration in buffer = 7.72E-04 M 10-fold dilution was needed to obtain the concentration. All data was obtained as an average of three experiments.					

Based on the data from Table 6 and Figure 3.9, it can be concluded that dendrimer size has an obvious influence on Ibuprofen solubility. The G2.0, with eight OH groups, could encapsulate five moles of ibuprofen. Furthermore, for the G3.0 with 16 OH groups, 12 moles of ibuprofen were encapsulated, while for the G4.0 with 32 OH groups, only 9 moles were trapped inside the dendrimer. The solubility of hydrophobic molecules in dendrimer solutions clearly depends upon the dendrimer generation. [124] The initial increase in solubility was due to an increase in the internal groups and the size of internal cavities available to interact with Ibuprofen molecules. Although dendrimer concentrations increase with dendrimer size, we expect to see a huge increase in loading for higher-generation G4.0-OH **11**, but there were only 9 moles loaded, which is lower than expected. This is due to steric crowding within the structure, which decrease the amount of organized space and lead to reducing binding. It was considered that G3.0-OH **10** to be the most suitable generation for encapsulating hydrophobic molecules. As a result of these findings, it was then investigated how dendrimer concentrations relate to drug encapsulation.
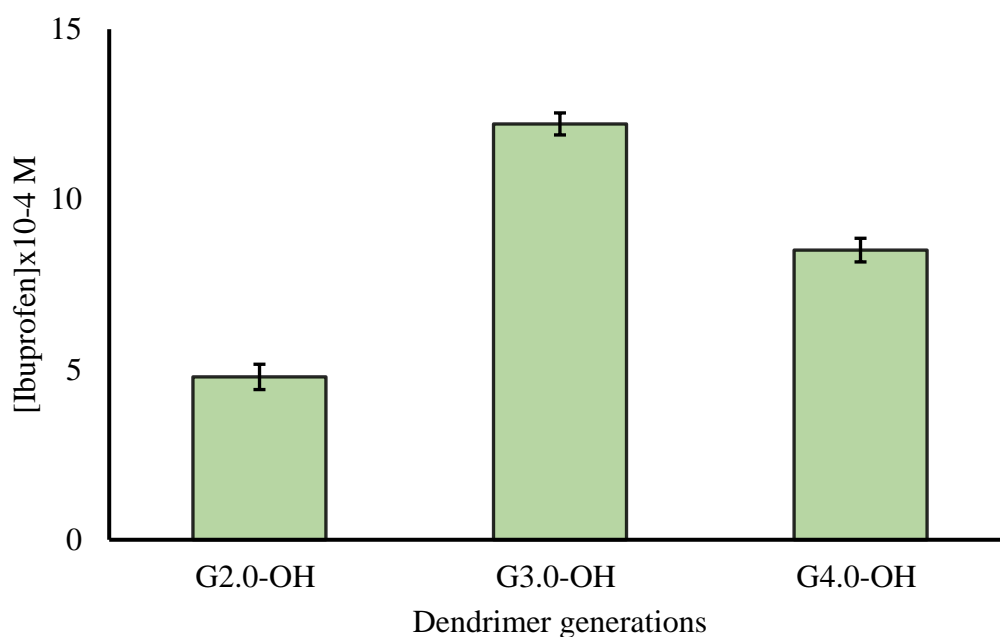
Figure 3. 9: Ibuprofen encapsulated in the different generations of PAMAM dendrimer

The next experiment was conducted to determine the effect of dendrimer concentration on loading and solubility of drug molecule. To achieve this, G3.0-OH PAMAM dendrimer with 16-OH groups was used in four different concentrations (1.0E-3, 1.0E-4, 1.0E-5 and 1.0E-6 M). Because the high generation (G4-OH **11**) is suffered from Dense packed which reduce cavities for hydrogen bonding, while G3. OH 10 was the optimal generation for encapsulating as discussed in above. In this experiment, we expect that the solubility of drug molecule in dendrimer solutions will be proportional to dendrimer concentration. To test these experiments were caried out using the same method used to calculate the maximum loading as previously described. To calculate the loading of ibuprofen in each dendrimer, we divided the encapsulated ibuprofen by the dendrimer concentration. The encapsulation data for different dendrimer concentrations are presented in Table 7.

*Table 7: The encapsulation of ibuprofen data in different concentrations of G3.0-OH **10**.*

Dendrimer concentration (M)	Δ- Absorbance (nm)	[Total Ibuprofen] M	[Encapsulated Ibuprofen] * M	Loading of ibuprofen per dendrimer
1.0E-6	0.0224	7.74E-05	1.800E-06	2±0.34
1.0E-5	0.0241	8.41E-05	6.96E-05	7±1.05
1.0E-4	0.0542	1.96E-04	1.2E-03	12±0.23
1.0E-3	0.0712	2.7E-04	1.9E-03	2±0.10
*Concentration of encapsulated ibuprofen after deducting freshly soluble ibuprofen in buffer 7.72E-4 M Concentration was obtained by dilution by 10-fold The data an average of three experiments				

The data summarised in Table 6 indicates that G3.0-OH **10** increase the solubility of ibuprofen linearly at lower concentrations (up to 1.0E-04 M). Above this concentration, the line is no longer linear Figure 3.10. In fact, the concentration dropped dramatically this could be due to self-association of dendrimers at higher concentrations. Furthermore, at concentrations (1.0E0-6 and 1.0E-05 and 1.0E-04 M), there was 2 ,7 and 12 equivalents of ibuprofen encapsulated

respectively. But just 2 equivalents of ibuprofen encapsulated at 1.0E-03. This is opposing to our prediction of higher loading at higher dendrimer concentrations.
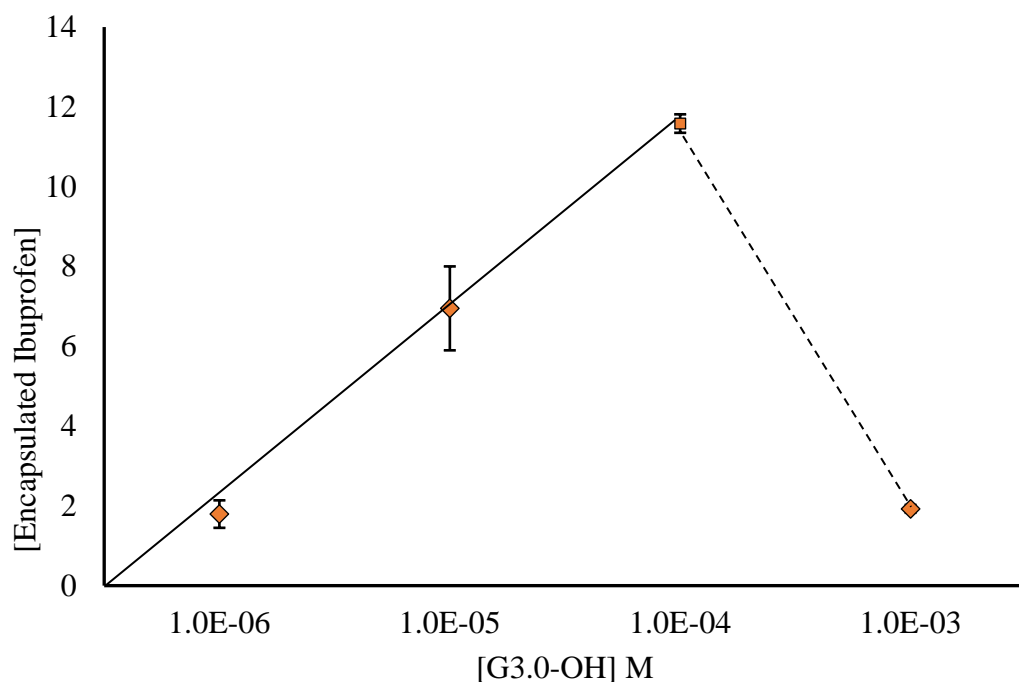
Figure 3. 10: The solubility of ibuprofen in different concentrations of G3.0-OH **10**

According to these results, we fine-tuned the study and looked at concentrations between 1.0E-4 M and 1.0E-03 M in order to explore the maximum loading of dendrimer during this stage. This was achieved by studying G3.0-OH in four different concentrations (2.50E-4, 5.0E-4, and 7.50E-4 M). The maximum solubility of ibuprofen inside G3.0-OH in shown in Table 8.

Table 8 : The solubility of ibuprofen G3.0 -OH dendrimer at concentration ranging from 1x10-4 to 7.5x10-4 M)

[G3.0-OH]	[Total Ibuprofen] M	[Encapsulated ibuprofen] M	loading per dendrimer
1.0E-4	1.86E-03	1.10E-03	10
2.5E-4	4.4E-03	3.6.20E-03	14
5.0E-4	8.62E-03	7.80E-03	16
7.5E-4	1.24E-02	1.20E-02	16
*Concentration of encapsulated ibuprofen after deducting freshly soluble ibuprofen in buffer 7.72E-4 M			

Ibuprofen solubility was 1.10E-03 M when dendrimer concentration was 1.0E-04M. When dendrimer concentration was 2.5E-04 M, we expect the solubility doubled, which was expected, but we expected 20 moles per dendrimer but were only able to load 14 moles. At dendrimer concentration of 5.0E-04 M we considered that should encapsulate roughly 60 moles of ibuprofen, however only 16 moles were encapsulated.
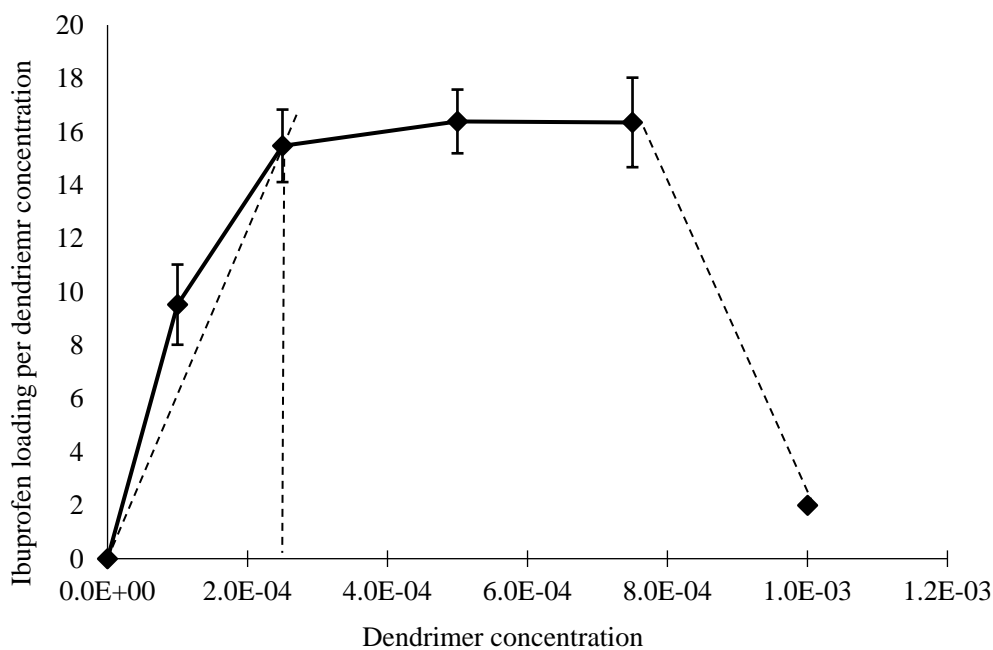
Figure 3. 11: An increase in G3.0-OH dendrimer concentration leads to increased ibuprofen solubility then plateaued.

Looking at the Ibuprofen concentration versus dendrimer concentration plot in Figure 3.11, it was evident that linearity had been broken at ~ 2.5E-4 M. It is possible that it is due to aggregation. This would reduce the space inside the dendrimers and limit the availability of functional groups due to interactions with other dendrimers.
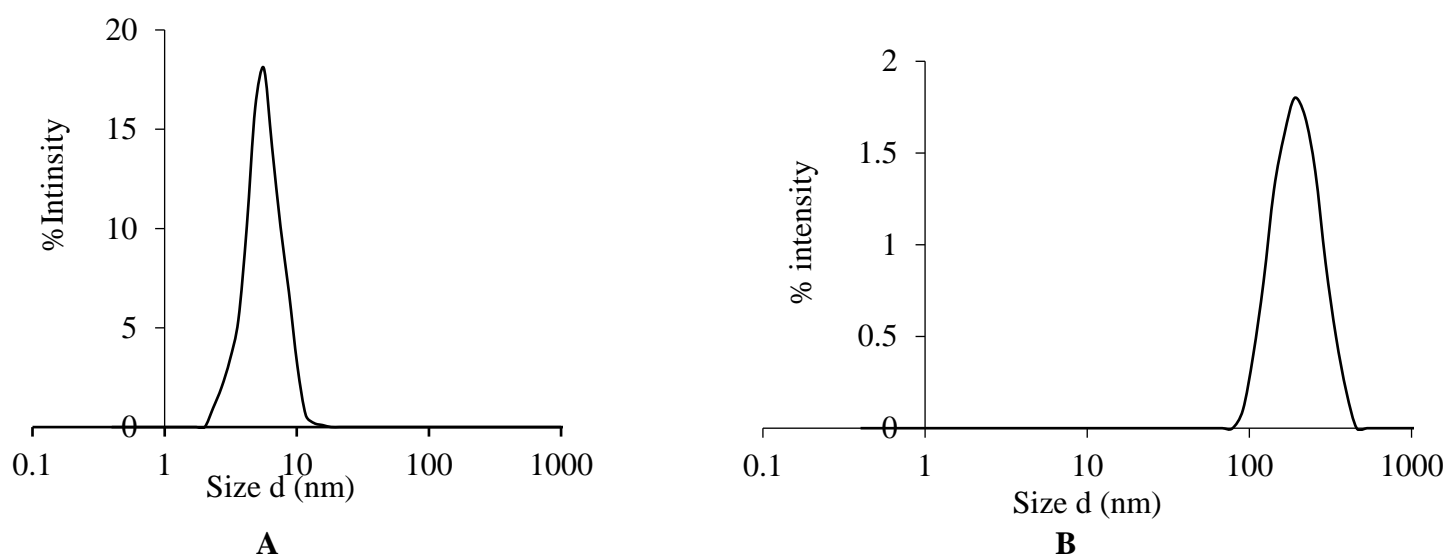
*Figure 3. 12: DLS data for G3. OH showing (**A**) dendrimer at concentration 1.0E-04 M (non-aggregated). (**B**) dendrimer at concentration 3.0E-04 M (aggregated).*

A light scattering (DLS) test was conducted to measure the size distribution for G3.0-OH at 1.0E-04 M and 3.0E-04 M, it was done in PBS pH 7.4 at 25 °C. PAMAM dendrimer G3.0-OH at a concentration 1.0E-04 M showed a very small particle size ~ 5 nm, indicating a non-aggregated structure. However, the PAMAM dendrimer at 3.0E-04 M aggregated into large species (200 nm) as shown in Figure 3.12. This could explain the reduction in encapsulation ability as concentration increases.

It is known that small molecule drugs (less than 1 nm) that are administered through the systemic route usually have a short time-to-circulation due to the rapid renal excretion mechanisms and are permeable to the whole body due to rapid extracellular transport. On the other hand, larger nanoscale therapeutics (more than 4 nm) can exhibit longer circulatory residency times, size-selective excretion modes and permeability patterns related with their nano-scale size and surface chemistry. [68]

In drug delivery the particle size that can promote accumulation in tumours should has hydrodynamic diameters above 100 nm, which may be optimal for tumour accumulation. As the vasculature within tumours is heterogeneous and abnormal, these nano particles can accumulate in tumours as the leaky vessels enable NP extravasation, this a phenomenon referred to the enhanced permeation and retention (EPR) effect. [134]

Additionally, NPs that are too small (less than 30nm) may not be capable of driving membrane wrapping enough to activate endocytic processes. [135] Multiple studies report good cellular uptake and intracellular delivery when particles ~50nm in diameter are used. [135,136,137]

3.7. Stability of the drug dendrimer complexes

As always, the co-precipitate method was used to prepare dendrimer–drug complexes for all dendrimer generations. Samples were kept in amber-coloured and colourless glass vials to achieve dark and light conditions, respectively. The samples were stored at room temperature for a period of 10 days in phosphate buffer at pH 7.4. Samples were analysed initially and then periodically every three days for any precipitation, turbidity, change in consistency and increase in drug loss. The dissociation rate of drug was indirectly determined by measuring the rate at which its concentration decreased. A total of five data points were analysed during a 10-day period using UV-vis spectroscopy. To determine Ibuprofen stability in the complex, the absorbance at 273 nm was monitored over time. The study was performed to determine the effect of dendrimer size on complex stability.
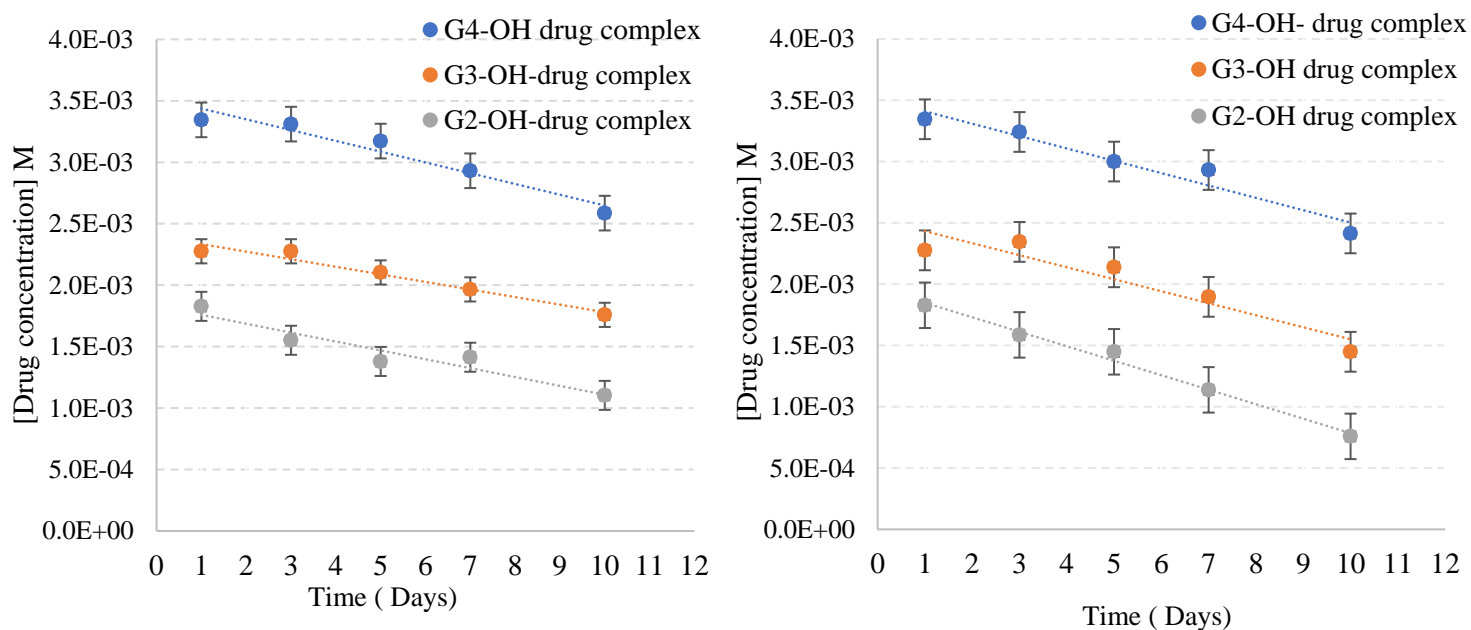
Figure 3. 13: Stability study for OH-PAMAM dendrimer- drug complexes in (Left) Dark storge and (Right) Light storge for 10 days.

To calculate the rate of dissociation the concentration of drug was obtained via divided the absorbance by extinction coefficient. Then the rate was obtained through the gradient (equation plot) and shown in Table 9.

Table 9: Rate of dissociation drug from complex in dark and light

Complex generation	Rate of dissociation in Dark mol/day	Rate of degradation in Light mol/day
G4-OH-Ibu complex	-5.00E-05	-1.0E-04
G3-OH-Ibu complex	-5.40E-05	-1.0E-04
G2-OH-Ibu complex	-5.20E-05	-1.0E-04

It is demonstrated that ibuprofen interacts with nitrogen atoms in the PAMAM cavity via hydrogen bonding or electrostatic interactions. Drug dendrimer complexes are stable at physiological pH for all generations based on the degradation rate. However, the graphs in Figure 3.13 show the rate is slightly faster in the light (1.0E-04 M Day^{-1}). In addition, all generations are slower in the dark (5.0-E-05 M Day^{-1}). It is likely that this was due to ibuprofen's hydrophobicity, which allows it to remain stable. [138]

Dissociation of the drug from the dendrimer complex occurs as a result of the release of the drug from the complex due to hydrogen bonding breaks. Despite of Ibuprofen's hydrophobicity allows it to remain stable in the complex. However, hydrogen bonding breaks cause the drug to be disassociated from the dendrimer, leading to drug releases into the solution. This process is faster in light, likely due to light providing more energy to the system, which increases the dissociation rate.

3.8. Summary

Three hydroxyl PAMAM dendrimers were synthesized and investigated for their ability to encapsulate small hydrophobic drug at 1.0E-04 M. The G3-OH was found to be the optimum generation size to encapsulate drug molecules. The encapsulation study was conducted to investigate the effect of concentration of dendrimer concentration on drug encapsulation. There was a significant impact of concentration on encapsulation, as discussed in Section 3.9 (pages 62-65). The aggregation was confirmed by DLS, which revealed a large hydrodynamic radius ~ 250 nm at dendrimer concentration 3.0E-04 M. The stability study of drug -dendrimer complexes revealed that were more stable in dark condition than in light. Despite dendrimers being monodispersed and having perfect structure. However, these generations exhibit increased stability and are capable of retaining the drug molecule in their internal cavities due to non-covalent interactions between the drug and the dendrimers. This caused the drug to release more slowly or to remain in the internal cavity of the dendrimer. On the other hand, the smaller generation would be less affected by strict hindrance, resulting in a greater amount of drug molecules encapsulated. Due to this, the ability of small generation dendrimers to hold the guest drug molecule within the dendrimer interior cavity is limited, this led to the ease of drug release.

Chapter 4 : Encapsulation of free base porphyrins and metal porphyrins within dendrimer for possible application to photo dynamic therapy

4.1. Introduction

Work in this chapter is to determine the effect of metal coordination (with the dendrimer internal is amins) on the encapsulation efficiency. Our research group has previously studied a Zn TPP, but the loading was extremely poor. [115] There is a possibility that low encapsulation could be explained by insolubility of Zn TPP during the encapsulation process, which required solubility in methanol. To address this problem of insolubility we proposed to use tetra hydroxyphenyl porphyrin (Zn TDHPP), whose 8-OH groups should produce some solubility in methanol.

Porphyrins are commonly synthesized by reacting pyrrole with an aldehyde of choice in stoichiometric amounts. It was known that porphyrins are UV-active molecules, and their Spectroscopy absorption ranges between 400-600 nm, depending on whether the porphyrin is β- or meso substituted.[139]

4.2. Synthesis of Tetrakis (3, 5-dihydroxyphenyl)-porphyrin (TDHPP)

The synthesis of TDHPP **13** was carried out in a two-step reaction, as illustrated in Scheme 4.1. In the first step, 3,5-methoxybenzaldehyde and pyrrole are reacted in refluxing propionic acid for 45 minutes to produce tetrakis (3,5-dimethoxyphenyl)-porphyrin (TDMPP) **12**. The second step, preparing Tetrakis (3, 5-dihydroxyphenyl)-porphyrin, was performed by the demethylation of TDMPP **12** using boron tribromide as the demethylation agent.
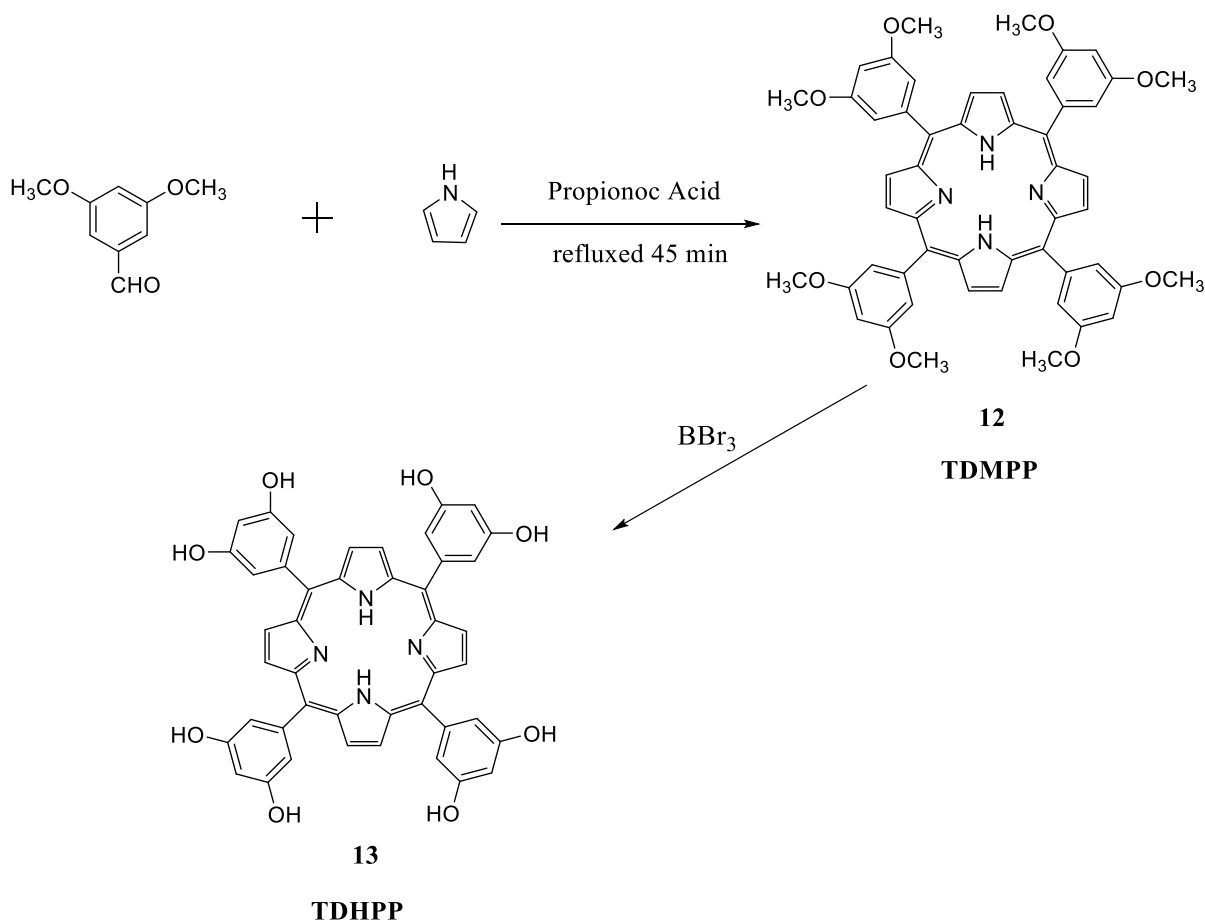
*Scheme 4. 1: The synthesis of Tetrakis (3, 5-dihydroxyphenyl)-porphyrin (TDHPP) **13***

In the first step, the successful synthesis of TDMPP **12** was confirmed in the UV spectrum by observing the porphyrin Soret band at 420 nm and four Q-bands at 513 nm, 548 nm, 586 nm and 643 nm. The ^{1}H NMR spectrum also showed a large singlet at 3.98 ppm for methoxy protons and a peak at -2.9 ppm for porphyrin nitrogen protons. Additionally, mass spectrometric analysis of methoxy porphyrin detected a molecular ion peak at 855.

In step two, TDHPP **13** was prepared by dissolving methoxy porphyrin (TDMPP) **12** in anhydrous dichloromethane and stirring under nitrogen for ten minutes, then adding boron tribromide dropwise, which turned the solution green. This reaction was conducted at room temperature under nitrogen with stirring for 6 hours, then it was quenched with distilled water.

The reaction mixture was then neutralised with sodium hydrogen carbonate solution and extracted with ethyl acetate. The product was highly soluble in methanol and dichloromethane, but insoluble in water, whereas the starting material (TDMPP) **12** was soluble in water.

The ^{1}H NMR spectroscopy confirmed the successful synthesis of the compound, there was no longer a visible peak for methoxy at 3.98 ppm. Additionally, the peak at 8.96 ppm corresponds to the pyrrolic *β*-H of the porphyrin ring. Two peaks were detected at 7.06 ppm and 6.70 ppm related to the resonances of phenylic protons (*ortho* and *para*, respectively). A Further signal was observed in the low field region of 9.72 ppm, which corresponded to the phenylic OH protons. The inner pyrrolic N–H proton resonance of TDHPP **13** was observed in the highest field region (-2.9 ppm) due to strong shielding. The UV spectrum showed strong absorption at 418nm corresponding to the Soret band. There were also four Q bands seen at 520 nm, 560 nm, 595 nm, and 655 nm. The product was further confirmed by mass spectroscopy analysis, showing a peak at 743, and by FT-IR analysis, showing a broad peak at 3420 cm-1 indicating phenylic OH groups. The next step was encapsulation of TDHPP **13** within the dendrimer; to monitor the encapsulation process and calculate the increased concentration of TDHPP, we monitored the peak ~418 nm shown in the UV spectrum Figure 4.1.
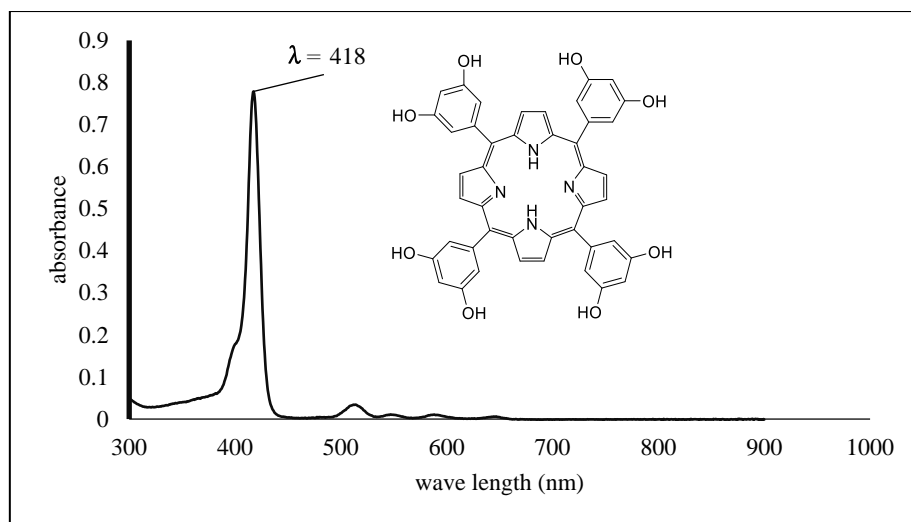
Figure 4. 1: The UV-vis spectrum of TDHPP in methanol. This peak will be monitored during encapsulation study.

4.2.1. Encapsulation of Tetrakis (3, 5-dihydroxyphenyl)-porphyrin (TDHPP) within hydroxyl dendrimers

The encapsulation was performed to study the ability of dendrimer to solubilise hydrophobic photosensitiser (TDHPP) **13**. In this study, the encapsulation results will be used as a control for the metal coordination study in the next section. The encapsulation efficiency was also investigated based on dendrimer size. The co-precipitate method was used with 1.0E-04 M PAMAM-OH, G2.0-OH, G3.0-OH, and G4.0-OH in methanol as previously described. The concentration of (TDHPP) **13** was calculated using its maximum absorbance (Sort band) and, the molar absorption coefficient (ε) and correcting for any dilutions and inherent solubility in PBS Buffer pH 7.4. The molar extinction coefficient for (TDHPP) was obtained graphically from a Beer-Lambert plot and found to be 9091 dm^3 mol^{-1} cm^{-1}. The resulting UV-vis spectrum is shown in Figure 4.2 and Table 10.

Table 10: The Characterisation of TDHPP 13

Parameter	TDHPP
λ max (nm)	418
Extrintion cofficient	9091 dm^3 mol^{-1} cm^{-1}
Solubility of ibuprofen in buffer	6.82E-07 M
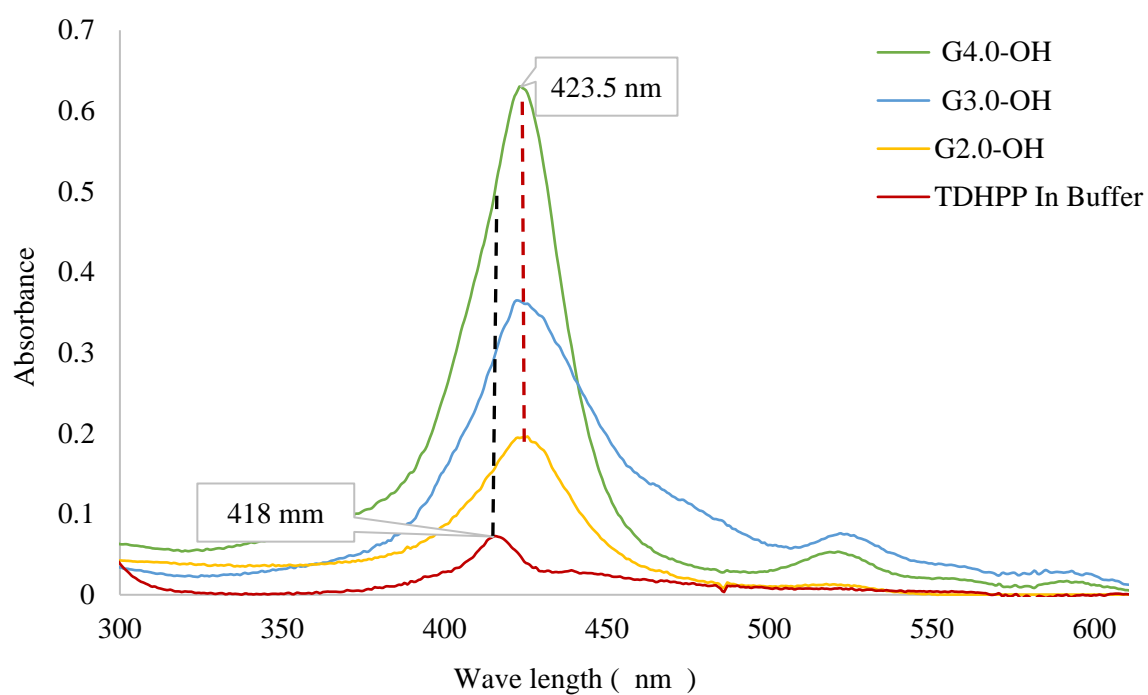
Figure 4. 2: The UV absorbance data before and after encapsulation of TDHPP (excess amount-3 fold) 13 in different generations of PMAMA-OH at 1.0E-04 M . The spectra of encapsulated porphyrin show a small shift to longer wavelength.

*Table 11: Analysis of the encapsulation of tetrakis (3, 5-dihydroxyphenyl)-porphyrin (TDHPP) **13** in PAMAM-OH*

Dendrimer generation	Absorbance	[Average total TDHPP] M	[Average encapsulated TDHPP] M	Loading /dendrimer
G2.0-OH **9**	0.20	1.91E-05	1.90E-04	2.0±0.30
G3.0-OH **10**	0.36	4.18E-05	4.18E-04	4.0±0.41
G4.0-OH **11**	0.64	7.66E-05	7.66E-04	8.0±0.73
Free TDHPP in buffer 6.82E-07 M The molar extinction coefficient 9091 dm^3 mol^{-1} cm^{-1}. Dendrimer concentration 1.0E-04 M				
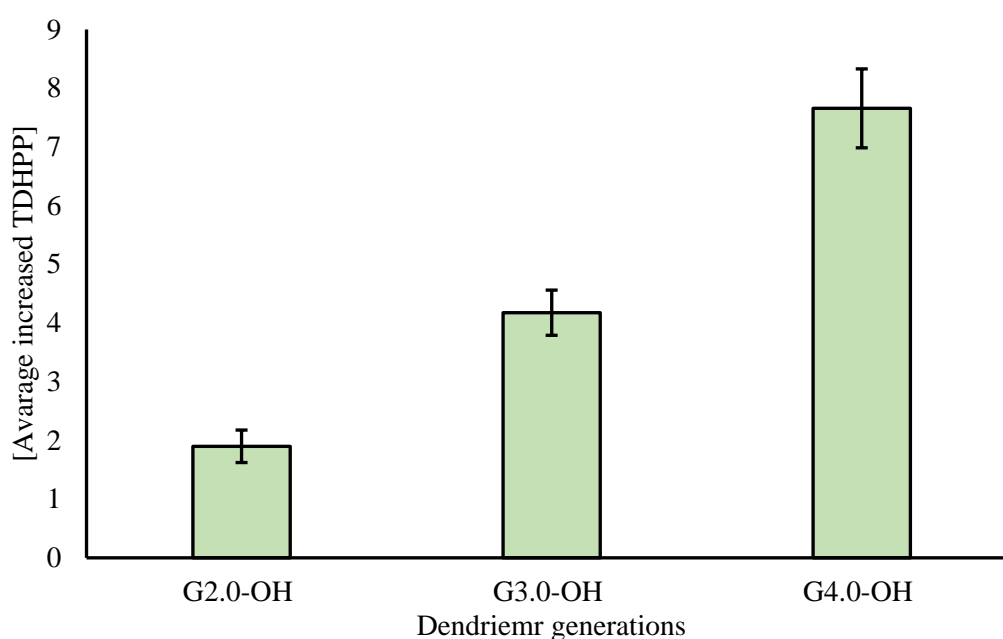
Figure 4. 3: The average increased concentration of TDHPP 13 in PAMAM dendrimer generations

It is clear from the above results that dendrimer size generation affects TDHPP solubility. It can be seen in Figure 4.3 that the solubility of dendrimer increases with increasing dendrimer size. The generation G2.0 with eight OH groups could encapsulate two TDHPP into the dendrimers' hydrophobic void. In addition, four moles were encapsulated for the G3.0 with 16

OH groups. For the G4.0 with 32 OH groups, eight moles of TDHPP were encapsulated inside the dendrimer. The low loading for smaller dendrimers could be attributed to the lack of organised structure. In fact, this is a well-known effect and is related to the lack of a densely packed structure for these small dendrimers. [140] In this case the encapsulated TDHPP concentration was increased with increasing in the dendrimer generations, which is unlike the results observed with Ibuprofen encapsulation. It could be because the TDHPP is bigger molecule and interact strongly with inner amines, as the G4.0-OH has more tertiary amines. In a Figure 4.2, the absorption of TDHPP in buffer was at 418 nm. However, after encapsulation λ max shifted to 423.5 nm for all dendrimer generations. This indicates that the binding environment inside the dendrimer is different to bulk water. It is known that the internal tertiary amines are basic and could be protonated. These basic amines can therefore deprotonate the phenolic groups, which can be stabilized by resonance. Once this happens, an ion-pair can form ($R_3N^{\oplus}H + O\text{-}R$) which increases bindings a secondary interaction to support any hydrophobic binding. In addition, the phenolates will perturb the aromatic structure of the porphyrin, result in a shift of λ max.
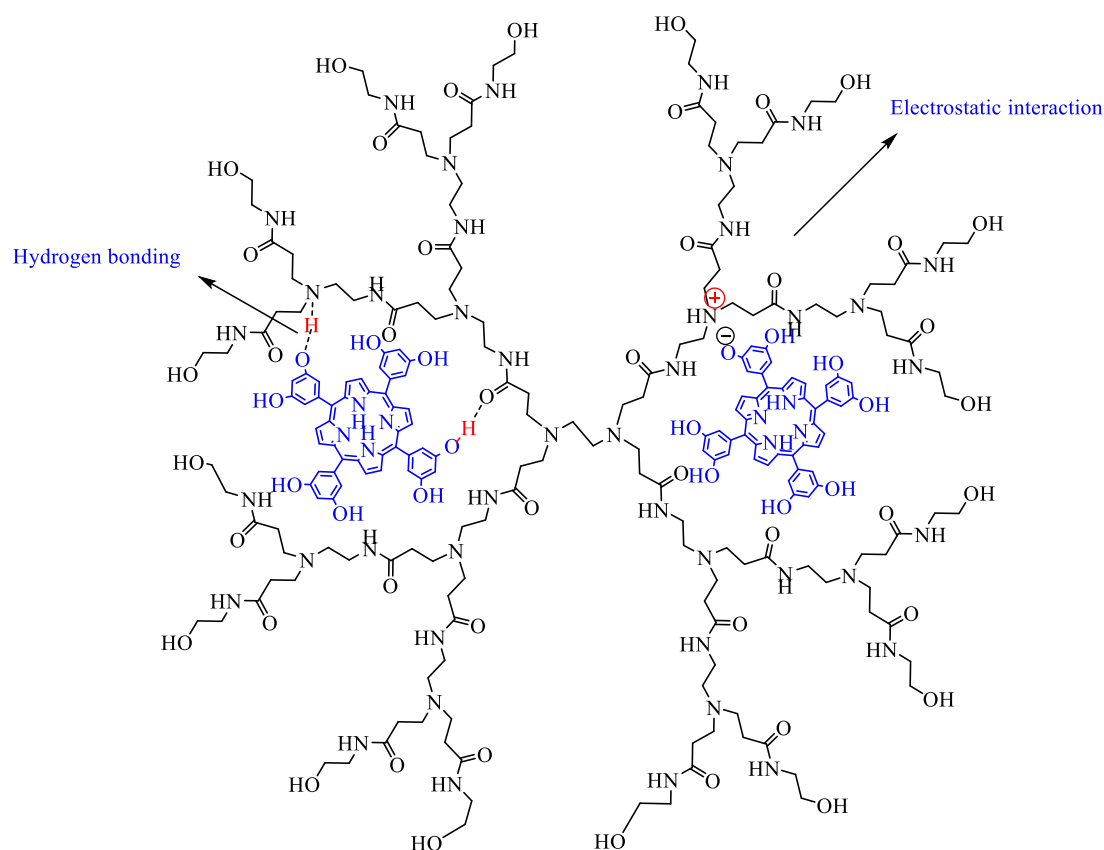
Figure 4. 4: The possible encapsulation via hydrogen bonding and electrostatic/acid base interactions between dendrimer and TDHPP

4.3. Synthesis and characterization of the zinc metalated porphyrin (ZnTDHPP)

Having studied the hydrophobic and electrostatic/acid base interactions by encapsulating TDHPP in dendrimer hydrophobic cavities. we aimed to maximize interactions coordination. As such the porphyrin (TDHPP) was metalated by adding zinc acetate in dichloromethane and methanol as illustrated in Scheme 4.2. The reaction was carried out for 45 min at room temperature. The evidence of the complete metalation of the porphyrin macrocycle cavity was also proved by ^{1}H NMR. The absence of a peak at high field - 2.9 ppm (NH) indicates that the macrocycle void is now occupied by a metal. Mass spectrometry confirmed insertion of zinc with a molecular ion peak detected at 806 (MH[+]).
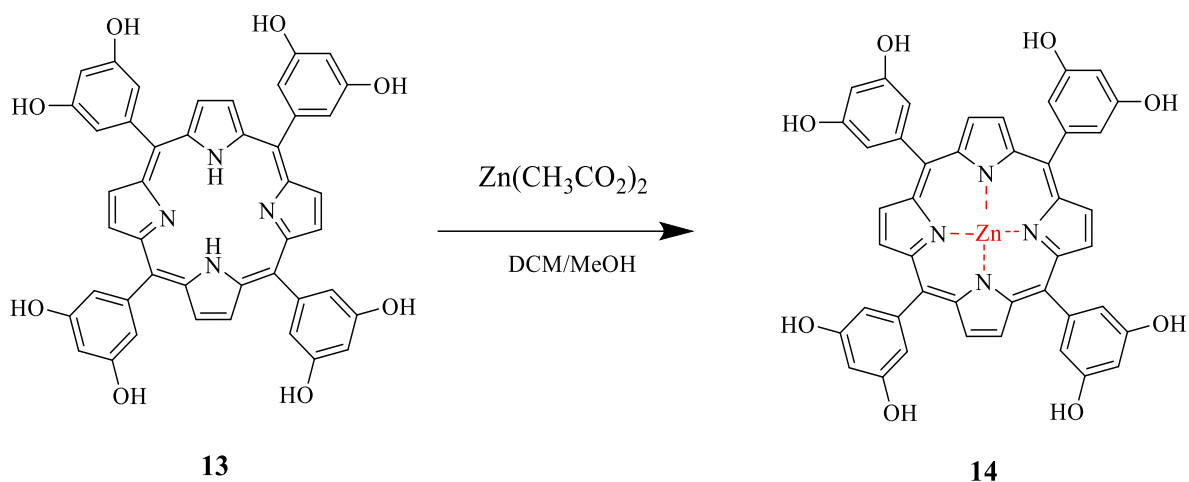
Scheme 4. 2: Synthesis of Zinc Tetrakis (3, 5-dihydroxyphenyl)-porphyrin (ZnTDHPP)
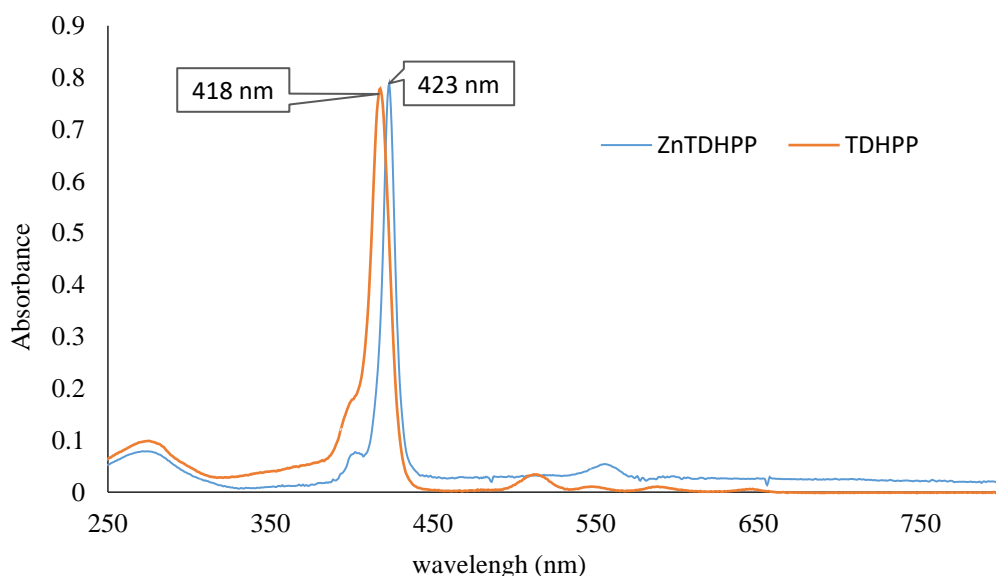
Figure 4. 5: The UV-vis spectrum Zn TDHPP and TDHPP in methanol

The UV-Vis spectrum indicated that there is a clear difference between bands of free-base and metalated porphyrins. ZnTDHPP **14** exhibits the Soret band at 423 nm, which is shifted from that of free base TDHPP **13** at 418. In addition, only two Q bands are observed at 560 and 596 nm instead of four as shown in Figure 4.5, which is typically indicative of metalated porphyrins. Following this, ZnTDHPP **14** was encapsulated by PAMAM dendrimers via coordination.

4.3.1. Coordination of ZnTDHPP 14 with PAMAM dendrimer

The encapsulation of ZnTDHPP was identical to those used for encapsulation TDHPP. As a pre-encapsulation step, the extinction coefficient of Zn TDHPP in methanol was obtained using a Beer Lambert plot (ε Zn TDHPP = 37356 dm3 mol^{-1} cm^{-1}). The maximum concentration of Zn TDHPP in phosphate buffer was 7.76E-6 mol dm-3. All measurements were analysed using UV-VIS spectroscopy. For monitoring the encapsulation procedure and to calculate the encapsulated concentration of Zn TDHPP, the peak at ~ 423 nm was monitored in the UV spectrum as shown in Figure 4.6.
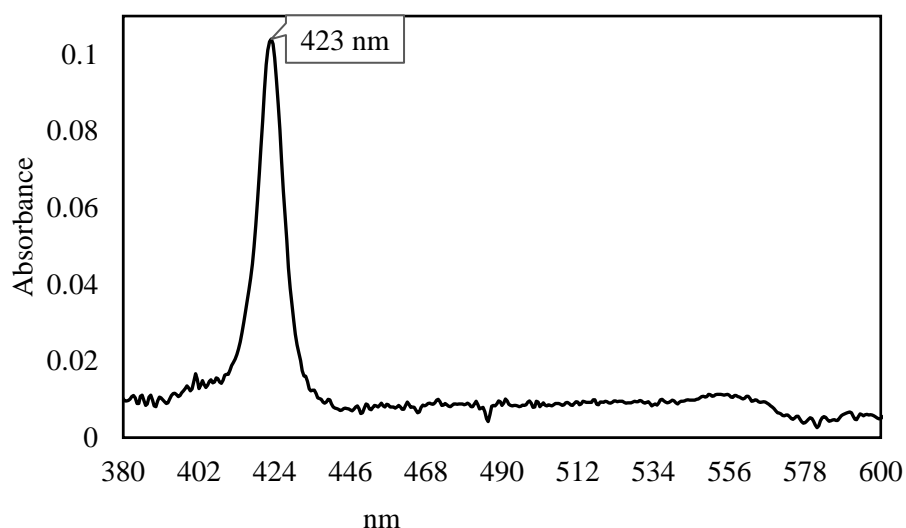
Figure 4. 6: The UV-vis spectrum of Zn TDHPP 14 in phosphate buffer pH 7.4, 0.01 M, which shows Sort band at 423 nm
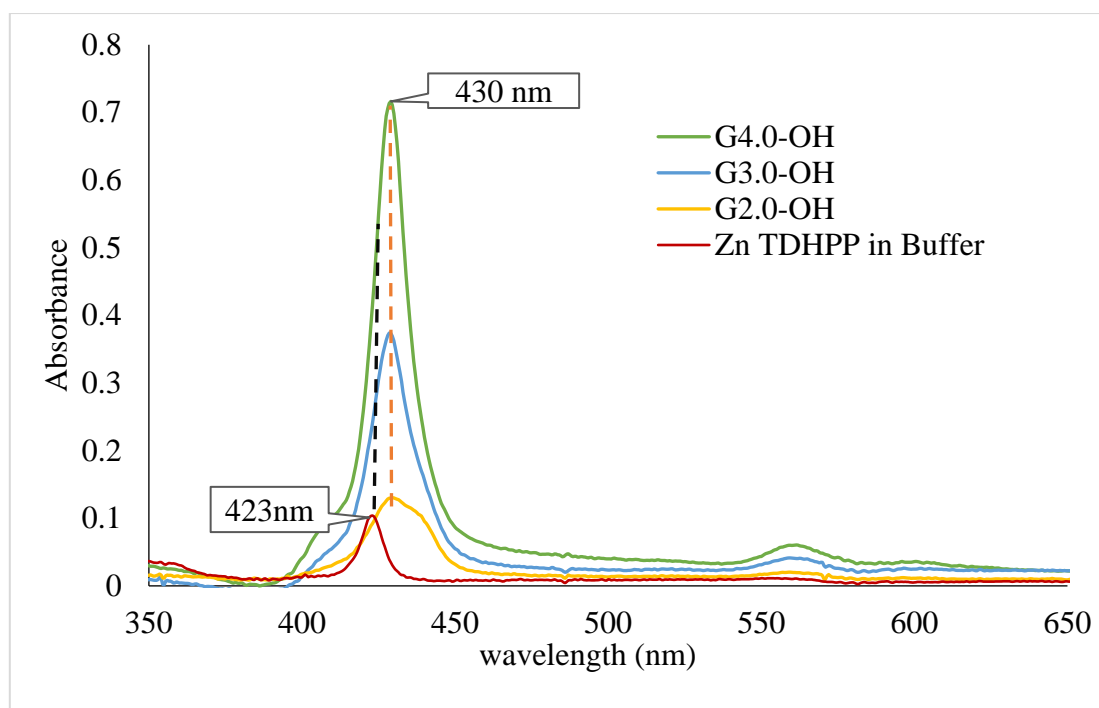
*Figure 4. 7: The UV-vis spectrum showing the absorbance of Zn TDHPP **14** before and after encapsulation*

*Table 12: The encapsulation of Zn TDHPP **14** in phosphate buffer pH7.4 within PAMAM dendrimer generations*

Dendrimer Generation	Absorbance	[average total Zn TDHPP] M	[Average encapsulated Zn TDHPP] *	[loading per dendrimer
2.0-OH **9**	0.13	4.13E-06	4.05E-04	4.0±2.04
3.0-OH **10**	0.37	7.44E-06	7.39E-04	7.0±0.35
4.0-OH **11**	0.71	1.73E-05	1.73E-03	17.0±0.85
*Concentration of Zn TDHPP after subtracted with 7.76E-6 M Dendrimer concentration 1×10^{-4} M				
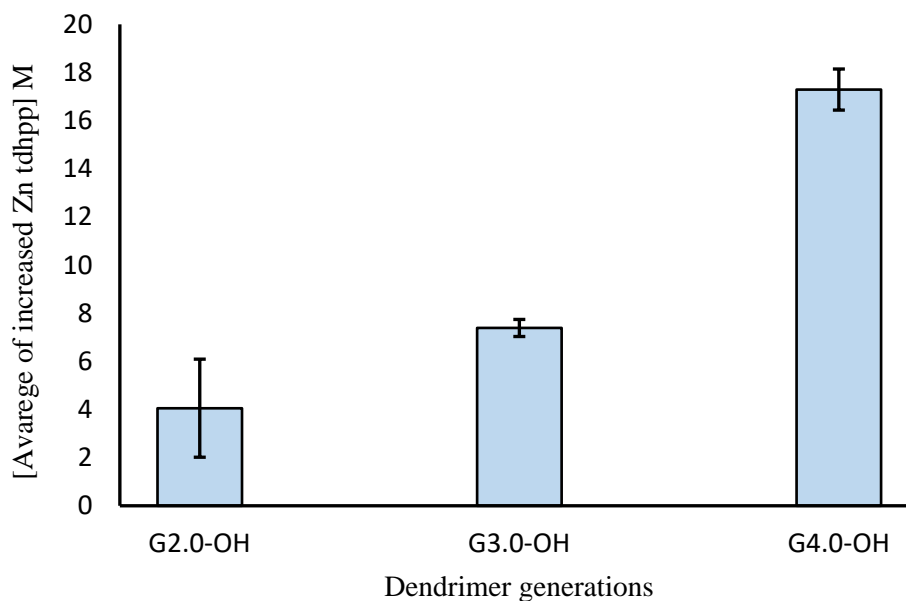
Figure 4. 8: The average increased concentration of ZnTDHPP in PAMAM dendrimer generations

According to Figure 4.7 the porphyrin Sortet band in all dendrimers shifted to 430 nm after encapsulation. The change was probably caused by the strong coordination binding between ZnTDHPP and the nitrogens within dendrimer and not by deprotonation and week ion pairing as was the case with TDHPP **13**. The zinc metal forms a coordination complex with the four nitrogen atoms of the porphyrin ring. The size of the dendrimer also plays a crucial role in the enhanced solubility of Zn TDHPP **14**. As shown in Table 12, the higher the generation of dendrimer, the more Zn TDHPP is bound. In comparison to free-base porphyrin, G2.0-OH it was observed 50% improvement. We did not expect a big improvement because of the opening structure and the fact the G2.0 dendrimer only has four accessible tertiary nitrogens available for coordination. However, there two more porphyrin molecules were encapsulated, these molecules could be bonded through hydrogen bonding with hydroxyl terminal groups.

Whereas the solubility has been increased from 4 to 7 moles in G3.0-OH and reached to 17

moles in G4.0-OH with TDHPP **13**, an increase from 8 as shown in Figure 4.8. As the free base

porphyrin interacts primarily via hydrogen bonds with the internal amines of dendrimers, the

insertion of metal has resulted in a significant improvement in encapsulation efficacy they

enable better coordination and hydrogen bonding interactions through their internal amines as

well as hydroxyl groups on the dendrimer periphery. Moreover, with increasing dendrimer

generation, internal amines and hydroxyl groups are increased, resulting in increased loading

of porphyrins. Figure 4.9 shows that metal coordination interaction between Zn and tertiary

amine dendrimer combined to ion pairing interaction.
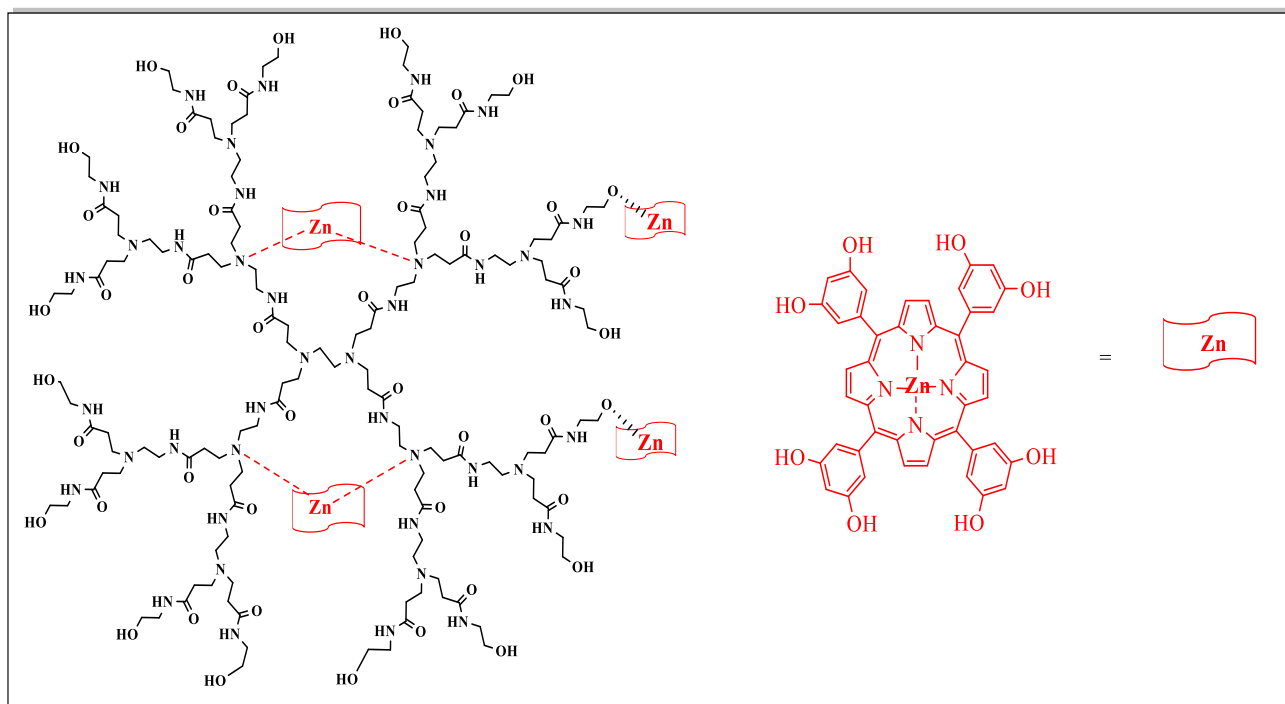
Figure 4. 9: The coordination interaction between G3.0-OH dendrimer nitrogens and Zn TDHPP 14.

4.4. Summary

In this chapter, PAMAM dendrimers were studied to determine their ability to improve the solubility of poorly soluble porphyrins for photodynamic therapy. Using the non-covalent encapsulation method, TDHPP was compared with Zn TDHPP to determine the impact of coordination interaction on PAMAM dendrimer as drug delivery system. The free-base porphyrin TDHPP was successfully synthesized. The insertion of Zn metal to TDHPP was confirmed by ^{1}H NMR, the absence of a peak at a high field - 2.9 ppm (NH) indicates that the macrocycle void is now occupied by a metal. In comparison with porphyrins alone, encapsulation and the solubility of both porphyrins in PAMAM dendrimers have improved. The coordination of Zn in porphyrin added more potential interaction with PAMAM dendrimer, this could explain the significant enhancement of the solubility of Zn metal porphyrin compared to a free base porphyrin.

Chapter 5 : Synthesis and characterisation of hyperbranched polymers

5.1. Introduction

Researchers developing drug delivery systems are increasingly interested in hyperbranched polymers because of their tuneable structure. [141, 142] One of the most distinctive features of hyperbranched polymers is their ease of synthesis using one pot. [143,144] The high end-group functionality and structural versatility of HBPs allow them to be attached to a high density of targeted ligands via non-covalent or covalent interactions, leading to stimuli-responsive drug release at the target site compared to other polymeric variants. HBPs have been extensively studied along with comparison of dendrimers and hyperbranched polymers. [145, 12] A researcher has previously compared hyperbranched polyglycerol with tris PAMAM dendrimers. [112] These dendritic polymers have similar molecular weights and the same hydroxyl termini. However, they differ in their construction and have very different internal functionality. In this study we will synthesise HBPs with terminal OH groups, but also internal amine and amide groups. In this respect they will match the internal and external functionality of PAMAM dendrimers and therefore allow a better comparison between dendrimers and HBPs.

5.2. Synthesis of hyperbranched PAMAM polymer (HBPAMAM)

The HBPAMAM **15** was chosen for this study because it offers similar functionality to dendrimer, which allows for a fair comparison. In order to mimic dendrimers, the selected polymer was synthesized with amide groups and terminal amines. Also, the terminal amines can be converted into hydroxyl functional groups, thus ensuring that dendrimers and HBPs share the same functionality HBPAMAM was synthesized with several multifunctional monomers using methylene bisacrylamide (MBA) and ethylenediamine (EDA) in a one-pot reaction (Scheme 5.1). MBA is an A_2-monomer with two acrylamide groups, whereas EDA is a B_4 monomer, which has two primary amine groups. This method was identified in the

literature, [146] and we chose to use it, since it had the same internal functionality as a PAMAM dendrimer.

We carried out Michael addition reactions with commercially available N, N′-methylene bisacrylamide (MBA) and ethylenediamine (EDA) monomers in deionized (DI) water to determine if hyperbranched polyamnioamide synthesis is feasible as shown in Scheme 5.1. The molar ratio of MBA/EDA was set to be 1:1. the reaction was stirred for 6 hours at 60 ^{0}C under nitrogen atmosphere, then precipitated into acetone. Assumed that equal amounts of MBA and EDA (molar ratio of MBA to EDA is 0.5) would consume all vinyl groups while preserving the primary amine groups as end groups. In general, polymerization of multifunctional monomers such as A$_2$ and B$_4$ produces crosslinked polymers. However, when A2 is slowly added to the reaction mixture, the remaining reactive groups only become B, thus preventing a gel-forming species from forming. Since MBA is relatively insoluble in water, the slow feeding of the A2 monomer (with low concentration of vinyl groups in aqueous solution) leads to a favourable reaction between the vinyl group and the readily available primary amines of EDA that generates covalent bonds with secondary amines. In the initial stages of polymerization, the formation of crosslinking points (e.g., tertiary amines) is prevented by the low concentration of secondary amines.

MBA(A₂ monomor)

EDA (B₄ monomor)

60 °C/30 min

MA

15

ETA

17

16
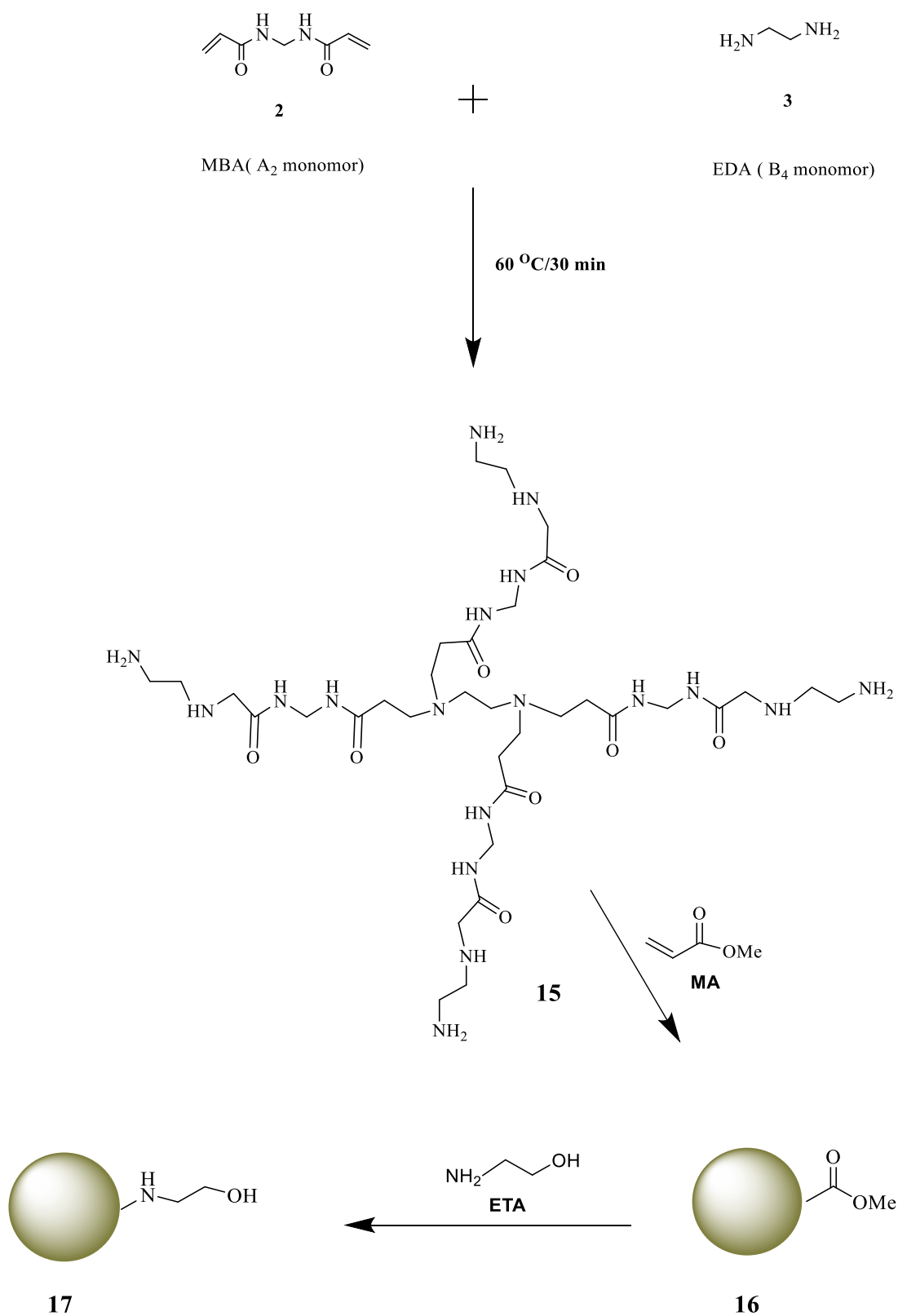
*Scheme 5. 1: Proposed synthesis of HBPAMAM **15** via polymerization of MBA and EDA. In the next step, the amine-terminated HBPAMAM **15** was reacted with MA to produce ester-terminated HBPAMAM **16**. The last step, the ester-terminated polymer reacted with ETA to synthesize HBPAMAM-OH **17**. MA: methyl acrylate. ETA: Ethanolamine*
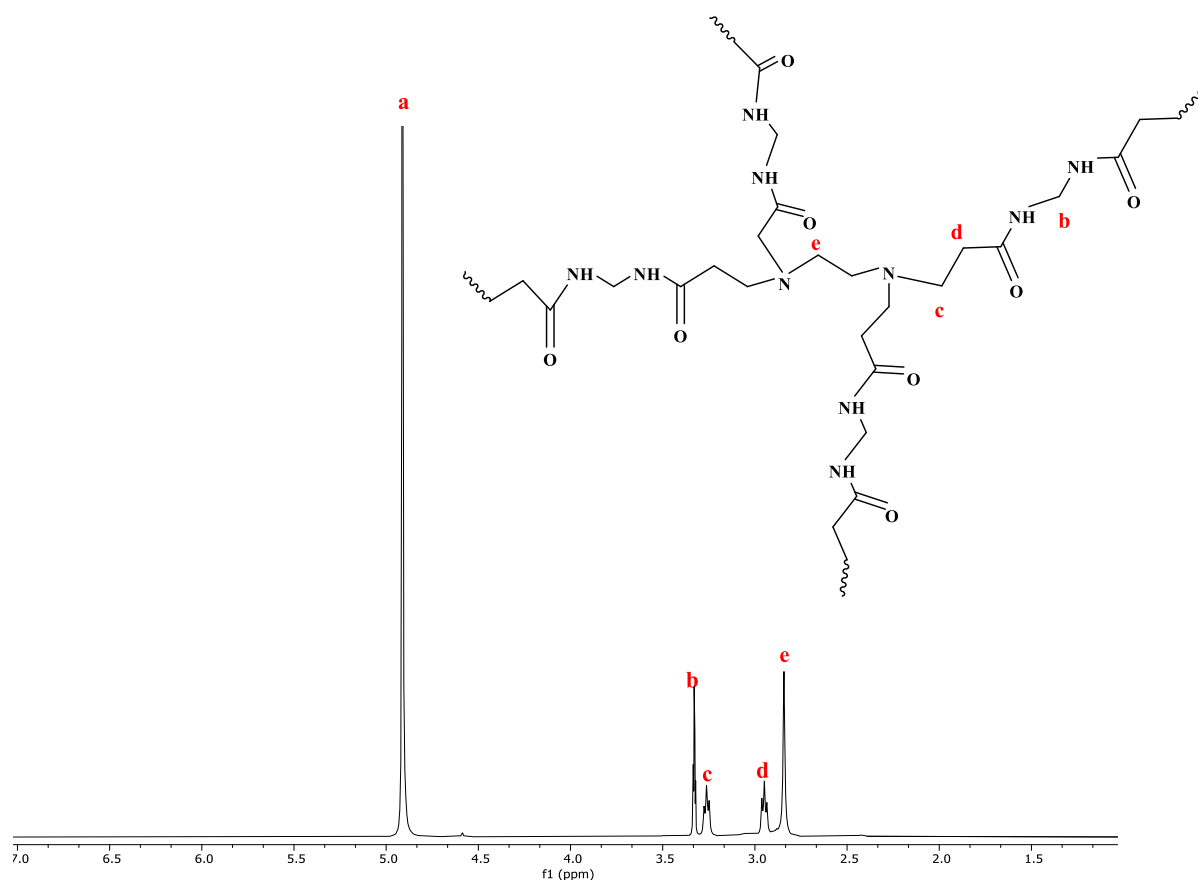
*Figure 5. 1: ^{1}H NMR spectrum of HBPAMAM **15** in methanol-d.*

The ^{1}H NMR of the synthesized HBPAMAM **15** is shown in Figure 5.1. The ^{1}H NMR spectrum

shows the peak 2.8 ppm is a singlet and corresponds to the EDA repeat unit. Additionally, the

signal (b) at 3.32 ppm is related to a new methylene group, which corresponds to -

CONHCH$_2$NHCO- in the repeat unit of HBPAMAM **15**. The signals labelled d and c at 2.91

and 3.25 ppm, correspond to the methylene protons connected with the carbonyl and the

methylene protons linked to secondary and tertiary amines. This means that there has been a

reaction between the monomer A$_2$ and monomer B$_4$. A more important point is that no signal

is detected at 6 ppm, which indicates that no alkene units remain, and all MBAs have reacted.

Mass spectrometry provided an estimate of the average weight of the HBP. The mass spectra

indicated small HBP clusters, the largest gave an m/z value of around 1270 and 1490. The determination of molar mass of dendritic polymers is difficult due to their polydispersity and their highly branched nature. Therefore, the mass spectrum is not precise enough to determine the MW of hyperbranched polymers due to the possible underestimation of the higher molar mass fraction. However, the m/z values indicate relatively large polymer. Consequently, we must perform the analysis in aqueous GPC since the HBP was insoluble in THF. At this point, we were unable to access the aqueous GPC (due to covid pandemic).

5.2.1. Effect of reaction time on the synthesis of HBPAMAM

Although, it would be necessary to perform the analysis in aqueous GPC since the HBP was insoluble in THF. Due to the covid pandemic, it was unable to access aqueous GPC. Therefore, in an attempt to obtain bigger HBPAMAM, the effect of time on molecular weight was studied. This study was performed to investigate the effect of time on the synthesis, and to determine the end time of the reaction. The polymerization progress was studied by sampling the reaction at various times, 30, 90, 240, 360 minutes, with a constant molar ratio of MBA to EDA and heating at 60 °C, using deionized water as solvent. The products of these reactions are labelled as HBPAMAM **16.1** HBPAMAM **16.2** HBPAMAM **16.3** and HBPAMAM **16.4** respectively**.** The products were analysed by NMR. A small amount was then reacted with an excess methyl acrylate and methanol in sample vial to converted to the ester terminated polymers. This would make them soluble in THF, allowing analysis by GPC.

The ^{1}H NMR spectra of HBPAMAM **16**.1 HBPAMAM **16.2**, HBPAMAM **16.3** and HBPAMAM **16.4** obtained are shown in Figure 5.2. It is significant to note that all peaks in Fig.4.3 (a), (b), (c), (d) are similar but not identical. The four polymers have signals corresponding to -CONHCH2NHCO- at (3.32 ppm) and MBA (3.24 ppm and 2.90 ppm) and EDA (2.81 ppm) repeating units, indicating that HBPAMAM was synthesized during all four

phases. Also, all four 1H NMR spectra showed that MBA was completely reacted by 30 minutes since no alkene peaks were found at (6 ppm).
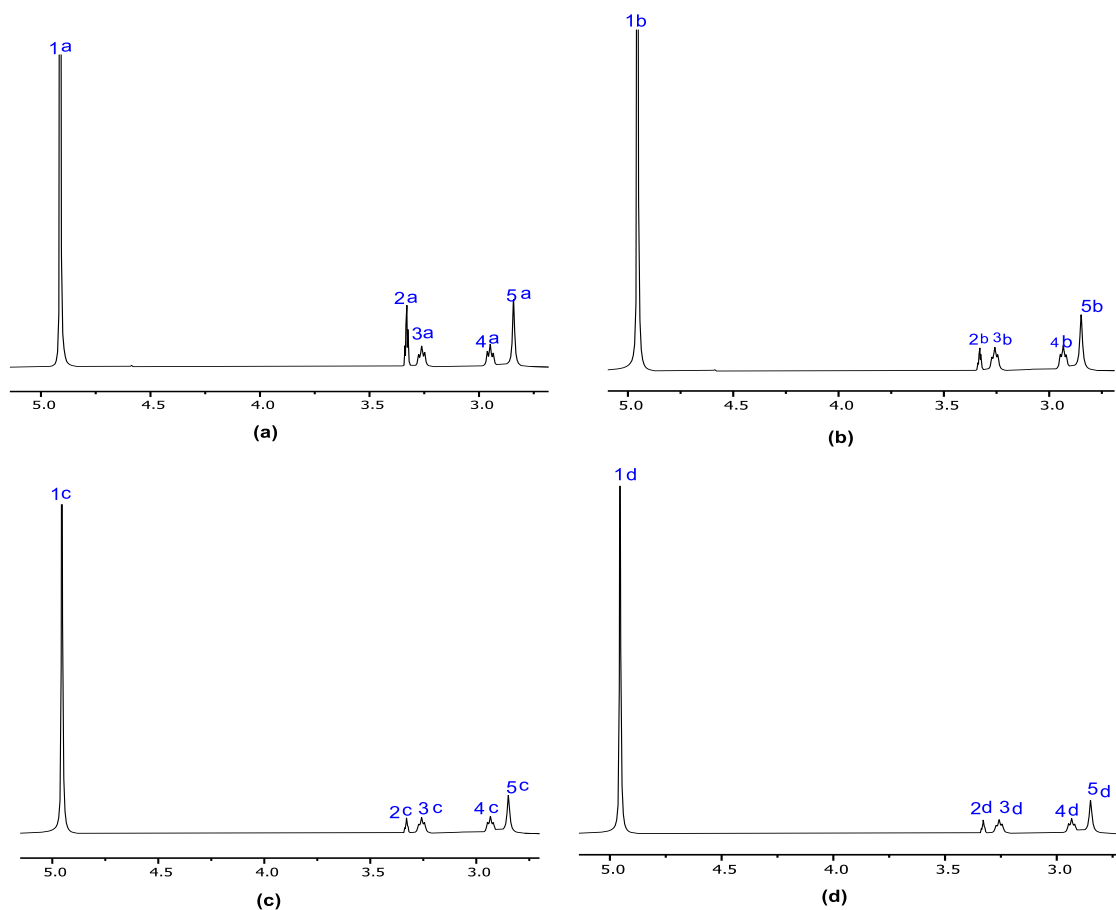
*Figure 5. 2: ^{1}H NMR spectrums of HBPAMAM **16** synthesized at different reaction times. (a) 30 min, (b) 90 min, (c) 240 min, (d) 360 min*

HBPAMAM **16.1.**, HBPAMAM **16.2**, HBPAMAM **16.3** and HBPAMAM **16.4** were then analysed by GPC after conversion to the esters. The data is shown in Table 13. The Mn values for HBPAMAM **16.1** and HBPAMAM **16.2** were the same, with 620 g/mol and 630 g/mol respectively. On the other hand, HBPAMAM **16.3** and HBPAMAM **16.4** had lower Mn of 500 g/mol and 440 g/mol. The molecular weight values for different reaction times are plotted in Figure 5.3. It is clear from the graph that reaction time has negative effect on HBPMAM synthesis. The graph clearly indicates that the molecular weight of the synthesized HBPAMAM

decreases as the reaction time increases. In addition, since the Mn values for both HAPMAM **16.1** and HBPAMAM **16.2** are the same, it was assumed that the reaction was completed and optimized within 30 minutes. This drop in molecular weight is due to the reversible reaction of polymerization, which lead to generating the starting monomers. Therefore, the next step to try and improve the molecular weight, was changing the molar ratio of the starting materials.

Table 13: Values of molecular weight of polymers synthesized at different reaction time

Sample	Time (h)	Mn (g/mol)	Mw (g/mol)	Mz+1 (g/mol)
HBPAMAM **16.1**	0.5	620	630	648
HBPAMAM **16.2**	1.5	630	632	638
HBPAMAM **16.3**	4	502	582	773
HBPAMAM **16.4**	6	440	520	882
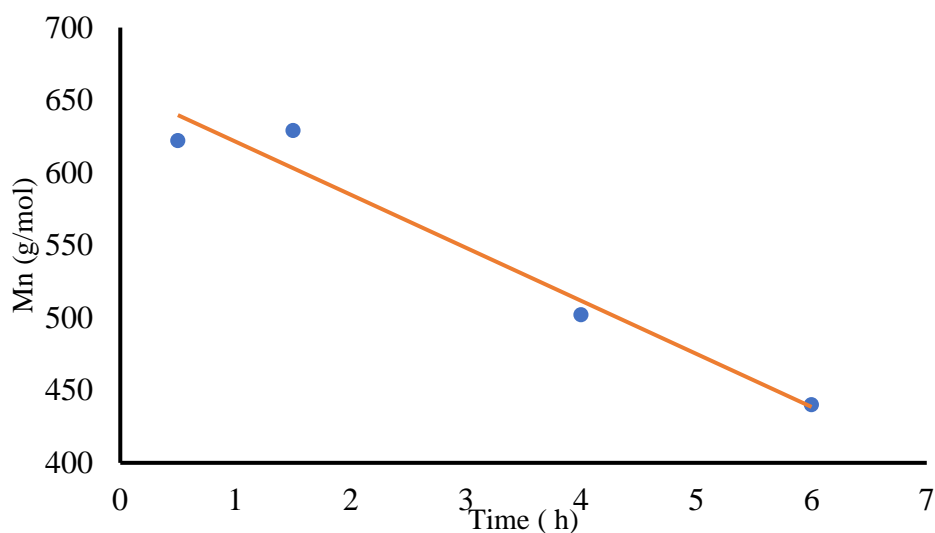
Figure 5. 3: The variation of Mn with different reaction times for HPAMAM synthesized by MBA and EDA at constant ratio 1:1.

5.2.2. Effect of the molar ratio on the synthesis of HBPAMAM

In previous experiments, it was shown that the synthesis of HBPAMAM was completed within 30 minutes. However, the molecular weights determined by GPC experiments were not very large. In an attempt to obtain a bigger polymer with hight molecular weight, we varied the monomer molar ratios of MBA and EDA. All mixtures kept the reaction time to 30 minutes at 60 °C and used deionized water as the reaction solvent. There was no change in the volume of deionized water during the study. Because if it increases, the concentration of monomers will be decreased. It also reduces the chances of collisions between monomers, reducing the speed of HPAMAM synthesis and affecting its molecular weight. Moreover, it was not considered changing the molar ratio of EDA to MBA. It's due to of the fact that an increase in amine groups would cause the reaction to terminate prematurely.

The products obtained from polymerisation between (MBA: EDA) were reacted with MA to convert them to an ester terminal HBPs before analysing by GPC. The data for all products is presented in Table 14. The data show that Mw values of the resulted HBPAMAMs were similar, indicating that changing the molar ratio of the reactants does not generate larger HBPs. However, there were three products (HBPAMAM 17.3, HBPAMAM 17.5 and HBPAMAM 17.6), with an average molecular weight (Mw) of 688 g/mol, 637 g/mol and 654 g/mol respectively, which were relatively high compared to the other samples. A conventional calibration curve based on linear polystyrene standards was used to calculate the molecular weights; therefore, the results may significantly underestimate actual molecular weights, because the hydrodynamic volume of branched polymers is smaller than that of linear polymers with the same molecular weight.

The next step was conversion of HBPAMAM to hydroxyl ended groups, we selected the 3 largest polymers (HBPAMAM 17.3, HBPAMAM 17.5 and HBPAMAM 17.6) to take forward.

Table 14: The GPC in THF characterisation data for HBPAMAM with different molar ratio of EDA:MBA in water at 60 ^{O}C

Sample code	Molar ratio EDA: MBA	Mn (g/mol)	Mw（g/mol)	Mz+1 (g/mol
HBPAMAM 17.1	1:1.1	506	586	935
HBPAMAM 17.2	1:1.15	512	604	940
HBPAMAM 17.3*	1:1.2	533	688	1692
HBPAMAM 17.4	1:1.25	499	595	896
HBPAMAM 17.5*	1:1.3	509	637	1242
HBPAMAM 17.6*	1:1.35	513	654	1330
HBPAMAM 17.7	1:1.4	474	574	974
HBPAMAM 17.8	1:1.45	506	584	828
HBPAMAM 17.9	1:1.5	514	621	1037
HBPAMAM 17.10	1:2	588	657	868
HBPAMAM 17.11	1:3	500	590	927
HBPAMAM 17.12	1:4	497	543	760

5.2.3. Converting of amine terminated HABAPAM to OH terminated HBPAMAM-OH

As discussed previously in section 5.2.2, it found that (HBPAMAM 17.3, HBPAMAM 17.5 and HBPAMAM 17.6) had a higher Mn, accordingly these three polymers were chosen for structural modification. First, the terminal amine polymers should be converted into ester-terminated polymers by reacting with methyl acrylate. Second, the ester-terminated polymers should be reacted with ethanolamine to yield the hydroxyl-ended polymers.

The first experiment was conducted at room temperature by taking small amounts of (HBPAMAM 17.3, HBPAMAM 17.5 and HBPAMAM 17.6) and reacting them with methyl acrylate in methanol for 30 minutes.
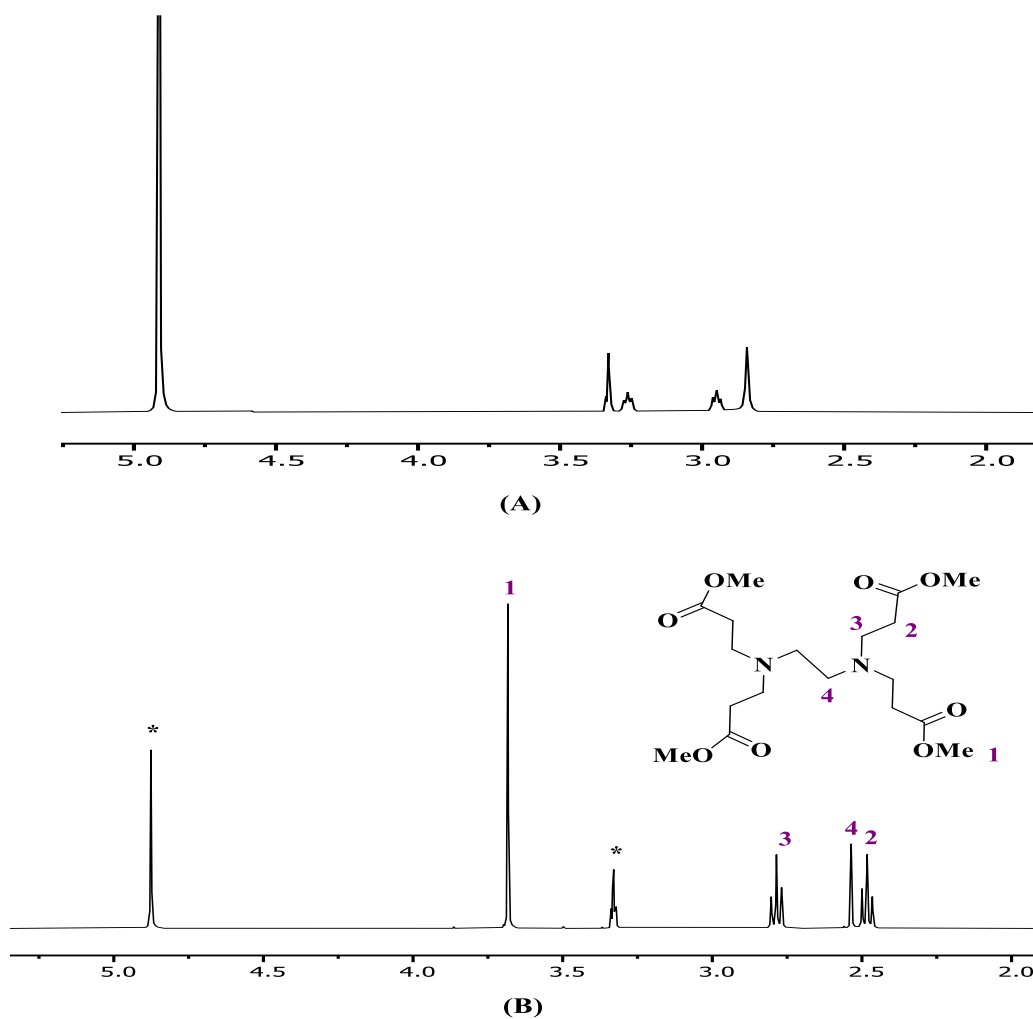
*Figure 5. 4: ^{1}H NMR spectrum of HBPAMAM 17.3 (**A**) and its modified product (**B**).*

The ^{1}H NMR spectra of modified (HBPAMAM 17.3, HBPAMAM 17.5 and HBPAMAM 17.6) were identical, Figure 5.4. There were four peaks in the ^{1}H NMR spectrum for the modified product (B). It was found to have a unique signal at 3.66 ppm, which was not observed in the spectrum of HBPAMAM 17.3 (A). This corresponds to the chemical shift of the methoxy protons. Moreover, triplets at 2.78 ppm and at 2.48 ppm, correspond to the two methylene groups respectively. Furthermore, the peak at 2.53 ppm could be related to the EDA repeat units. However, peak at 3.32 from the polymer was not observed, which corresponds to - CONHCH$_2$NHCO- in the repeat unit of HBPAMAM. This could be the degradation of polymer

instead to give repeated unit peak and ester-terminated polymer, obtained peak related to methoxy group.

The modified B product of HBPAMAM 17.3 was analysed by GPC in THF the Molecular weight (Mn) was only 400, which is lower than the starting polymer and not as expected. It can be concluded that the reaction of HBPAMAM with MA did not result in an ester terminated HBPAMAM-OMe despite, repeating this experiment several times, which developed product with different peaks. However, a new material whose was unknown or closer inspection of the NMR we began to notice a very familiar looking spectrum. Specifically, the spectrum of the G 0.5 PAMAM dendrimer. If this was the case, we can assume that HBPAMAM degraded over the course of the experiment by adding methanol, and that the EDA resulting from the degradation then undergoes a 1,4 Michael addition with the rest of the methanol as well as methyl acrylate. A mass spectrum of the product had an m/z of 405, confirming the formation of the G 0.5 dendrimer. It was now clear why the optimization results (time and ratio) did not generate reasonable GPC data in THF, as the analysis was always performed after (attempted) conversion to the ester.

At this stage the Aqueous GPC became available for analysis. The (HBPAMAM 17.3) with anime terminal was selected, which was discussed in Section 5.2.2 that it has the higher molecular weight than the other samples. The aqueous GPC data also demonstrate the presence of higher molecular weight species than the THF GPC data as shown in Table 15. This suggests that some of the polymer chains are more flexible and can adopt a variety of conformations. Therefore, it's important to consider the effect of the solvent on the polymer solution when performing GPC analysis. Amine-terminated polymers are insoluble in THF GPC as they need to be converted to a tester group before analysis, and the ester terminated polymer was not achieved due to degradation of the polymer and undergo to retro 1,4 Micheal reaction. Buffer

solution (pH 7.4) was used as an eluent that could better reduce the interactions between the cationic polymer and the packing materials of the column. Hence, this led to a higher and more accurate molecular weight determination.

*Table 15: Aqueous GPC data for amine terminated HBPAMAM **17.3**.*

Peak	Mn (g/mol)	Mw (g/mol)	Mz+1 (g/mol)	Mv (g/mol)	PD
Peak 1	4526	4605	4776	4675	1.017

Although conversion was not achieved, the synthesized amine terminal HBPAMAM as confirmed by GPC has a relatively high molecular weight. Therefore, it was suggested that comparing it to the amine terminal PAMAM dendrimer. This is discussed in (Chapter 7 Section 7.2).

Since our objective was to synthesize HBP that would possess both internal and terminal functionalities similar to PAMAM dendrimer. Therefore, the next section was studied shoulder to shoulder with another researcher in the Twyman group. In this part, aromatic Ar-HBPMAM is synthesized and its modification to have hydroxyl terminal groups is discussed.

5.3. Synthesis of new monomer for the Aromatic Hyperbranched Polymer (Ar-HBPAMAM)

Due to the inability to functionalize the HBPAMAM, we needed to find a new approach. Since our objective was to synthesize HBP that would possess both internal and terminal functionalities similar to PAMAM dendrimer in order to compare them fairly. Our research group have synthesised an Aromatic Hyperbranched Polymer (Ar-HBPAMAM) that possessed amide groups, internal and terminal amines. [147] In this respect they mimic the functionality of PAMAM dendrimers. Additionally, the terminal amines can be modified into hydroxyl groups, to give a HBP with the same functionality as the OH terminated PAMAM dendrimers.
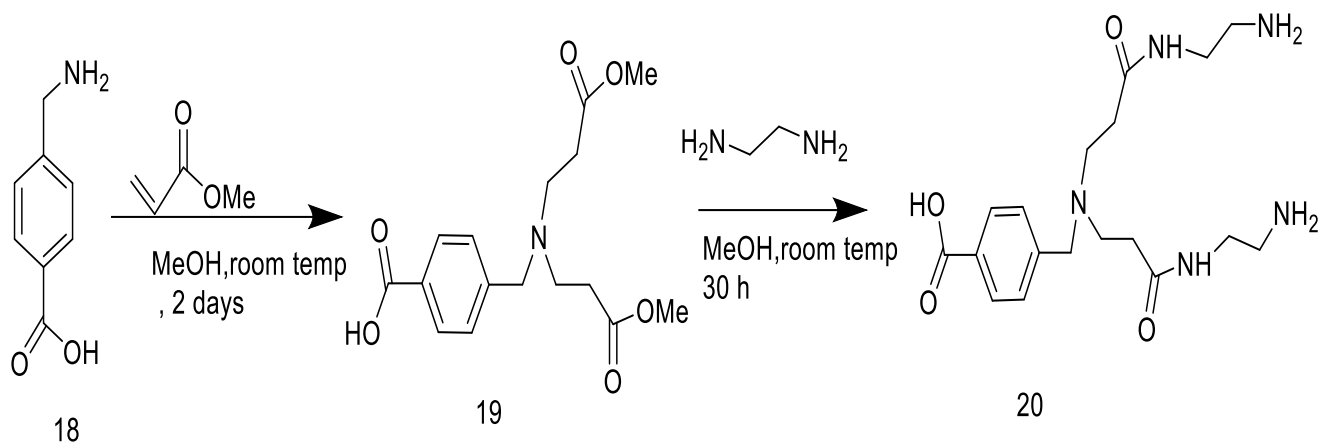
*Scheme 5. 2: Synthesis of monomer **20** via intermediate **19**.*

The monomer for Ar-HBPPAMAM was synthesized in two steps. First step was to prepare monomer **19**, which could be easily synthesised via conventional PAMAM synthesis. Starting from 4-aminomethyl benzoic acid **18**, MA was added to produce diester **19**. To ensure the reaction had run to completion, it was stirred for 48 hours at room temperature. Diester **19** was obtained after purification. During the next reaction, a similar process to that used in dendrimer amidation was followed. the diester **19** was added with a large excess of ethylenediamine to produce monomer **20** as shown in Scheme 5.2. It was necessary to use an excess of EDA to prevent the side reactions previously mentioned (Chapter 3, Scheme 3.6, Pages 46-49). Step two involved heating monomer 20 at 165°C for 30 hours under vacuum, as shown in Scheme 5.3. A honey-coloured glassy solid was obtained at the end of the polymerisation (hyperbranched polymer **21**).
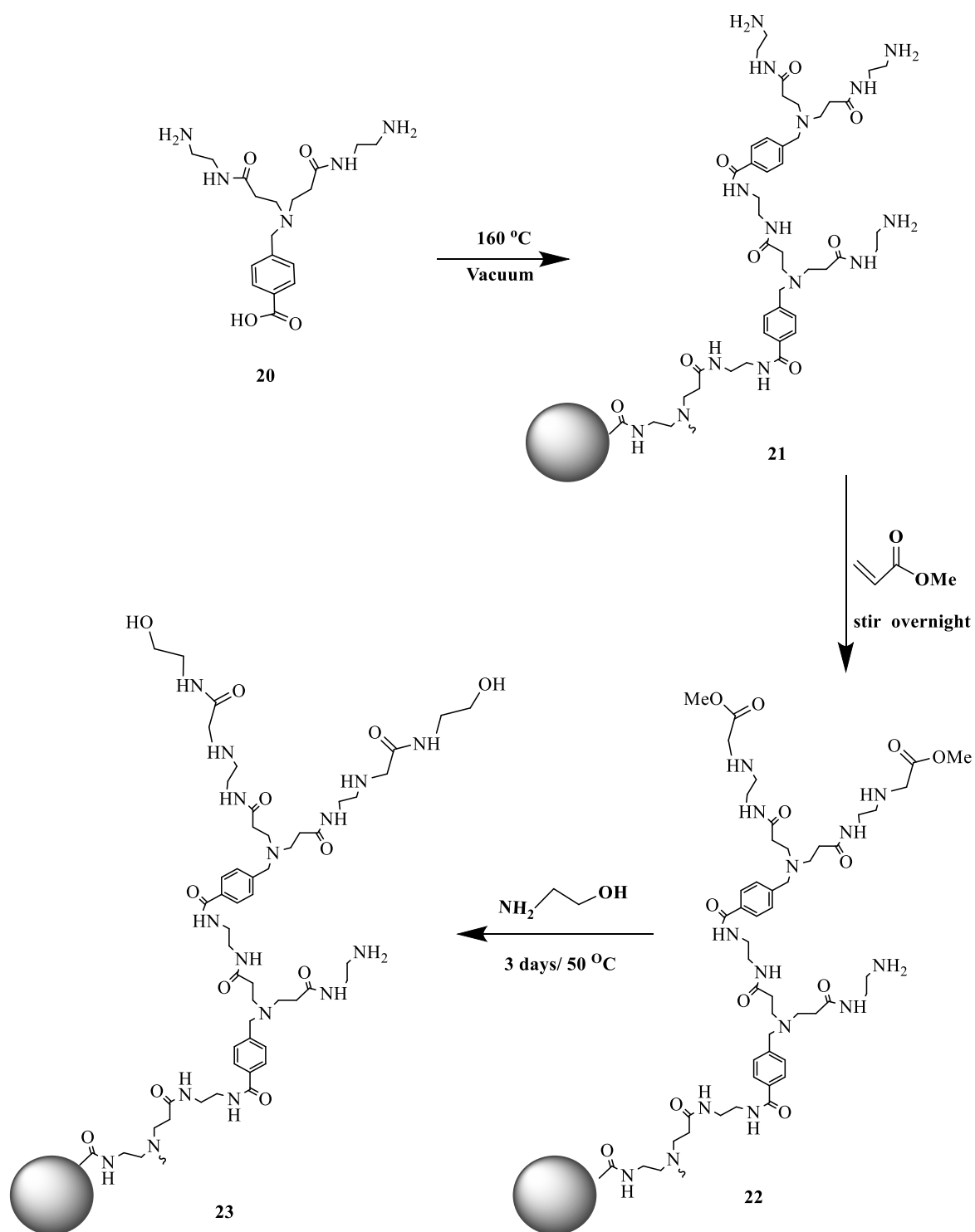
*Scheme 5. 3: illustrates the synthesis of Ar-HBPAMAM. Firstly, reaction of monomer **20** to give amine terminal Ar-HBPAMAM (**21**). Then the ester-terminated Ar-HBPAMAM (**22**) was obtained by reacted **21** with MA. Finally, product (**22**) reacted with ethanolamine to synthesis the hydroxyl terminated Ar-HBPAMAM-OH (**23**) (some arms not shown for simplification).*

5.3.1. Characterisation of ester and amine terminal monomers for aromatic hyperbranched polymer

The characterisation tools used for Ar-HBPAMAM were the same as those for PAMAM dendrimer. Both the ^{1}H NMR and ^{13}C NMR spectra were useful in determining the conversion from diester 19 to monomer 20. It was expected that 19 diester would exhibit methoxy peaks in ^{1}H NMR and an ester carbonyl in ^{13}C NMR. Whereas in monomer 20, these peaks should be absent after conversion to amides. Based on the data presented in Tables 16 and 17 , diester 19 is clearly converted to monomer 20. The absence of characteristic ester peaks (Methoxy or C-O peaks) in monomer 20 indicates a successful conversion.

*Table 16: ^{1}H NMR data for diester **19** and monomer **20***

^{1}H NMR (δH ppm)	Molecule	
	Diester **19**	Monomer **20**
Aromatic	(d, 8.00-7.33)	(m, 7.71 - 7.25)
Methoxy	(s, 3.63)	x
CH_2NH_2	x	(t, 3.11)

Table 17: ^{13}C NMR data for diester 19 and monomer 20

^{13}C NMR (δC ppm)	Molecule	
	Diester **19**	Monomer **20**
Aromatic	(141.8 - 135.4)	(135-122)
C=O	(172)	(174)
C-O	(77.3 – 76.7)	x
C-N	x	(57.03 – 32.94)

IR spectroscopy was also used to identify the functional group changes. the diester 19 has an ester C=O stretch at 1732 and no amide group. However, monomer 20 has a carbonyl amide stretch at 1642 and the carbonyl ester is no longer visible. Mass spectrometry indicated

molecular ion of 324 and 380 m/z for the diester 19 and monomer 20, respectively, that were similar to those calculated. therefore, the conversion can be considered successful.

The characterisation of anime terminal Ar-HBPAMAM **21** was difficult, mainly because of its increasing molecular weight and polydispersity. The ^{1}H NMR spectrum showed peaks in the expected regions, but the peaks were broad and overlapped. Multiplets were observed at 7.71 -7.25 ppm, associated with aromatic protons. It suggested that due to the broadness of the peaks, some overlap is seen between these signals for aromatic protons and the repeat units derived. For polymers however, resonance signals from repeating units often coalesce as broad peaks, this is largely due to poor molecular rotation and repeating units being situated in marginally different chemical environments.[148] We also find multiple broad multiplets at 3.40 – 1.88 ppm, which are corresponding to all the aliphatic protons on the Ar-HBPAMAM.

A ^{13}C NMR provided some further clarification. The carbonyl peak of the amide group was observed at 174 ppm, and two peaks were identified at 135.0 ppm and 122.7 ppm and confirming an aromatic unit present. The spectrum also showed multiple peaks at 47.27 – 36.68 ppm which are from increasing number of C-N and C-C groups that exist in many environments within the polymer.

The IR spectrum of Ar-HBPAMAM exhibited an amide stretch at 1634 cm-1 and was absent of carbonyl ester stretches. Consequently, it helped to confirm that structural assumption of Ar-HBPAMAM as it was expected that all esters are converted to amides. Furthermore, the molecular ion peak at 1460 was observed via MALDI mass spec, as we expect the molecular mass to be higher than 1000 g/mol. The aqueous GPC was performed to determine an Mn for the Ar-HBPAMAM. The GPC determined Mn to be 2300. Following confirmation that Ar-HBPAMAM was synthesized successfully.

5.3.2. Synthesis and characterisation of hydroxyl-terminated aromatic hyper branched PAMAM polymer (Ar-HBPAMAM-OH 23)

The terminal amines Ar-HBPMAM **21** were converted to hydroxyl groups using the same procedure as used for PAMAM dendrimers. The amine group was first modified to ester terminal groups (Ar-HBPAMAM-OMe **22)**, by treatment with methacrylate. To determine whether Ar-HBPAMAM-OMe **22** had converted to Ar-HBPAMAM-OH **23**, characterisation was required. Our expectation was to loss the ester methyl peak, and new peaks for the methylene protons were observed.

^{1}H NMR spectrum for Ar-HBPPAMAM-OMe **22** revealed a sharp peak at 3.62 ppm which represented methoxy protons, however there is no such peak in the Ar-HBPAMAM-OH **23** spectrum. In the Ar-HBPAMAM-OH **23** spectrum, multiplets between 3.58 - 2.35 ppm indicate additional proton environments associated with the ethanolamine group. The success of the reaction was also confirmed by ^{13}C NMR, Ar-HBPAMAM-OH **23** spectra revealed a new peak at 62.81 ppm related to c-o environment. Moreover, Ar-HBPAMAM-OH had more peaks in the C-N region compared to Ar-HBPAMAM-OMe **22**, which indicates that new amide bonds are being synthesized. IR spectroscopy was further performed to characterise Ar-HBPAMAM-OH **23** and to be sure that all esters have been converted to amide groups. in this case, it was anticipated to indicate abroad peak at 3000 cm-1 and the ester C=O stretch would be no longer visible. This is confirmed by IR data in Table 18.

*Table 18: IR data for Ar-HBPAMAM-OMe **22** and Ar-HBPAMAM-OH **23***

IR Stretch (cm^{-1})	Type of Ar-HBPAMAM	
	Ar-HBPAMAM-OMe **22**	Ar-HBPAMAM-OH **23**
C=O (ester)	1731	x
O-H	x	3266
C=O (amide)	x	1639

5.4. Summary

The HBPPAMAM-NH$_2$ was successfully synthesised. The 1,4 Michael addition converted the amine group to an ester terminal group. The effect of time on the reaction was studied. The results revealed that the molecular weight of the synthesized HBPAMAM decreases as the reaction time increases. The reaction was completed and optimized within 30 minutes. The series of HBP was prepared to investigate the effect of the molar ratio on HBPAMAM synthesis. There were three polymers that were relatively bigger, they were selected to be converted to ester-terminated polymers. The amine-terminated polymers were insoluble in THF and could not be analysed by GPC. Therefore, HBPAMAM-NH$_2$ was first reacted with methyl-acrylate. Nevertheless, the aqueous GPC showed a molecular weight of 4526 g/mol for HBPAMAMNH$_2$. The conversion of HBPPAMAM-NH$_2$ to an end-hydroxyl group was not achieved due to certain reaction conditions. In contrast, HBP containing the same internal and external groups as PAMAM dendrimers was successfully converted to a hydroxyl ending group.

Chapter 6 : The encapsulation studies for hyperbranched polymers

6.1. Introduction

In order to evaluate the binding and release potential of both synthesised HBPs, it was essential to establish the possibility of encapsulating drug or host molecules. We expected that the HBPs would be able to encapsulate the drug molecule since both of HBPs had internal cavities with the same functionality as the dendrimers (hydrophobic and hydrogen bonds). In the first encapsulation experiment, the host/guest complex was formed by the co-precipitation technique and using ibuprofen as a model of drug. An accurate molar concentration of dendrimers can be obtained easily, due to dendrimers being mono-disperse and having a unique and identifiable molecular weight. In the case of HBPs, molar concentrations cannot be calculated, because they are polydisperse and do not have a defined molecular weight. As it was mentioned in the previous Section, the GPC's characterisation of HBPs with respect is not accurate and only provide an estimate of the average molecular weight. Therefore, mass per volume (g/L) was used as the unit of concentration when studying HBPs. Because we aimed to compare the systems have the same functionality, we propose to study the encapsulation of HBPAMAM-NH$_2$ **17.3** amine terminal specially after the aqueous GPC gave molecular weight of 4526 g/mol.

6.2. Encapsulation of Ibuprofen by HBPAMAM-NH$_2$ 17.3

The encapsulation of HBPAMAM-NH$_2$ **17.3** was performed at two concentrations, and a mass/volume concentration of 0.05 mg/ml and 0.75 mg/ml have been used. This to investigate the ability of HBPAMAM at high and low concentration. In the first step, the extinction coefficient of Ibuprofen (ε Ibuprofen = 290 dm^3 mol^{-1} cm^{-1}). It was found that the maximum free concentration of Ibuprofen was approximately 7.72E-4 mol dm^{-3}. We used (Δ Abs) absorption values between 274 and 276 nm to compensate for potential baseline drift.

Table 19: Encapsulation data of Ibuprofen using low and high concentrations.

[HBPAMAM-NH$_2$] mg/ml	Δ Abs	[average of total Ibu] M	[* average of encapsulated Ibu] M
0.005	0.56	1.67E-03	9.01E-04 ±3.65E-04
0.75	0.421	1.55E-03	7.80E-04±1.46E-04
* Concentration of encapsulated Ibuprofen after substruction with 7.72 x 10-4 M All data was obtained as an average of two experiments ± standard deviation.			

It is clear that HBPAMAM-NH$_2$ **17.3** can encapsulate ibuprofen and improve its solubility. The concentration of Ibuprofen was increased to 9.01E-04 M at polymer concentration 0.005 mg/mL.   This is as we expected, due to the presence of internal and external amines. Moreover, the presence of a carboxylic functional group in the ibuprofen structure, a second interaction could occur with the tertiary amines inside the HBPAMAM-NH$_2$. The results in Table 19 shows that the encapsulation ability of HBPAMAM-NH$_2$ has been reduced when the polymer concentration increased to 0.75 mg/ml. Therefore, another experiment was carried out to investigate what happens between the two concentrations discussed, and to determine the best concentration for the maximum drug encapsulation. It was anticipated that increasing concentration of polymer would lead to increase in the concentration of encapsulated ibuprofen. The experiment studied different concentrations of HBPAMAM-NH$_2$ **17.3** ranging as follows (0.01, 0.02, 0.04, and 0.06 mg/ml. The results are shown in Table 20 and Figure 6.1.

Table 20: Encapsulation data of ibuprofen using different concentrations of HBPAMAM-NH2 17.3

[HBPAMAM-NH2] mg/ml	Δ Abs	[Average incapsulated Ibu] x10⁻³ M	[* Average of increased Ibu] X 10⁻³ M
0.01	0.43	1.66	1.02±6.35E-05
0.02	0.83	2.90	2.23±1.11E-04
0.04	0.93	3.65	2.65±9.2E-05
0.06	0.82	2.97	2.33±3.9E-05
* Concentration of encapsulated ibuprofen after subtracting with 7.74×10^{-4} M.			
- All data was obtained as an average of three trails ± standard deviation			
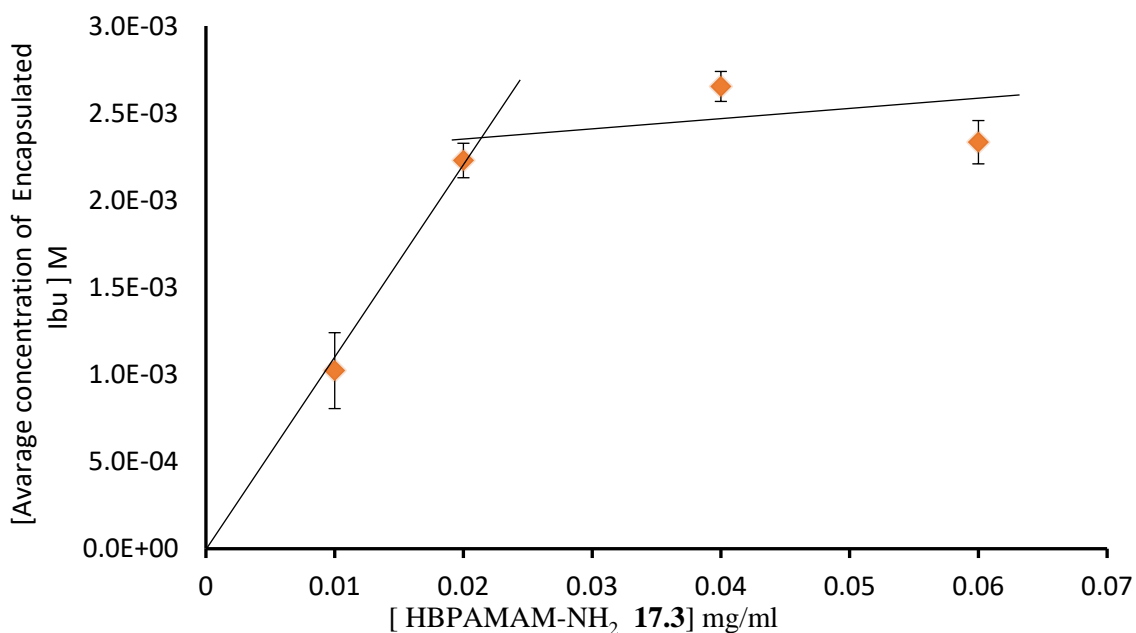
Figure 6. 1: The increased concentration of encapsulated ibuprofen with increased concentration of HBPAMAM-NH2 17.3

According to data, the concentration of encapsulated ibuprofen initially increases as the polymer concentration increases. This is due to the increased number of internal amines and amides required for hydrogen bonding or electrostatic interactions. The encapsulated ibuprofen concentration increased linearly until it reached 0.04 mg/mL, at which point it plateaued. This could be due to the formation of large aggregated species at higher concentrations. Moreover,

at a concentration of 0.06 mg/mL, the concentration of ibuprofen decreased to 2.33E-03 mg/mL

It is possible that the aggregation of polymer will lead to be less internal space being available to encapsulate drug molecules. The HBPAMAM-NH$_2$ was next examined at these concentrations to assess its possible aggregation behaviour. This will be discussed in the following section.

6.2.1. Dynamic light scattering (DLS) study of the aggregation of HBPAMAM-NH2

The concentration-dependent aggregation of HBPAMAM-NH$_2$ 17.3 was studied using dynamic light scattering (DLS). In DLS, macromolecules are analysed for their diffusion behaviour in solutions to determine their diffusion coefficients. This coefficient can be used to determine the hydrodynamic radius. The encapsulating ability of macromolecules is lowered when their branches become intertwined, which leaves less space to encapsulate the gust molecules. We postulated that the HBPs at higher concentrations are more likely to aggregate because they are closer together. We discussed in previous sections that we are concerned about macromolecule aggregation at high concentrations. DLS experiments were done for HBPAMAM-NH$_2$ at four different concentrations that covered the range studied for encapsulation (0.01 mg/mL, 0,02mg/mL,0,04 mg/mL, and 0.06 mg/mL. The DLS spectra shown in Figure 6.2.
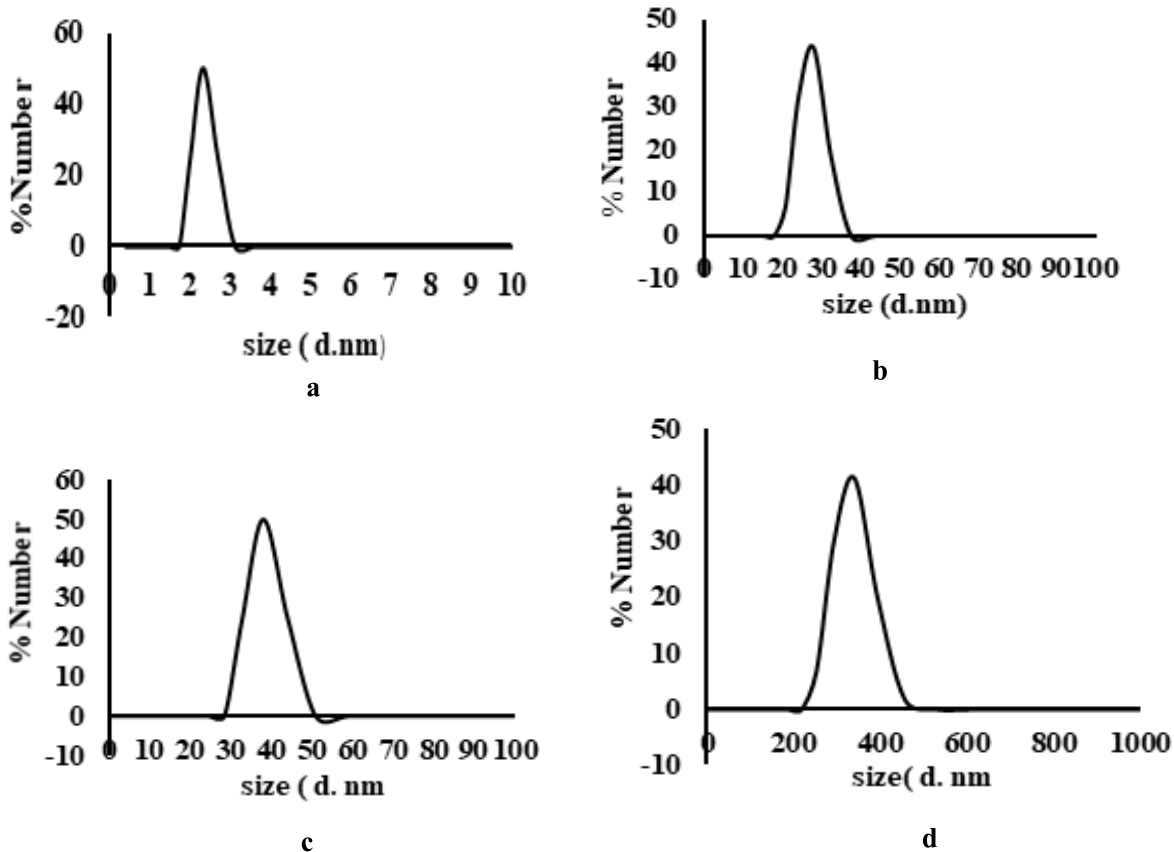
*Figure 6. 2: DLS data of HBPAMAM-NH$_2$ at different concentrations (**a**) polymer at 0.01 mg/mL. (**b**) polymer at 0.02 mg/mL. (**c**) polymer at 0.04 mg/mL. (**d**) polymer at 0.06 mg/mL.*

The DLS data in Figure 6.2 shows, increasing in polymer concentration the hydrodynamic radius increased in stages. At 0.01 mg/mL the diameter size was 2.3 nm. Then increased to around 30-40 nm at 0.02 and 0.04 mg/mL respectively. However, at 0.06 mg/mL the HBPAMAM-NH$_2$ **17.3** become very large, confirming aggregation. This data broadly overlaps with encapsulation data. In accordance with the present results, previous studies have demonstrated that the hyperbranched polymers tend to further aggregation at higher polymer concentration.[149] Moreover, the results showed that Hyperbranched polymer aggregates were capable to encapsulate small hydrophobic molecules.

It was suggested that the presence of a mixture of individual macromolecules of different masses reduces association, leading to aggregates of different sizes.[150] it is well known that HBPs are polydisperse and irregularly structured, and they are more dynamic. This could reduce the amount of controlled space, thereby reducing the amount of drug molecules encapsulated. Furthermore, the release of drug molecules from an inner cavity where drug molecules have been encapsulated might be faster. This is due to the fact that the drug might be encapsulated in aggregates that have dynamic activity between polymer molecules. The ideal scenario can be seen in the cartoon in Figure 6.3. We can conclude that simple HBPAMAM-NH$_2$ **17.3** have the ability to encapsulate drug molecules as we expected.

A	B	C	D
Rh = 2.3 nm	Rh = 28 nm	Rh = 40 nm	Rh = 342 nm
Conc = 0.01 mg/mL	Conc = 0.02 mg/mL	Conc = 0.04 mg/mL	Conc = 0.06 mg/mL
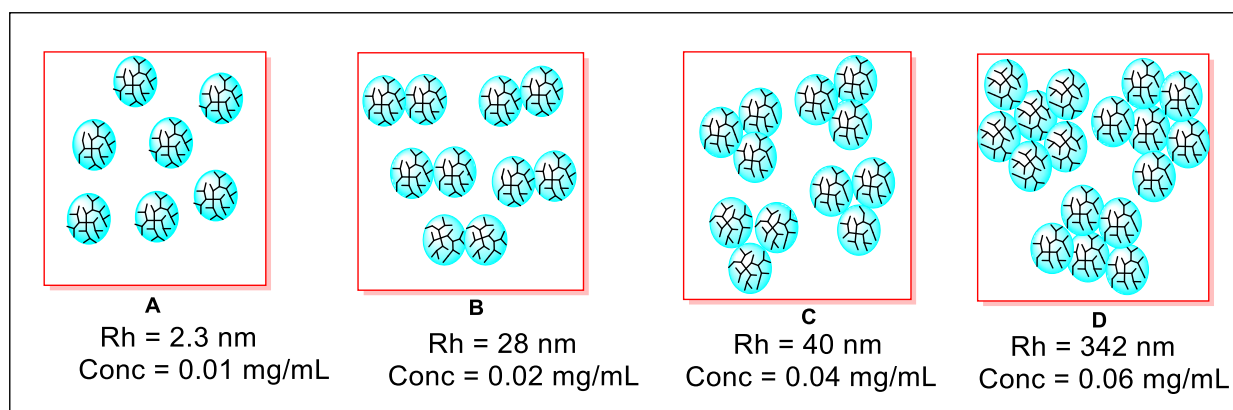
Figure 6. 3: The expected cause of decreased the encapsulated ibuprofen at high concentration. Rh: Hydrodynamic Radius. Conc: Polymer Concentration.

We also work on improving poorly soluble anticancer therapeutics used in photodynamic therapy. It will allow us to develop a deeper understanding of the effect of secondary interactions between the drug molecule and HBPAMAM-NH$_2$. The encapsulation study was therefore undertaken by using Zn TDHPP. Based on our previous DLS data, it was necessary to use a concentration below the aggregation limit to prevent aggregation.

6.2.2. Encapsulation of Zn TDHPP 14 using HBPAMAM-NH$_2$

The Zn THDPP **14** was synthesized and characterized previously in Chapter 3 Section 3.3.2. The encapsulation was carried out as previously described via the co-precipitate method. The extinction coefficient of Zn THDPP **14** was determined to be 3.7x 10^{-4} dm^3 mol^{-1} cm^{-1}. The maximum concentration of Zn THDPP **14** in phosphate buffer was 7.76E-6 mol dm^{-3}.

It was determined earlier that high concentrations of polymer were susceptible to aggregation. Therefore, in this work, the experiment was conducted at three concentrations below the aggregation limit (0.005 mg/mL, 0.01 mg/mL, and 0.04 mg/mL). We expected the HBPAMAM-NH$_2$ would be able to increase the concentrations of the Zn THDPP, due to the secondary interactions via of Zn with internal tertiary amines within the HBPAMAM-NH$_2$. The data is shown in Table 21.

Table 21: Encapsulation data of Zn TDHPP 14 using HBPAMAM-NH$_2$ 17.3

| HBPAMAM-NH$_2$ mg/ml	Abs	[Average of total Zn TDHPP] M	*[Average of encapsulated Zn TDHPP] M
0.005	0.34	2.5E-06	9.1 ±2.5E-06
0.01	0.41	4.3E-05	2.2±2.7E-06
0.04	0.65	1.6E-05	7.8±7.3E-06
* Concentration of encapsulated Zn TDHPP after subtracting with 7.76E-06 M.			
- All data was obtained as an average of three trails ± standard deviation			
ε = 3.7x 10^{-4} dm^3 mol^{-1} cm^{-1}			

The effect of different concentrations of HBPAMAM-NH$_2$ on the solubility of Zn THDPP can be clearly observed. A linear relationship was found between the concentration of polymer and Zn THDPP solubility. The concentration Zn THDPP in buffer alone was 7.76E-06 M. After encapsulation within the polymer, it was significantly improved to1.2E-05 M at HBPAMAM-NH$_2$ concentration of 0.005 mg/mL. At HBPAMAM-NH$_2$ concentration of 0.01 mg/mL the porphyrin concentration increased doubled. The concentration of porphyrin was four times

higher at 0.04 mg/mL than it was at 0.01 mg/mL. In this case, the porphyrin concentration was increased as predicted with increased polymer concentration as shown in the Figure 6.4. If we look it at the results of Ibuprofen encapsulation over the same HBPAMAM-NH$_2$ concentration range, the concentration of Ibuprofen was non-linear behaviour for example at 0.04 mg/mL the Ibuprofen concentration plateaued. But porphyrin over the same [HBP] range is linear, due to the porphyrin is bigger molecule than Ibuprofen, which can form strong bond to HBP and overcome aggregation.
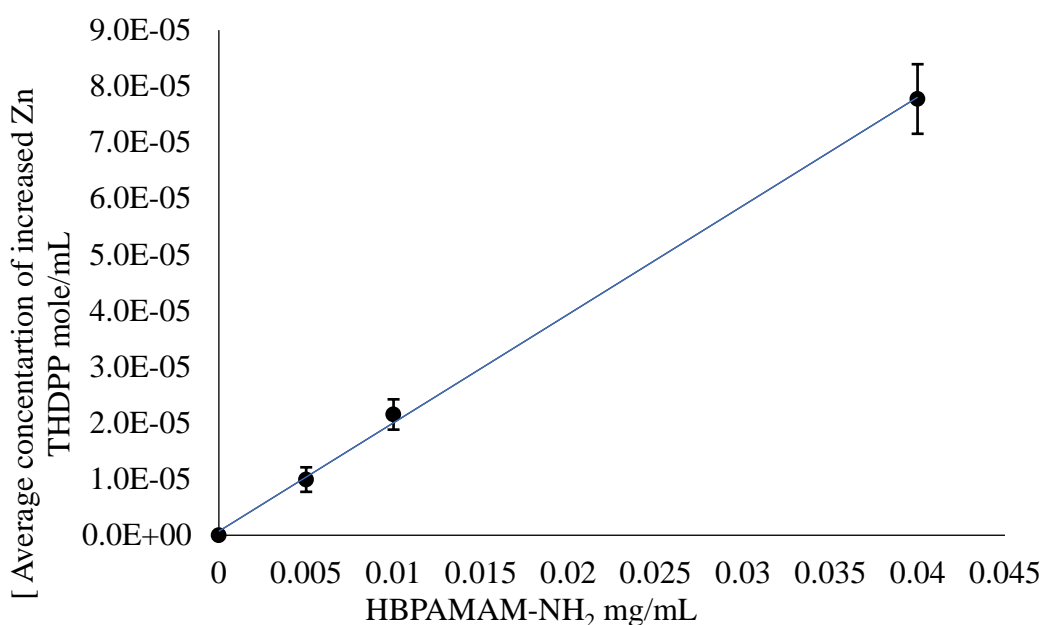
*Figure 6. 4: Increased concentration of encapsulated Zn TDHPP **14** with increased polymer concentration*

HBPAMAM-NH$_2$ **17.3** possessing terminal primary amines (cationic). In the literature, it was reported that cationic (NH$_2$) dendrimers are exhibited cytotoxicity, however, anionic and neutral dendrimers are rarely toxic.[76] Moreover, the surface charge significantly affects the bioavailability, immunogenicity, and in vitro and in vivo toxicity of dendrimers. Therefore, a polymer with neutral terminal groups and water solubility is required for minimal cytotoxicity.

We then need a HBP that has the same structural and functionalised features of PAMAM-OH dendrimers. The following section describes our investigation using an aromatic hyperbranched PAMAM (Ar-HBPAMAM-OH **23**) polymer, that is more robust than the HBPAMAM-NH$_2$ 17.3 discussed above and should be suitable for derivatisation.

6.3. Encapsulation of Ibuprofen using aromatic hyperbranched PAMAM polymer (Ar-HBPAMAM-OH 23)

This polymer was synthesised successfully in collaboration with a research member (**Lucy Hamson**). The synthesis and the characterisation data were discussed Section 5.3.2. The aqueous GPC analysis revealed a tri-modal set of peaks, which meant that, the molecular weight of Ar-HBPAMAM-OH could not be confidently defined. However, the molecular weight was estimated using the average determined by GPC, which was 2300 D. however, it should be noted that the PD was very high (> 10). Nevertheless, the Ar-HBPAMAM-OH **23** was studied for its ability to encapsulate drug molecules at two concentrations (0.327 mg/ml and 0.70 mg/ml). Following the results for the HBPAMAM-NH$_2$ **17.3.** It was expected that the concentration of encapsulated ibuprofen would increase two-fold with a similar two-fold increase in polymer concentration. As before the encapsulation experiment was done via the co-separation method. The initial choice of HBP concentration was made based on the dendrimer concentrations previously described.

*Table 22: Encapsulation data of ibuprofen using Ar-HBPAMAM-OH **23** in different concentrations.*

[Ar-HBPAMAM-OH **23**] mg/ml	▲ [Average total Ibu] M	*[Average encapsulated Ibu] M
0.32	1.52E-03	7.05E-03±7.46E-05
0.70	1.40E-03	6.00E-03±5.484E-05
▲Concentration of ibuprofen determined via absorbance divided by $\varepsilon= 290$ dm^3 mol^{-1} cm^{-1}		
*Encapsulated Ibuprofen after subtracting from free Ibuprofen concentration 7.72E-04 M		
- all data was obtained as average of two experiments ±standard deviation.		

The data indicated that Ar-HBAPAMAM-OH encapsulate more than that with HBPAMAM-NH$_2$. This increasing must be due to the extent of π-π stacking interaction between an aromatic ring in ibuprofen and the Ar-HBPAMAM-OH caused by the presence of aromatic groups in the polymer backbones. The concentration of ibuprofen in buffer alone was 7.72E-04 M. It increased to 7.05E-03 M and 6.00E-03 at 0.32 and at 0.70 mg/mL respectively as shown in Table 22. This clearly indicates that Ibuprofen concentration dos not really increase as the Ar-HBPAMAM-OH 23 concentration approaches 0.70 mg/mL presumably, this is due to the same aggregation as observed for the HBPAMAM-NH$_2$ and OH-dendrimers.

6.4 Summary

The ability of HBPAMAMNH$_2$ **17.3** to encapsulate hydrophobic molecules was evaluated at low and high concentrations. At a polymer concentration of 0.75 mg/ml, the concentration of encapsulated ibuprofen was reduced. The concentrations of HBPAMAM-NH$_2$ **17.3** ranging from 0.01, 0.02, 0.04, and 0.06 mg/ml was studied, to determine the effect of concentration on HBP and determine the maximum HBP concentration. Encapsulated ibuprofen concentration increased with increasing polymer concentration. However, at a concentration of 0.04 mg/ml the encapsulated ibuprofen plateaued. The DLS data revealed that HBP tend to aggregate gradually with increasing in concentration. The encapsulation of porphyrin revealed that the

encapsulated concentration of porphyrin increased linearly compared with ibuprofen at the same polymer concentration. The encapsulation using Ar-HBPAMAM-OH **23** has the ability to encapsulate more of ibuprofen than HBPAMAMNH2. Overall, both polymers HBPAMAM-NH$_2$ and Ar-HBPAMAM-OH 23 are promising polymers for encapsulating hydrophobic drug molecules (Ibuprofen and porphyrin).

Chapter 7 : Comparisons of PAMAM dendrimer and HBPs for drug delivery

7.1. Introduction

Having synthesised and studied encapsulation properties of several dendrimers and hyperbranched polymers, we were now in a position to partly answer the question set out in the aims. That is, "are dendrimers superior to hyperbranched polymers as drug delivery systems?" Although attempts to answer this question have been reported in the literature, the systems compared were often very different with respect to size and (more importantly), internal and external functionality. The work in the previous chapters describes the synthesis and properties of various systems with similar internal and external functionality. This chapter compares the results obtained from the encapsulation experiments carried out using an amine ending PAMAM dendrimer and amine terminated HBP PAMAM (HBPAMAM-NH2 17.3), as well as the OH ended PAMAM dendrimers and OH terminated aryl PAMAM HBPs (Ar-HBPAMAM-OH 23). In both cases encapsulation depended on a variety of non-covalent interactions, including hydrophobic, ionic and hydrogen bonding.

When comparing different systems, it is important that concentrations remain constant between systems. As dendrimers possess a monodisperse structure, we can easily determine the molecular weight and use this to calculate a molar concentration. However, we cannot calculate a unique and accurate molecular weight for the HBPs, due to polydispersity. Although we have used GPC to obtain molecular weight data, this is only an estimate and the numbers obtained are simple averages. As such, we cannot calculate molar concentrations for the HBPs reported in previous chapters. For this reason, mass per volume (g/L) was used for the units of concentration when studying the dendrimers and HBPs. This method works, because for a given mass of polymer, the number of repeat units is constant across all molecular weights (and is a common method used for polymer concentrations). The final aim of the

project involved comparing PAMAM dendrimers to hyperbranched polymers in their efficiency as drug delivery systems.

7.2. Comparing the ibuprofen encapsulation efficiencies of an amine terminated PAMAM dendrimers and an amine terminated HBPAMAM

To compare the properties of these two systems, amine terminated dendrimer and HBPAMAM-NH_2 of similar molecular weights was required. As such, a G 3.0 **6** PAMAM dendrimer with a molecular weight of 3256 g mol^{-1}, was used and compared with the HBPAMAM-NH_2 **17.3** with an Mn of 4526 (as determined by aqueous GPC). We have previously determined an extinction coefficient ε of 290 dm^3 mol^{-1} cm^{-1}) and a maximum free concentration of 7.72E-4 mol dm^{-3} for Ibuprofen. The difference values in absorption between 274 nm and 276 nm were used to determine encapsulated concentrations (Δ Abs was used to compensate for potential baseline drift). A concentration of 0.32 mg/mL was used for both of the amine terminated systems, as this corresponded to the previous dendrimer concentration of $1x10^{-4}$ M. The encapsulation data for the amine terminated dendrimer and HBPAMAM-NH_2 are shown in Table 23 and compared graphically in Figure 7.1.

Table 23: Data for the encapsulation abilities of ibuprofen by G3 and HBPAMAM-NH_2

Host System	Trial one			Trial two		
	Δ Abs	[Total Ibu] M	*[Encapsulated Ibu] M	Δ Abs	[Total Ibu] M	*[Encapsulated Ibu]M
G3 **6**	0.3959	1.37E-03	5.93E-03	0.4147	1.43E-03	6.58E-03
HBPAMAM-NH_2 **17.3**	0.3861	1.33E-03	5.59E-03	0.4099	1.41E-03	6.41E-03
* The encapsulated Ibuprofen after subtracting from 7.72E-4 M The data was obtained as two data sets						

Host System	[Average Encapsulated Ibu] M
G3	6.26E-03±4.58E-04
HBPAMAM-NH$_2$	6.00E-03±5.80E-04
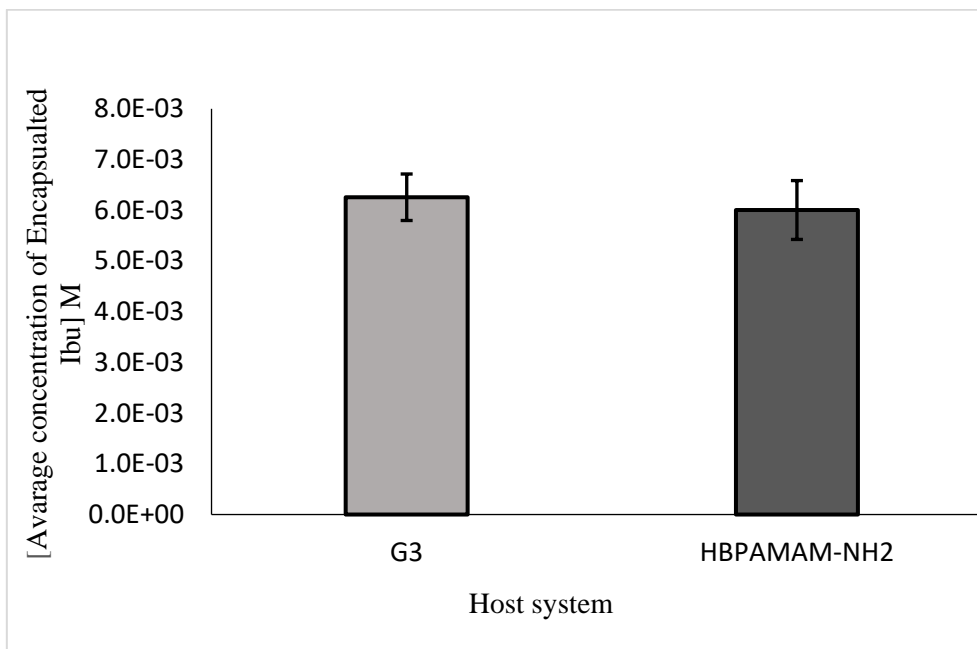
Figure 7. 1: The comparison in average concentration of encapsulated ibuprofen between G3 and HBPAMAM-NH$_2$, the host systems concentrations at 0.32 mg/mL.

The dendrimer's encapsulation ability was not significantly different from the HBP's; therefore, it was clear that there was no difference in the ability to encapsulate Ibuprofen. In this respect, it is clear that the HBP is performing at as well as the more complicated dendrimer-based system. At this point we decided to compare the smaller G2.0 amine terminated PAMAM dendrimer (M =1429) with the amine ended PAMAM HBP. However, it was possible that the above-mentioned systems were aggregates at a concentration of 0.32mg/mL, the new experiments were conducted at a corresponding concentration of 0.143mg/mL for each of both systems (G 2.0 **4** Dendrimer vs. HBPs). The data is shown below in Table 24 and Figure 7.2.

Table 24: Encapsulation study of ibuprofen by G2 and HBPAMAM-NH₂ into two datasets

Host System	Trial one			Trial two		
	Δ Abs	[Encapsulated Ibu] M	*[Increased Ibu] M	Δ Abs	[Encapsulated Ibu] M	*[Increased Ibu] M
G2 **4**	0.427	1.47E-03	7.00E-03	0.418	1.44E-03	6.69E-03
HBPAMAM-NH₂ **17.3**	0.445	1.53E-03	7.62E-03	0.436	1.50E-03	7.31E-03
* The concentration of encapsulated Ibuprofen after subtracting free concentration of ibuprofen in buffer 7.72E-4 mol dm-3						

Host System	Average [Encapsulated Ibu] M
G2	6.85E-03±2.19E-04
HBPAMMA-NH₂	7.47E-03±2.19E-04
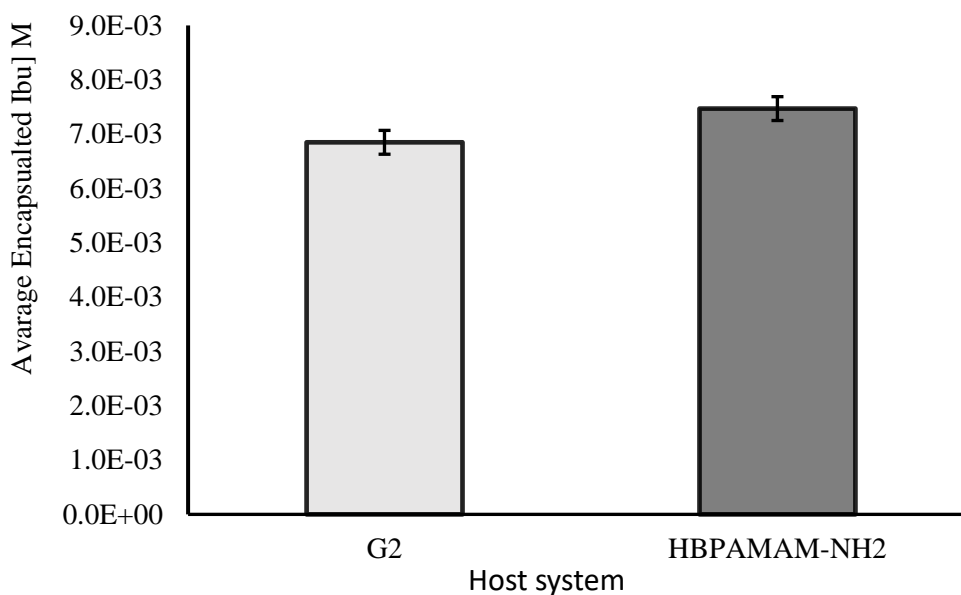
Figure 7. 2: The comparison in average concentration of encapsulated ibuprofen between G2 and HBPAMAM-NH₂ at concentration of 0.143 mg/ml.

Interestingly, at this lower concentration, the HBPAMAM-NH$_2$ encapsulates a significant amount of Ibuprofen in comparison to the G2 **4** dendrimer. It is due to the higher molecular weight and larger size of the HBP, which provides more space for encapsulation. However, the size of encapsulation levels in comparison to polymer concertation, it was found that at the lower concentration (0.14 mg/ml) of the same HBP, ibuprofen binds significantly more than at the higher concentration (0.32 mg/ml). To a certain extent, this was predictable based on our earlier observations regarding aggregation (and the negative effect on encapsulation). Less obvious, was the observation that the smaller dendrimer at 0.14 mg/mL could bind more ibuprofen than the larger dendrimer at 0.32 mg/mL. Again, the reason for this is probably due to aggregation of the G3.0 **6** dendrimer.

The results of these experiments suggest that the much simpler and more accessible HBPs can indeed be used as efficient drug delivery systems. When compared to similarly functionalised dendrimers, it looks as if the HBP was able to encapsulate more small drug molecules than an equivalently functionalised dendrimer. However, it is also clear that the level of aggregation influences the amounts of drug that can be encapsulated. In addition, the amine ended systems represented a valuable model to make an initial evaluation that could test our aims, these molecules cannot be used clinically. Due to the amine ended systems when added to aqueous solution, it can be protonated, which leads to a densely packed surface charge leading to homolysis.[151] To overcome this problem a series of neutral dendrimers were synthesised, and studies and the bulk of this data was reported in a previous chapter. The following section simply reports and compares the data obtained for equivalently functionalised OH terminated systems. The following section compares equivalently functionalised dendrimers and HBPs but examines neutral OH-terminated dendrimers.

7.3. Encapsulation of Ibuprofen using Hydroxyl ended PAMAM dendrimer (G3.0-OH) and Hydroxyl ended Ar-HBPAMAM-OH

It was essential to compare HBP-OH with both dendrimers since Ar-HBPAMAM-OH **23** aqueous GPC analysis reveals a tri-modal hyperbranched polymer. Because of this, it is not possible to confidently state the molecular weight of the Ar-HBPAMAM-OH. Additionally, It is difficult to distinguish which fraction produced the observed results; it could be any one of the three fractions or a combination of them. However, there is one peak, inside the calibration curve, with an estimated Mn value of 2300. Due to the possibility of Mn being greater or less than this value, we compare Ar-HBPAMAM-OH with G3.0-OH 10 with a molecular weight of 3272 g mol^{-1}. Dendrimer would be anticipated to be superior at encapsulation in this study. Dendrimers are monodispersed, so we are confident that each molecule in solution has the same amount of Mr and drug loading capability. However, the HBPs are polydisperse, therefore we expect the average encapsulated concentration would be lower because of their polydisperse nature. It is because HBPs are composed of a combination of large HBPs and smaller polymers, which lead to poor encapsulation efficiency.

The comparison of encapsulation studies was conducted with Ar-HBPAMAM-OH and G3.0-OH, using ibuprofen as the model drug. This encapsulation was performed similarly to what was conducted before. All parameters that were used in this experiment are stated in the current chapter in Section 7.2. The data of the encapsulation are showed in Table 25.

Table 25: Encapsulation data for G3.0-OH and Ar-HBPAMAM-OH into two datasets

Host system	Trial one			Trial two		
	Δ Abs	[Total Ibu] M	[Encapsulated Ibu] M	Δ Abs	[Total Ibu] M	[Encapsulated Ibu] M
G3.0-OH **10**	0.4063	5.12E-03	4.60E-02	0.4047	5.10E-03	4.58E-02
Ar-HBPAMAM-OH **23**	0.4131	5.21E-03	4.69E-02	0.3923	4.94E-03	4.42E-02

Host System	[Average concentration of Encapsulated Ibu] M
G3.0-OH	4.59E-02 ± 1.01E-4
Ar-HBPAMAM-OH	4.55E-02 ± 1.31E-3
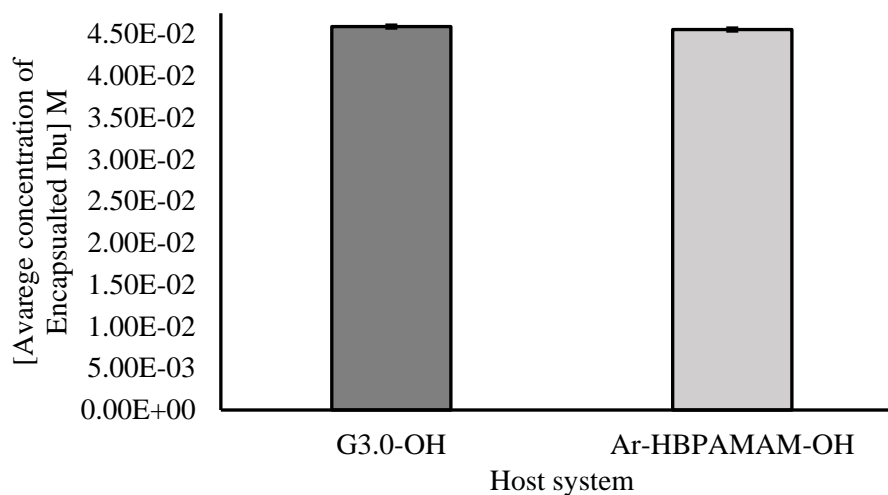
Figure 7. 3: The comparison in average encapsulated concentration between G3.0-OH and Ar-HBPAMAM-OH at concentration 0.32 mg/mL. In both sets of data, error bars overlap, indicating there are no significant difference

According to the data based on Table 25, the G 3.0-OH **10** dendrimer and the Ar-HBPAMAM-OH **23** were able to encapsulate similar amounts of drug, the data is also shown graphically in Figure 7.3. This result is similar to the one obtained for the amine ended systems discussed above. However, there is a major difference and that relates to the levels of encapsulation.

Specifically, the OH ended macromolecules appeared to encapsulate significantly more than the amine ended systems. For example, the amine encapsulation concentrations were 6.0E-03 M, but the OH ended systems had a much higher level of encapsulation and encapsulated around 4.50E-02 M ibuprofen. This difference could be due to a lack of aggregation for neutral OH end systems (G 3.0-OH and Ar-HBPAMAM-OH) .It is well known that charged systems aggregate at much lower concentrations than neutral molecules. [152]

7.4. Encapsulation of Zn TDHPP using G2 and HBPAMAM-NH$_2$

Having successfully demonstrated that the OH ended systems could encapsulate ibuprofen with equal levels of efficiency, we wanted to see if the same was true for a different drug. Specifically, one that was larger and also could interact with the systems in a different way. As such we investigated a metallo-porphyrin. Specifically, zinc tetra-dihydroxy-tetraphenyl porphyrin (Zn-TDHPP **14**). This porphyrin could interact with the OH systems through the same hydrophobic, H-bonding, and electrostatic interactions involved during ibuprofen encapsulation but could also form strong metal to ligand bonds with the internal amines. Zn THDPP was encapsulated and the concentration Zn-TDHPP was determined as previously described. An extinction coefficient of 37,356 dm^3 mol^{-1} cm^{-1} and a maximum solubility of 7.76E-6 mol dm^{-3} (in phosphate buffer) was determined for the Zn TDHPP. Polymer concentrations were selected so that they would be below any aggregation limits previously determined for the amine ended dendrimer. Therefore, the G2.0 amine terminated PAMAM dendrimer was used at a concertation of 0.05 mg/mL and the encapsulation data is shown in Table 26 and graphically in Figure 7.4.

Table 26: Encapsulation study of Zn TDHPP by G2 and HBPAMAM-NH2 into two datasets

Host system	Trial one			Trial two		
	Abs	[Total Zn TDHPP] M	[Encapsulated Zn TDHPP] M	Abs	[Total Zn TDHPP] M	[Encapsulated Zn TDHPP] M
G2	0.3270	8.75E-06	9.94E-07	0.3321	8.89E-06	1.13E-06
HBPAMAM - NH$_2$	0.3222	8.6330E-06	8.73E-07	0.3283	8.78E-06	1.03E-06

Host System	Average [Encapsulated Zn TDHPP] M
G2 **4**	1.060E-06 $\pm$ 7.3616E-08
HBPAMAM-NH$_2$ **17.3**	9.75E-07 $\pm$ 7.76314E-08
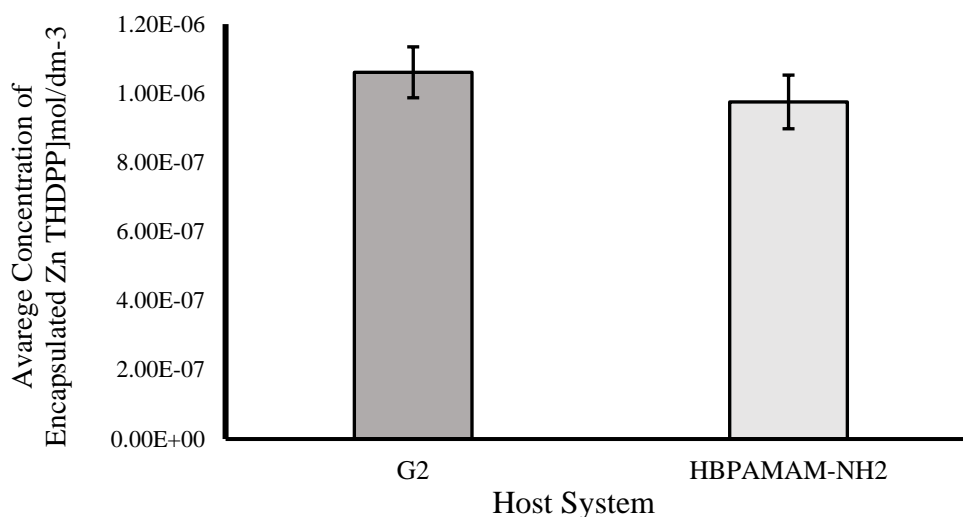
*Figure 7. 4: The comparison in average concentration of encapsulated Zn TDHPP **14** between G2 **4** and HBPAMAM-NH$_2$ **17.3** at concentration 0.05 mg/mL.*

As with the ibuprofen results, it is clear that there is no real difference between the encapsulation ability of the HBPAMAM-NH$_2$, and the G2.0 amine ended dendrimer. Therefore, there does not seem to be a significant advantage in using the less accessible and more complicated dendrimer systems. However, this conclusion needs to be considered alongside the fact the HBP studied was bigger than the dendrimer. The only real difference is

again related to the level of encapsulation. That is, considerably less porphyrin is encapsulated relative to ibuprofen. This is presumably due to the size difference between the two drug molecules.

7.5. Summary

A comparison was conducted between the HBPAMAM-NH$_2$ and G2/G3 PAMAM NH$_2$ dendrimers. It was found that the ability of HBP-NH2 and G2/3 to encapsulate drug molecules was not significantly different. A similar comparison was performed using Zn TDHPP. Based on the data, both systems encapsulated porphyrin equally well, with a concentration of 1.0E-06 M. The difference between the two values is insignificant. The comparative study between the Ar-HBPAMAM-OH and the G3.0-OH dendrimer, showed that both could encapsulate similar amounts of Ibuprofen at concentrations of 4.50E-02 M and 4.60E-02 M, respectively. This means that both dendrimers and HBPs are equally effective in encapsulating drug molecules and the differences in their encapsulation properties are not significant.

Chapter 8 : Conclusions

8.1. Conclusions

In recent years, dendrimers have demonstrated considerable promise as drug carriers. Among their superior characteristics is their ability to encapsulate small host molecules in their globular structures at high generations. The ability to modify functionality opens up opportunities for active and passive drug targeting, which suppresses side effects associated with them. However, dendritic systems are not perfect, as previously discussed. Consequently, both academia and industry have been looking at other macromolecules that are capable of delivering drugs like dendrimers. A simpler alternative may be offered by HBPs because their synthesis is effortless often entailing just one pot. Although HBPs and dendrimers have been compared before, they have not been like for like comparisons to address the shortfall currently present in the literature, this project studied the two macromolecules like for like with respect to their size and functionality.

First, we synthesized a series of PAMAM dendrimers. were synthesized, ranging from G 0.5 to G3.5. The steps of Michael addition and amination were repeated sequentially to build the desired dendrimers. A water soluble PAMAM dendrimer (OH-ended PAMAM dendrimers) was synthesised by modifying the ester terminal groups to the hydroxyl groups, result in OH-ended dendrimers (8OH, 16 OH and 32 OH). Initially, a study was conducted to investigate the dendrimers' ability to encapsulate drug molecule based on dendrimer size and determine any dense packing effects. We studied three generations of dendrimers (G2.0-OH, G3.0-OH, G4.0-OH) at a concentration of 1×10^{-4} M. The ability of the dendrimers to encapsulate a drug molecule was dependent on the size of PAMAM dendrimer generation. It was found that the G 3.0-OH was the best generation for encapsulation of Ibuprofen, with a loading of 12. The higher-generation G4.0-OH could only encapsulate 9 equivalents due to a more densely packed structure. As such, the G3.0-OH dendrimer was determined as the most suitable generation for encapsulation of small hydrophobic drugs. The concentration limits with respect to the

G3.0-OH dendrimer were studied at different concentrations ranging from $1.0E^{-3}$ to $1.0E^{-6}$ M. The results demonstrated that the amount of ibuprofen that the G3.0-OH dendrimer could encapsulate increased (roughly) linearly up to a dendrimer concentration of 2.50E-04 M. Above this concentration the loading remained constant and plateaued. Dynamic light scattering (DLS) indicated that dendrimers at concentrations above 2.50E-04 M were much larger than those measured at lower concentrations (200 nm vs 5 nm respectively). study carried out to measure the size distribution for G3.0-OH at 1.0E-04 M and It was therefore concluded that the observed decrease in encapsulation ability was due to aggregation of dendrimer at higher concentrations. As such, it was important to keep concentrations below 2.50E-04 M for future encapsulation experiments (when comparing to equivalent HBPs).

The stability of the ibuprofen dendrimer complexes was studied in a light and dark environment for ten days. The study was performed to determine the effect of dendrimer size on complex stability, and used the G2.0-OH, G3.0-OH and G4.0-OH dendrimers. In dark conditions, drug complex stability was observed to be 50% better than same complex in the light (1.0E-04 M Day^{-1}). and (5.0-E-05 M Day^{-1}), respectively).

A similar encapsulation study was also undertaken to investigate the effect of metal coordination on the encapsulation ability of porphyrin molecules with potential application in photodynamic therapy (PDT). Tetradihydroxyphenyl porphyrin (TDHPP) was selected as our test species, as this has previously been used clinically for the successful treatment of cancers by PDT.TDHPP and Zn TDHPP were synthesised and characterised successfully. Encapsulation studies using the same PAMAM dendrimers (G2.0-OH, G3.0-OH and G4.0-OH) were then undertaken. The results showed that significant improvements in the levels of encapsulation and solubility occurred for the metalated species. For the G3 .0 OH, encapsulation increased from 4 to 7 equivalents for the free base and metalated porphyrins respectively. For the G4.0-OH the change was more significant, rising from 10 to 17

equivalents for the free base and metalated porphyrins respectively. In both cases (G 3.0 and 4.0), the amount of encapsulation was more than the total number of available tertiary nitrogen within the dendrimers. However, UV spectroscopy clearly indicated that all of the ted porphyrins were coordinated (a large shift in the wavelength of the Soret band was observed). As such, we postulate that some of the increase may come from additional coordination to the terminal OH group. This may also account for the fact that the amount of encapsulated porphyrin increased with higher dendrimer generation, which was not observed when ibuprofen was used. Clearly, the secondary coordination interactions contribute significantly to porphyrin loading and encapsulation.

Two HBPs were successfully synthesised (HBPAMAM-NH$_2$ and Ar-HBAPAMAM-OH). However, the HBPAMAM-NH$_2$ was not stable to particular reaction conditions and could not be converted to hydroxyl ended groups. Nevertheless, encapsulation studies were carried out for both polymers and compared to similar dendrimers (with respect to terminal group). For HBPAMAM-NH$_2$, the Ibuprofen concentration increased linearly until it reached at 0.04 mg/mL, and then it plateaued. DLS analysis showed a more gradual aggregation of the HBPs, compared to the more quantised aggregation of the dendrimers. The encapsulation study using Ar-HBPAMAM-OH confirmed that they could encapsulate more Ibuprofen molecule than HBPAMAM-NH$_2$.

The final part of this project and one of its main aims, was to compare the encapsulation ability of similar HBPs and dendrimers, with a view to their use as potential drug delivery systems. First, the comparison between the HBPAMAM-NH$_2$ and the G2/G3 PAMAM NH$_2$ dendrimers were studied. This revealed that HBP-NH$_2$ and G2/3 abilities to encapsulate drug molecule was not significant different. For example, the G2 PAMAM dendrimer could encapsulate ibuprofen with maximum concentrations of 7.5E-03 and 7.0E-03, respectively. A similar comparison was carried out using Zn TDHPP. According to the data, both systems could encapsulate equally

well, with both encapsulating the porphyrin with a concentration 1.0E-06 M. Since there is an infinitesimal difference between the two values, their difference is not significant.

The comparative study using the Ar-HBPAMAM-OH and the G3.0-OH dendrimer, again revealed that both systems could encapsulate similar amounts of Ibuprofen with concentration of 4.50E-02 M and 4.60E-02 M, respectively.

If we compare the amine-terminated systems (HBPs and dendrimers) with the OH terminated systems (HBPs and dendrimers), we could see a big difference in their encapsulation ability. For example, the NH_2-terminated HBP could encapsulation 6.0E-03 M of the Ibuprofen whereas in the OH terminated Ar-HBP could encapsulate 4.50E-02 M of Ibuprofen, an amount nearly 10 times higher.

Overall, it seems clear that HBPs are plausible and cheaper alternatives to dendrimers as drug delivery systems. However, it's worth mentioning that dendrimers possess a regular and perfectly balanced mono-dispersed structure that satisfies drug approval agencies with respect to size and dispersity and potential clinical application. On the other, HBPs are often very polydisperse with respect to molecular weights and structures. As such, it is more difficult to obtain the types of narrowly dispersed materials required by drug approval agencies. Therefore, if HBPs are to be used as drug delivery systems, it will be necessary to improve both their synthesis and purification techniques.

Future work is required to compare the systems in vitro and obtain a better comparison of the delivery abilities of the two systems (HBPs and dendrimers). This will also enable us to study the ability of both systems to improve the delivery and therapeutic effects of the drugs they carry. Another area for future study will be to develop the ideas around the solubilisation and site-specific delivery of photosensitizers for PDT. Intrinsic cytotoxicity can be overcome by specific chemical modifications with respect to amine terminated ($HBbPAMAMNH_2$).

Complexation with different bioactive molecules allows for optimal delivery while being delivery-independent and safe for the cell as well as the payload. additional research may be carried out within the research group to study the degradation of HBPAMAM. Other related considerations for instant: controlled release mechanism, controllable aggregation; need investigations to develop more efficient nanocarrier systems under physiological conditions. Further research should involve PDT studies, toxicity test for both systems. The future of hyperbranched nanocarriers is bright as they will move more into applications with ease of synthesis and scale up being the major driving forces. It is expected that different topologies, flexibility, and compositions of nanocarrier systems will expand the categories and functionalities of functional hyperbranched polymers presented here. Due to these factors, hyperbranched polymers will continue to be a promising platform for a variety of applications.

Chapter 9 : Experimental

9.1. Experimentations

9.1.1. Solvent and glassware

Most of the chemicals and reagents were obtained from a commercial supplier (primarily from Sigma-Aldrich) and were used directly without further purification. Dry solvents were obtained from the University of Sheffield Chemistry Department Grubbs solvent supply system. The glassware used for this project was cleaned and oven-dried at 500 °C for about 2 h.

9.1.2. Nuclear magnetic resonance spectroscopy (NMR)

All samples were analysed using a Bruker 'AV3HD-400' machine at the University of Sheffield Chemistry Department NMR Facility. Roughly 2 mL of each sample was introduced into the NMR tube, along with approximately 2 mL of deuterated solvents supplied by (Sigma Aldrich). The NMR spectra were examined using Topspin 3.0 NMR software.

9.1.3. Mass spectroscopy (MS)

Two types of mass spectrometry were performed to determine the mass of compounds. Electrospray Ionisation Mass Spectrometry (ES-MS) was used for low molecular weight products (less than 1000 Da) and recorded using a Micro mass Prospect spectrometer. For the molecular weight of compounds more than 800 Da, Matrix-Assisted Laser Desorption Ionisation Time of Flight (MALDI-TOF) mass spectrometry was used. Using dithranol or dihydroxy benzoic acid matrices, the experiment was carried out on Bruker III mass spectrometer.

9.1.4. UV-vis spectroscopy

The ultraviolet absorbance was recorded using an Analytik Jena AG Specord S-600 Specord instrument. All solutions were prepared in an appropriate solvent, before measurements, the instrument was calibrated using a standard solution.

9.1.5. Dynamic light scattering (DLS)

The diameters of particle size for polymer were determined by dynamic light scattering (DLS) on a Zetasizer Nano ZS instrument (ZEN 3600) at 25 ^{0}C.   The DLS measurements were typically made in triplicate.

9.1.6. Gel permeation column (GPC)

 Aqueous GPC data was implemented using Millipore Waters Lambda-Max 481 LC spectrometer with an LMW/HMW column. Non-ionized water was used as eluent. Calibration of GPC system determined using polyethylene glycol (PEG) standards (Mn 2000-5000 Da). The raw data was then characterized using GPC online software.

9.1.7. Gel permeation Chromatography (GPC)

GPC experiments were carried out using an Agilent Technologies 1260 Infinity machine. Only the low molecular weight column E (3 x PLgel Mixed B with Guard), which can measure molecular weights up to 50,000, was used for the experiments. Samples were prepared with a GPC grade THF solution containing toluene as a flow marker at a concentration of 1 mg/mL and filtered through a filter prior to analysis. Using a polystyrene standard as a calibration, the machine is run for 30 minutes after injection and the data obtained are analysed using Agiernt GPC/SEC software.

9.8. Infrared (FTIR) Spectroscopy

 FT-IR Spectrometer was used, and the spectra was analysed by a Perkin Elmer.

9.1.9. pH measurement

The pH of the buffer solution prepared was measured using a pH 210 Microprocessor pH Meter from Hanna Instruments Ltd. (Leighton Buzzard, UK). The pH probe was calibrated using

calibration solutions at two reference standards pH 4.0 and pH 7.0, prepared with buffer tablets (Sigma-Aldrich, Poole, UK).

9.2. Synthesis of PAMAM dendrimers

9. 2.1. General synthesis of half anionic PAMAM dendrimers

In a 500 ml round bottom flask, Methyl acrylate in an excess amount was added dropwise over 30 minutes to a solution of the previous amine terminated PAMAM dendrimer (or EDA in case of synthesizing PAMAM G 0.5 dendrimer) dissolved in MeOH then the reaction serried at room temperature for a period depending on the generation of the dendrimer. The unreacted solvents of excesses methyl acrylate and MeOH were removed via rotary evaporation at 40°C and placed under a high vacuum for definite purity of the ester terminated PAMAM dendrimer products.

9.2.2. General synthesis of full generation cationic PAMAM dendrimers

In a 500 ml round bottom flask, the previous ester terminated PAMAM dendrimer was dissolved in methanol, then EDA was added dropwise over a period of 30 minutes to a stirred without heat applied. After that, the reaction was stirred at room temperature for several days. the solvent was removed via rotary evaporation at 45 °C. Then for purification, the excess EDA was removed by the addition of a 9:1 azeotropic mixture of toluene: MeOH, this step was repeated as many times as necessary to remove all the EDA and give the full generation PAMAM dendrimer product.

9.2.3. Synthesis of G 0.5 PAMAM dendrimer

The ethylene diamine EDA (3 g, 0.04 mol) was dissolved in methanol (50 mL). then methyl acrylate was added dropwise to the reaction solution in an excess amount (25.11 g, 0.29 mol) at 0°C for 40 mins. The reaction mixture was kept stirring overnight at room temperature. Excess methyl acrylate and methanol were removed by rotary evaporator, this step was repeated three times until yellow oil product was obtained (17 g. 85 %).

ES-MS, 405 (MH$^+$), ^{1}H NMR (MeOD, 400 MHz): δ 3.69 (s, 12H), 2.77 (t, 8H), 2.55 (s, 4H), 2.49 (t, 8H); 13C NMR (MeOD, 400 MHz) δ ppm 173.1, 51.3, 50.5, 49.4, 47.5, 31.8. FTIR (cm^1), 3287 (mide, NH), 2945 (OCH3, stretch), 1730 (C=O, ester), 1465 (CH2, bend).
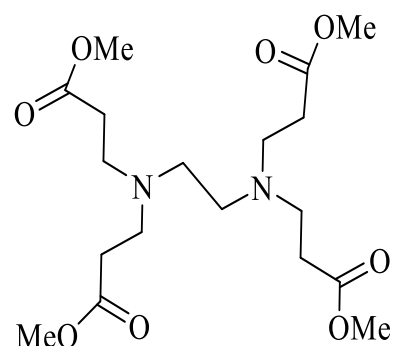
9.2.4. Synthesis of G 1 PAMAM dendrimer

The ester terminates PAMAM G 0.5 dendrimer (17 g, 0.042 mol) was added dissolved in methanol (150 ml) and ethylenediamine (50g, 0.84 mol) was then added dropwise and kept stirring for 5 days. The excess EDA and solvent were then removed by washing the mixture with an azeotropic combination of 9:1 toluene: methanol solution. This purification procedure was carried out several times until all EDA was completely removed. The product was then dried under a high vacuum for 3 h. the product was a honey-coloured oil (45 g, 93%).

Mass spec ES-MS, 516 (MH+), ^{1}H NMP (MeOD, 400 MHz):3.69(s, 8H), 3.33-3.27 (mm, 16H), 2.81-2.41 (m, 20H). 13C NMR (MeOD) δ ppm 173.5, 51.1, 49.9, 48.2, 38.1, 33.3. FTIR λ (cm^{-1}) 3280 (amide, NH, Stretch), 2979, 2953 (CH), 2859, 1636 (amide, C=O stretch), 1546, (amide NH bend), 1436 (CH2 bend), 1356, 1283, 1112, 1030, 940.
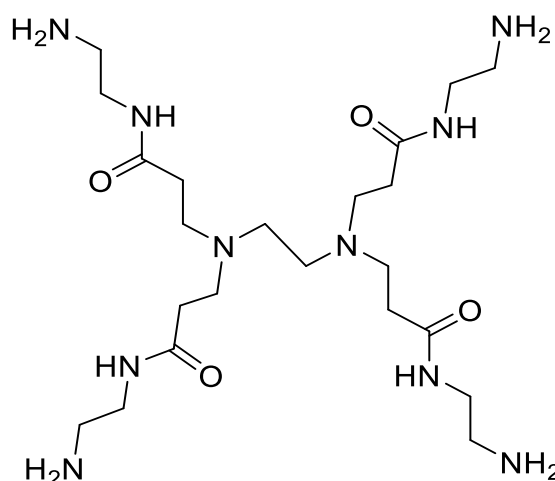
9.2.5. Synthesis of G 1.5 PAMAM dendrimer

The PAMAM dendrimer with four amine terminal groups G 1 (20.25 g, 0.042 mol) was dissolved in methanol (150 mL) in a round bottom flask (500 ml). Then, methyl acrylate (62.51 g, 0.73 mol) was dropped into the reaction solution. The solution was left stirring overnight at room temperature for three days. The solvent was concentrated at reduced pressure at 45 °C once the reaction was completed. The product was then dried and obtained as a yellow sticky oil (50 g, 90%).

Mass spec MALDI-TOF: 1206 (MH+): ^{1}H NMR (MeOD, 400 MHz), 3.69 (s, 24H), 3.38-3.23(m, 24H), 2.87-2.36 (mm, 44H):^{13}C NMR (MeOD, 400 MHz) δ ppm 173.5, 173.2, 52.4, 50.7, 49.8, 49.21, 37.1, 32.2, 31.9; FTIR λ (cm-1) 3311 (NH, stretch), 2952 (CH, stretch), 2877, 1735 ,1650 (C=O, ester), 1538(NH), 1436 (CH2, bend).
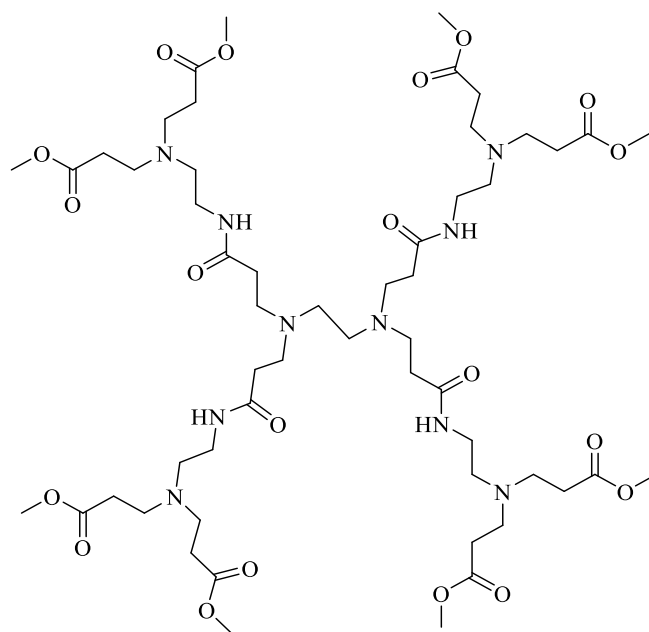
9.2.6. Synthesis of PAMAM G2.0 PAMAM Dendrimer

The generation 1.5 ester terminated groups PAMAM dendrimer (15.65 g, 0.013 mol) was dissolved in (100 ml) methanol, then EDA (12.5 g, 0.028 mol) was added to the reaction solution via dropwise Technique for 45 minutes. The reaction was stirred in the room temperature for 5 days. After the reaction was allowed to react completely, the azeotropic mixture of 9:1 methanol: toluene was used to wash the product and remove the unreacted EDA. The purifying procedure was repeated several times until all EDA was completely removed. This product of PAMAM dendrimer G 2.0 was honey /brown thick oil (19.78 g, 98 %). Mass spec MALDI-TOF:1429 (MH+), ^{1}H NMP (400 MHz, MeOD) δ, 4.91 (s, 4H), 3.65(s, 8H), 3.40-3. 24H), 2.88-2.26 (mm, 76H), ^{13}C NMR (MeOD): 173.2, 50.7, 48.3, 46.1, 41.2, 35.9, 32.0, 31.7; FTIR λ cm^{-1} , 3276 (NH, stretch), 2938 (CH, stretch), 1646 (C=O, amide), 1556 (NH - bend).

Mass spec MALDI-TOF:1429 (MH+), ^{1}H NMP (400 MHz, MeOD) δ, 4.91 (s, 4H), 3.65(s, 8H), 3.40-3. 24H), 2.88-2.26 (mm, 76H), ^{13}C NMR (MeOD): 173.2, 50.7, 48.3, 46.1, 41.2, 35.9, 32.0, 31.7; FTIR λ cm-^{1} , 3276 (NH, stretch), 2938 (CH, stretch), 1646 (C=O, amide), 1556 (NH - bend). **Synthesis of**
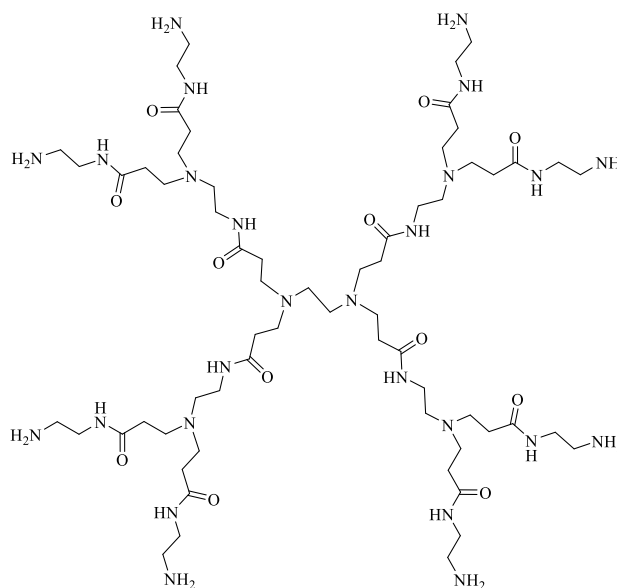
9.2.7. PAMAM G 2.5 PAMAM Dendrimer

A methyl acrylate (66.43 g, 0.77 mol) was added drop by drop to a stirred solution of the mine terminated product, which is dissolved in 150 ml methanol, from the previous synthesis (27.57 g, 19.28 mmol). The reaction was left stirring at room temperature for three days. After that, methanol and methyl acrylate were eliminated via a rotary evaporator. the product was dried under an ultra-high vacuum for 5 hours yielding a sticky honey-coloured oil (38 g, 70 %).
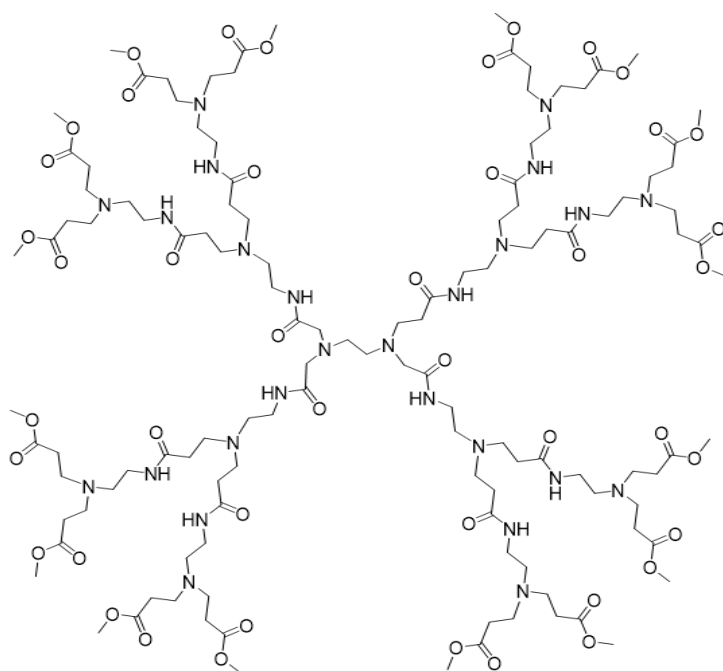
Mass spec MALDI - TOF 2805(MH+), ^{1}H NMR (MeOD, 400MHz) 3.69 (s, 48H), 3.37-3.22 (m, 12H), 2.91-2.32 (mm, 152H) ; ^{13}C NMR (MeOD, 400MHz) δ ppm 173.2, 173.3, 52.4, 51.2, 49.1, 48.7, 37.8, 34.1, 32.1; FTIR λ (cm^{-1}) 3297 (N-H, amide stretch), 2952 (CH, stretch), 2837, 1737 (C=O, ester), 1647 (C=O, amide), 1552 (NH, amide bend), 1438 (CH2, bend).

9.2.8. Synthesis of G3.0 PAMAM Dendrimer

A PAMAM G2.5 (31.88 g, 11.36 mmol) was stirred in 150 mL of methanol. Dropwise additions of EDA (79.33 g, 1.32 mol) were made for 30 minutes. the reaction solution was left to react at room temperature for 5 days. an azeotropic solution 2.0 L mixture of 9:1 toluene: methanol was used to remove EDA from the crude product. EDA was wholly eliminated by repeating the purification process, after washing with methanol (100 mL). The product was dried to yield a yellow oil (43 g, 95 %).

Mass spec TOF MALDI-MS, 3257 (MH+). ^{1}H NMR (400 MHz, MeOD), 3.27 (t, 24H, NHCH$_2$), 2.81 (t, 32H, CH$_2$N), 2.74 (56H, t, CH2N), 2.61 (32H, t, NCH2), 2.38 (56H, t, CH2C=O); FTIR λ (cm^{-1}), 3291 (NH, amide stretch), 3092 (C-H, stretch), 1638 (C=O) 1560 (N-H, amide bend), 1486 (CH2, bend).
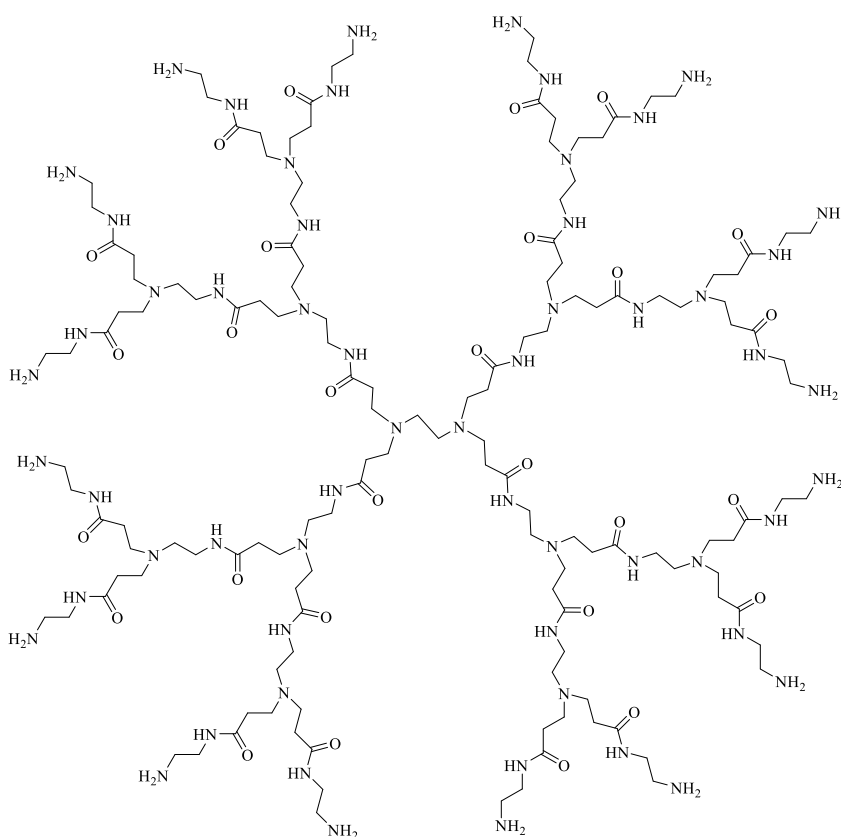
9.2.9. Synthesis of G 3.5 PAMAM Dendrimer

A PAMAM G 3.0 (33.43 g, 10.26 mmol) in methanol (100 mL) and stirred. Methyl acrylate (129 g, 1.5 mol) was added dropwise for 45 minutes. The reaction mixture was allowed to react for 5 days. Methyl acrylate and the excess solvent were eliminated at 4 ^{O}C

under reduced pressure. The product of G3.5 was obtained as a sticky yellow/brown (56 g, 85 %).

Molecular Weight: 6011.12
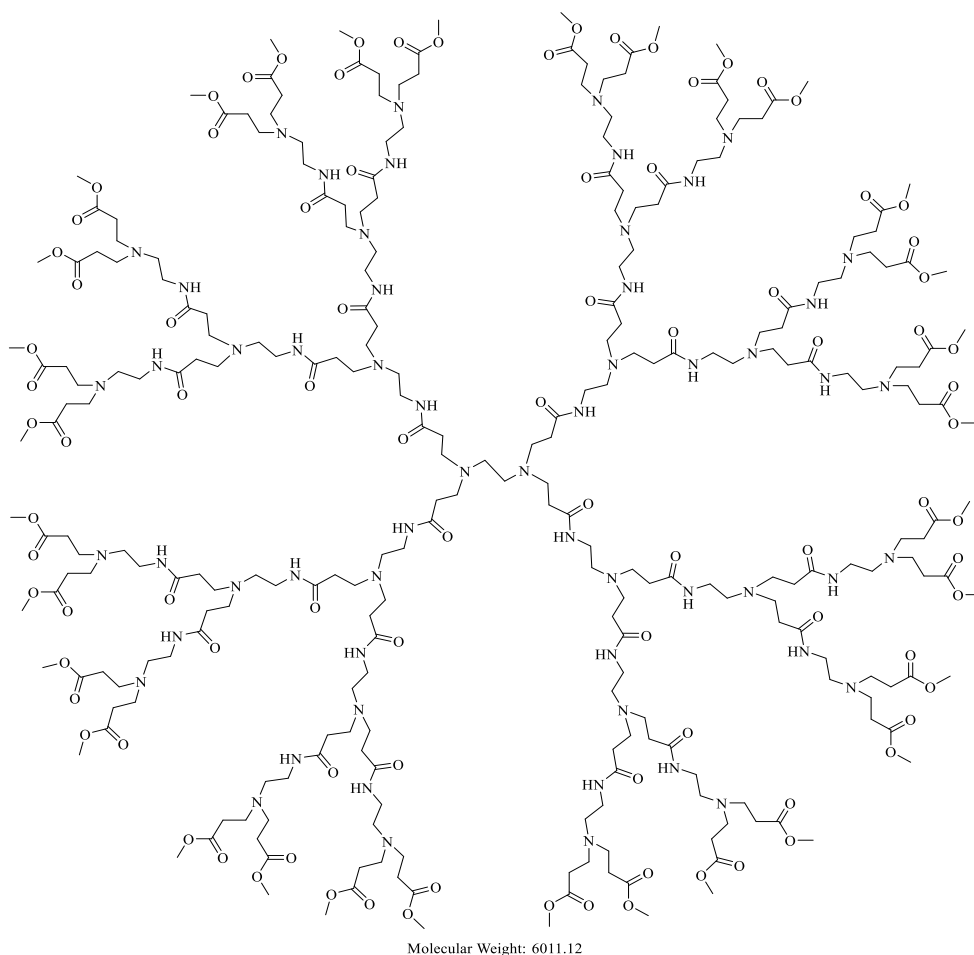
Mass spec TOF MALDI-MS, 6012 (MH+) ^{1}H NMR (MeOD, 400MHz) δ 3.69 (m, 96H), 3.39-3.27 (m, 56H), 2.9-2.36 (mm, 300H); ^{13}C-NMR (MeOD, 400MHz) δ ppm 174.5, 173.5, 52.7, 52. 51.3, 49.7, 49.0, 37.3. 37.2, 33.4, 32.1; FTIR (cm^{-1}): 3298 (N-H, amide stretch), 2953 (C-H, sp3 stretch), 2833, 2105, 1734 (C=O, ester), 1643 (C=O, amide), 1549 (N-H, amide bend), 1439 (CH2, bend), 1361, 1263, 1200, 1043.

9.3. Synthesis of Neutral PAMAM dendrimers

9.3.1. The general procedure of Synthesis Neutral OH terminated dendrimers

In 250 ml around the bottom flask, the generation of half dendrimer was added to DMSO, then the potassium carbonate and ethanolamine were added in droplets to the mixture. After that, the mixture was stirred and refluxed for 3 days at ^{0}C 50. Later, the crude mixture was filtered at reduced pressure to remove residues from potassium carbonate. The filtered product was purified by washing with acetone 200 ml three times. The oil product was settled in the bottom of the flask. The acetone layer was then poured off and 5 ml of distilled water was added to dissolve the product. The product was allowed to be precipitated and settled for 1 hour and the upper layer was poured off. The product was dried in a vacuum oven to give PAMAM-OH dendrimer.

9.3.2. Synthesis of G1-OH PAMAM dendrimer

The half-generation of PAMAM dendrimer (5 g, 12.3 mmol) was dissolved in 10 mL of DMSO. Potassium carbonate (6.77 g, 94.2 mmol) and ethanolamine (3.02 g, 94.2 mmol) were added portion-wise to the mixture. The reaction mixture was stirred and refluxed for 3 days at 50 °C. The purification procedure was followed as mentioned above. The product was dried to yield G 0.5-OH (6.74 g, 50 %) as a yellow oil.

ES-MS 521 (MH+), ^{1}H NMR (D2O,400Mhz) 3.57 (8H, t, CH2CH2OH), 3.24 (8H, m, NHCH2CH2), 2.74 (8H, m, N(CH2CH2), 2.54 (4H, t, CH2CH2N), 2.37 (8H, t, CH2CH2CO). ^{13}C NMR (400 MHz, D2O), 175.0 (C=O),
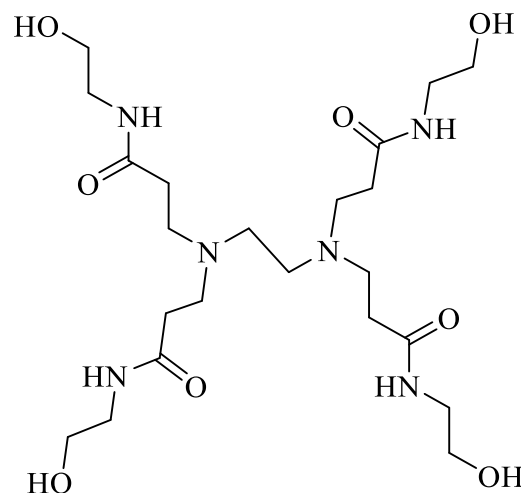
173.5 (C=O), 60.0, 55.0, 50.0, 47.0 , 41.5 , 37.0, 33.0, 33.0 (CH2); FTIR (cm-1) , 3295 (N-H stretch), 3123, 2948, 2845, 1653 (C=O), 1560 (N-H), 1445 (CH2), 1363, 1315, 1223, 1066.

9.3.3. Synthesis of G2-OH PAMAM dendrimer

The G 1.5 PAMAM dendrimer (10 g, 8.29 mmol) dissolved in 10 ml of DMSO. ethanolamine (4.88 g, 0.08 mol) and potassium carbonate (11.05 g, 0.08 mol) were added portion-wise with continuously stirring. The reaction was refluxed at 50 oC for 3 days. Then the crude product was purified as the procedure mentioned above. The product was dried in a vacuum overnight to give G 1.5-OH (18 g, 75 %).

Mass spec (ES), 1438 (MH); H NMR (400 MHz, D2O), 3.51 (16H, t, CH2CH2OH), 3.18 (24H, m, NHCH2CH2), 2.69 (24H, m, N(CH2CH2), 2.50 (12H, t, CH2CH2N), 2.30 (24H, t, CH2CH2CO); ^{13}C NMR (100 MHz, D2O), 175.0 (C=O), 173.5 (C=O), 61, 52.0, 50.0 , 47.0 , 41.5 , 37.0, 33.0 (CH2); FTIR (cm-1) , 3295 (N-H stretch), 3134, 2958, 2847, 1583 (C=O), 1564 (N-H), 1455 (CH2), 1373, 1311, 1213, 1046.
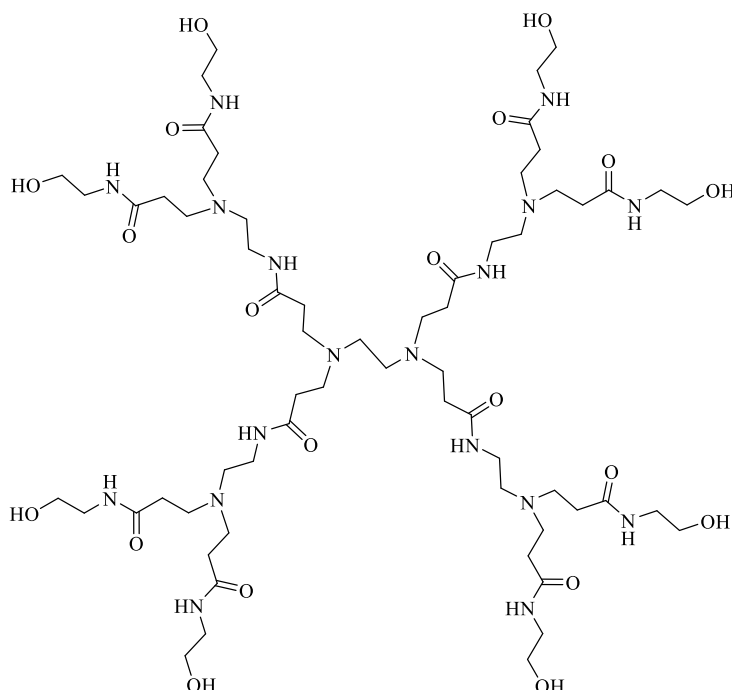
9.3.4. Synthesis of G3-OH PAMAM dendrimer

A PAMAM G 2.5 (6 g, 2.14 mmol) was dissolved in 10 mL of DMSO. ethanolamine (2.66 g, 0.043 mol) and potassium carbonate (5.92 g, 0.042 mol) were added portion-wise to the dendrimer solution. The solution was stirred and refluxed at 50 oC for 72 hours. After, this was followed by a purification process as mentioned in the general procedure (5.76 g, 80 %).
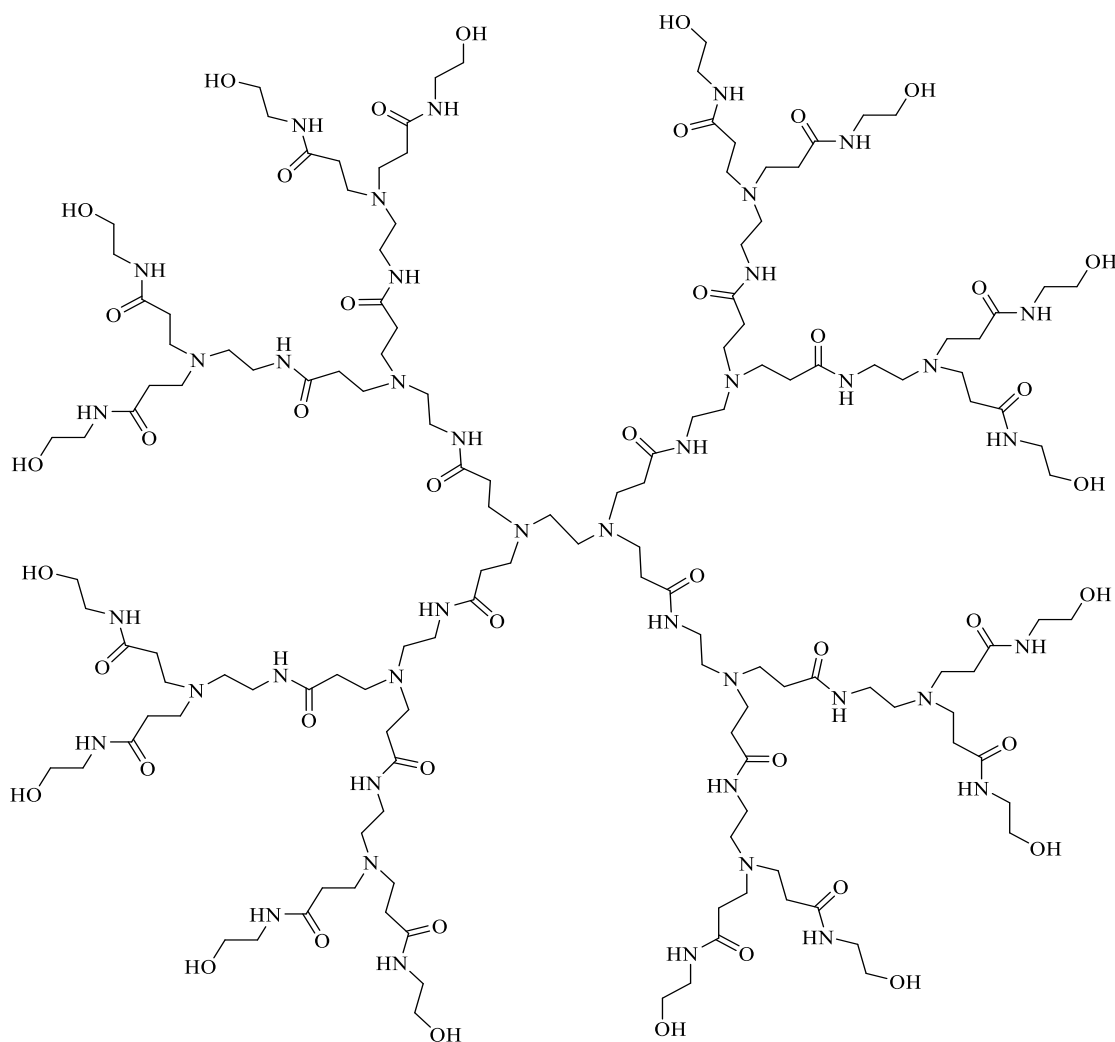
Mass spec TOF MALDI-MS, 3272 (MH+); ^{1}H NMR (400 MHz, D2O), 3.63 (32H, t, CH$_2$CH$_2$OH), 3.33 (56H, m, NHCH$_2$CH$_2$), 2.81 (56H, t, N(CH$_2$CH$_2$), 2.60 (28H, t, CH$_2$CH$_2$N), 2.40 (56H, t, J 7.0 Hz, CH$_2$CH$_2$CO); ^{13}C NMR (400 MHz, D2O), 175.5 (C=O), 174.5 (C=O), 60.0 , 51.5 , 49.0 , 41.5, 39.0 , 36.5 , 33.0 (CH2) ;FTIR (cm^{-1}) , 3423 (N-H stretch), 2945, 1640 (C=O), 1564 (N-H), 1445(CH2), 1317, 1072, 1035.

9.3.5. Synthesis of G4-OH PAMAM dendrimer

DMSO 10ml was used to dissolve G3.5 PAMAM dendrimer (5.12 g, 0.85 mmol) in a round bottom flask. Then ethanolamine (2.07 g, 0.034 mol) and potassium carbonate (4.60 g, 0.033 mol) were added to the dendrimer solution. The dendrimer solution was then stirred and

refluxed at 50 oC for 3 days. Following this, the product was purified and dried as described in the general procedure. The G 3.5-OH was obtained (6.45 g, 98 %).
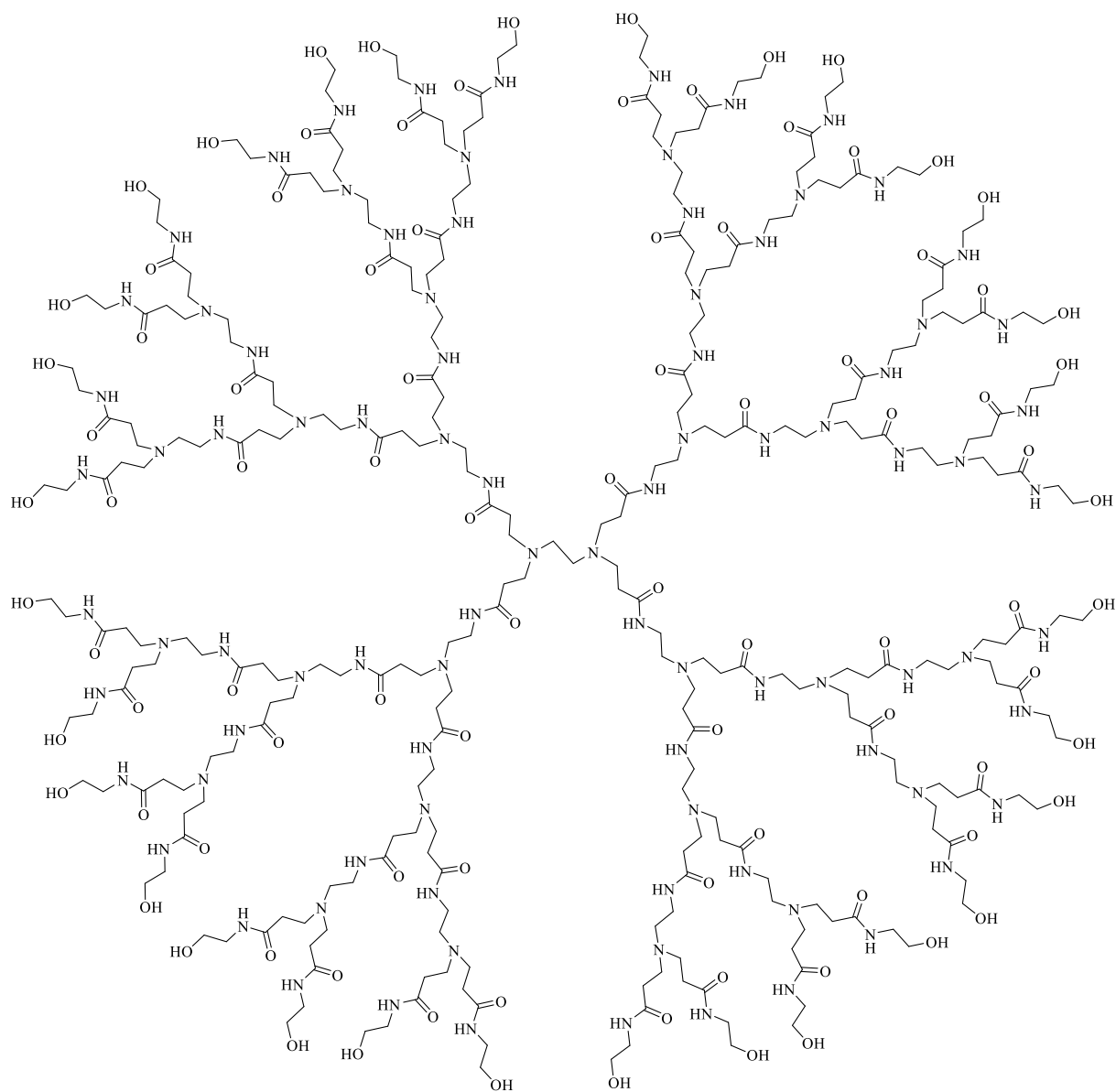
Mass spec TOF MALDI-MS 6940 (MH +); ^{1}H NMR (400 MHz, D2O), 3.55 (64H, t, CH2CH2OH), 3.23 (120H, m, NHCH2CH2), 2.73 (120H, m, N(CH2CH2), 2.54 (60H, t, CH2CH2N), 2.35 (120H, CH2CH2N); ^{13}C NMR (100 MHz, D2O), 176 (C=O), 174.5 (C=O), 59.87 , 60.0, 52.0, 49.0, 48.0, 42.0, 37.0, 32.0 (CH2); FTIR (cm-1) , 3265 (N-H), 3072, 2918, 2826, 1640 (C=O), 1549 (N-H), 1438 (CH2), 1364, 1295, 1030, 958, 885, 824.

9.4. Solubility and Beer-Lambert law experiment for ibuprofen

The solubility of ibuprofen was determined by adding the excess quantity of ibuprofen to a 100 ml conical flask containing 50 ml of phosphate buffer solution pH 7.4. the flask was covered and Shaked at 25 0C for 30 minutes. The sample was filtered via a 0.45 μm syringe filter diluted.

properly and the concentration of ibuprofen was determined by UV spectrophotometry. A 206 mg of ibuprofen was taken into a 100 ml volumetric flask and dissolved in methanol. The concentration of the stock solution was 1×10^{-3} mol/ml. different known concentrations of the standard solutions (0.1, 0.3, 0.4, 0.7, and 1 Mm) were prepared from this stock solution. the absorbance of ibuprofen was measured using UV/vis spectroscopy, and the Δ absorptions values were used at wavelengths from 273 to 278 nm.

9.4.1. Preparation of phosphate buffer

Sodium phosphate dibasic (2.021 g) and sodium phosphate monobasic (0.34 g) were efficiently dissolved in 1.0 L distilled water. The pH was adjusted to 7.43 with HCl or NaOH and the buffer solution was obtained with a concentration of 0.01 M.

9.5. General procedure for the encapsulation

Solutions of PAMAM dendrimer with hydroxyl terminal groups (G2, G3, and G4) and excess amount of ibuprofen were prepared in methanol. After that, the solutions were physically Shaked for 10 minutes. Later, the solvent was removed by a rota evaporator. then, the dendrimer/ ibuprofen complexes were dissolved in phosphate buffer pH 7.4 (10 ml) and filtered to remove any excess ibuprofen. Lastly, all samples were analysed using UV-Vis.

9.5.1. Preparation solutions of (1x10^{-4} M) PAMAM dendrimers (2, 3, and 4 -OH)

For preparing a stock solution of G2-OH (1 x10^{-4} M) a 14 mg was dissolved in 100 ml methanol. Whereas the solution of G3-OH was prepared by adding a 32 mg and dissolving in methanol in a 100 ml volumetric flask. While the G4-OH solution was made by diluting 70 mg in 100 ml methanol.

9.5.2. Preparation of four different concentrations (1x10^{-3}, 1x10^{-4} 1x10^{-5} and 1x10^{-6} M) of G3-OH PAMAM dendrimer

G 2.5-OH solutions of four concentrations were prepared by dissolved (0. 32, 0.032, 0.0032 and 0.00032 mg) in 100 mL volumetric flask to obtain (1x10^{-3}, 1x10^{-4} 1x10^{-5} and 1x10^{-6} M. respectively.

9.5.3. Preparation of four different concentrations of (x 10^{-4} M) G3-OH PAMAM dendrimer

32 mg, 82 mg, 160 mg, and 240 mg of G3-OH PAMAM dendrimer were dissolved in a 100 ml volumetric flask of methanol to make concentrations of 1, 2.5, 5, and 7.5 x10-4 M respectively.

9.6. Synthesis of 5,10,15,20-tetrakis (3, 5-dimethoxyphenyl) porphyrin (TDMPP)

In a round bottom flask a freshly distilled pyrrole (4.80 ml, 70 mmol) and 3, 5-dimethoxybenzaldehyde (11.5 g, 60 mmol) were added to propionic acid (300 ml). The mixture was left under reflux for 30 minutes at 150 ^{0}c. the mixture was cooled to room temperature for 2 hours. The crude mixture was filtrated and washed thoroughly with propionic acid and methanol. The obtained product was dried in a vacuum oven overnight to yield purple crystals (3.5 g, 30 %).
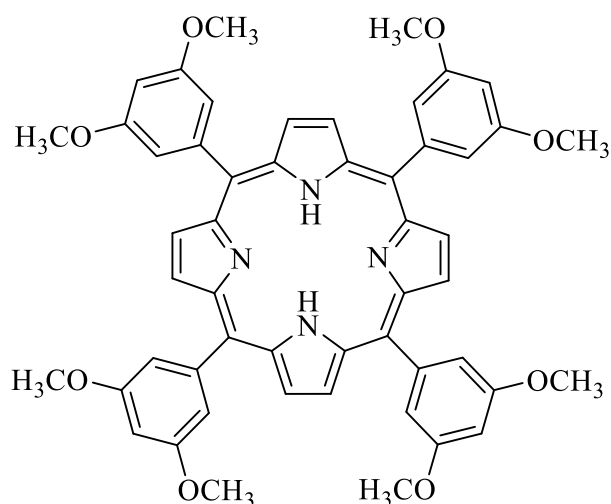
^{1}H NMR (400 MHz, CDCl$_3$): δH 8.94 (s, 8H, pyrrolic β-H), 7.43 (s, 8H, phenolic *o*-CH), 6.95 (s, 4H, phenolic *p*-CH), 3.97 (s, 24H, phenylic *m*-CH$_3$), -2.99 (s, 2H, NH); ^{13}C NMR δc (400 MHz, CDCl$_3$): δ 1591, 144.0, 119.8, 113.8, 101, 26.9; IR: vmax/cm^{-1}) 1150 (OMe); UV Absorbance (CH$_2$Cl$_2$) λ max (nm)= 420.5, 513, 548, 585.5, 643.5;(MH)$^+$ (ESI-MS) = 855 (calculated 855 gmol^{-1}).

9.7. Synthesis of 5,10,15,20-tetrakis (3, 5-dihydroxy phenyl) porphyrin (TDHPP)

the 250 ml two-neck a round bottom flask was charged with 5,10,15,20- tetrakis (3, 5-dimethoxyphenyl)- porphyrin (500 mg, 0.58 mmol) and a dry dichloromethane (50 ml) in the meantime the dropping funnel was fitted to the flask and all system was flashed with nitrogen. after carefully adjusting a dropping funnel a Boron tribromide (5 ml) was delivered to reaction mixture and stirred gently under nitrogen at room temperature for 5 hours. The reaction was quenched slowly with distilled water (5 ml) and stirred for another 15 mints.
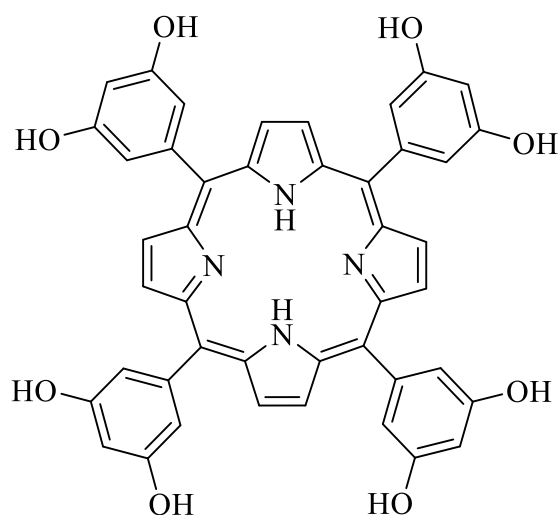
 Yield 1.3 g , 97%; ´¹H NMP (400 MHz, CDCl3) δH 9.04 (δ, 8H, pyrrolic β-H), 7.52 (δ, 8H,

phenylic o-CH), 6.96 (t, 4H, phenylic p-CH), 4.91 (s, 8H, phenylic m-OH), -2.89 (s, 2H, NH);

^{13}C NMR (400 MHz, CD$_3$OD) δ C 156.5, 143.7, 120.0, 114.4, 101.8; IR (cm^{-1}) 3431 (OH); UV

Absorbance (MeOH) λ max (nm) = 417, 512, 547.5, 587, 644.5; (MH)$^+$ (ESI-MS) 743

(calculated 743 gmol^{-1}).

9.8. Synthesis of zinc-porphyrin (ZnTDHPP)

A TDHPP (2.5 mg, 3.3 mmol) was dissolved in 100 ml dichloromethane in a round bottom

flask. Excess zinc acetate was dissolved separately in 5 ml methanol, this solution was then

added to the flask containing TDHPP. The reaction was refluxed and stirred for 1 hour at 50

^{O}C. then unreacted zinc acetate was filtrated under reduced pressure. The solvent was removed

by rotary evaporator, the product was purified by recrystallization. The resulting crystals then

dried to give dark purple crystals ZnTDHPP (2 g, 70 %).
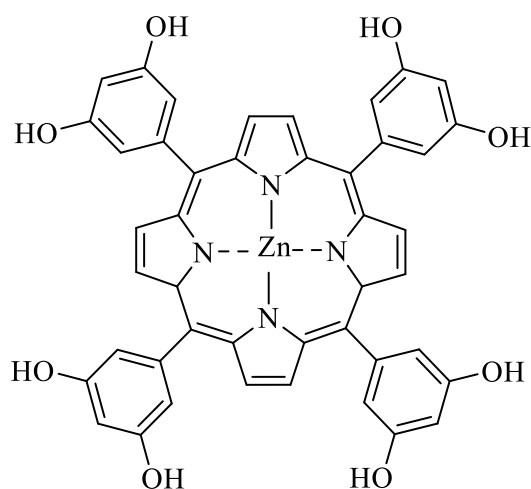
^{1}H NMR (400 MHz, DMSO) δ H 9.04 (d, 8H, pyrrolic β-H), 7.52 (d, 8H, phenylic o-CH), 6.96 (t, 4H, phenylic p-CH), 4.91 (s, 8H, phenylic m-OH); ^{13}C NMR (400 MHz, DMSO) δ C 156.5, 143.7, 120.0, 113.4, 102. UV Absorbance (MeOH) λ max (nm) 423.5 and 561.5); mass spec (ESI-MS) = 808 E (MH$^+$) (calculated 808 gmol^{-1}).

9.9. Beer-Lambert experiment for TDHPP and ZnTDHPP

In a volumetric flask, 5.2 mg of TDHPP 2 mg of ZnTDHPP were dissolved in methanol (1L) to prepare stock solutions of 5.2×10^{-6} M and 2.5×10^{-6} M. The UV spectrophotometer was used to measure the absorbance of compounds at their characteristic wavelengths 417nm for TDHPP and 423 nm for ZnTDHPP with methanol as a reference. Serials of dilutions at different concentrations were made to plot the beer lambert graph.

9.10. Encapsulation of TDHTP and ZnTDHTP using a different generation of PAMAM dendrimer

All PAMAM hydroxyl dendrimers were kept at 1×10^{-4} M concentration. The complex solutions were prepared in a vial of 10 ml methanol, where dendrimer solutions were dissolved with an equivalent amount of TDHTP or ZnTDHTP in methanol. Then, methanol was removed via rota-vap. After that, 10 ml of phosphate buffer solution pH (7.4) (0.01 M) was added to the

complex solution and filtrated, the absorbance of the solutions was measured by UV/Vis spectroscopy at 417nm and 423 nm.

9.11. Stability of the drug dendrimer complexes

The concentrations of All PAMAM dendrimer generations (G1.5, G2.5 and G3.5-OH) were kept the same (1×10^{-4} M). The stability of dendrimers was studied using excess amounts of ibuprofen in 20 ml phosphate buffer pH 7.4 up to 10 days at room temperature, in two conditions (Dark and Light). The degradation of ibuprofen in PBS was then measured as absorbance values at 273 nm by UV spectrophotometry.

9.12. Synthesis of hyperbranched Polyamnioamide Polymers (HBPAMAM-NH$_2$)

9.12.1. The main procedures for synthesis HBPAMAM 15

In the synthesis procedure of HBPAMAMA 15, EDA (1.06 g 17.63 mmol) was mixed in a minimum amount of water of 3.75 ml, then (2.7 g, 17.63 mmol) of MBA was slowly added to the reaction, which was equipped with a condenser and magnetic stirrer. the above-mixed solution was refluxed for 24 hours at 60 ^{O}C. after that, the reaction solution was allowed to cool at room temperature, and then the mixture was precipitated in 200 ml acetone, and the product was concentrated on a high vacuum yielding a light-yellow oily product (HBPAMAM 15). This method was repeated in all polymers under different conditions.

The products of this experiment were labelled as HBPAMAM **16**. N (N = 1, 2, 3,4) depending on the temperature duration of the reaction as shown in the **Table 1**

9.12.1.1. Synthesis of HBPAMAM by polymerization of EDA and MBA in a 1:1 mass ratio at different reaction times

Sample code	EDA:MBA ratio	Reaction time (minutes)
HBPAMAM **16.1**	1:1	30
HBPAMAM **16.2**	1:1	90
HBPAMAM **16.3**	1:1	240
HBPAMAM **16.4**	1:1	360

In four 100 ml round bottom flasks MBA (6.74 g, 43.75 mmol) were slowly added to a solution containing EDA (2.63 g, 43.75 mmol) and 3.57 ml distilled water. These reactions were left for 30 ,90 ,240 and 360 minutes at 60 ^{O}C to give products labelled as (HBPAMAM 16.1, HBPAMAM 16.2, HABPAMAM 16.3 and HBPAMAM 16.4) respectively. The following table shows the characteristic of the resulting products.

^{1}H NMR (δH ppm)	Sample code			
	HBPAMAM 16.1	**HBPAMAM 16.2**	**HBPAMAM 16.3**	**HBPAMAM 16.4**
-CONHCH$_2$NHCO-	(m, ~3.33)	(m, ~3.32)	(m, ~3.31)	(m, ~ 3.31)
-NCH$_2$CH$_2$CO-	(t, ~3.25)	(t, ~3.26)	(t, 3.25)	(t, 3.25)
-NCH$_2$CH$_2$CO-	(t, ~ 2.92)	(t, ~2.95)	(t, ~2.95)	(t, ~2.94)
- NCH$_2$CH$_2$N-	(s, ~ 2.81)	(s, ~ 2.80)	(s, ~ 2.81)	(s, ~ 2.82)
GPC Mn, Mw and PD	Mn= 623 Mw= 630 PD=1.013.	Mn= 630 Mw= 632 PD=1.005.	Mn= 502 Mw= 582 PD=1.16.	Mn= 440 Mw= 520 PD=1.15.
Yield	(5.45 g, 20.12 %)	(6.13 g, 22.53 %)	(5.84 g, 23.33%)	(5.32 g, 23.82 %)

9.12.3. Synthesis of HBPAMAM by polymerization of EDA and MBA for 30 min at different mass ratios

9.12.1.2. Synthesis of HBPAMAM 17.1 to HBAPMAM 17.12

The polymerization of MBA-EDA was carried out as shown in the Table at 60 ^{O}C. All the reactions were prepared for 30 min.

Sample code	Molar ratio EDA: MAB	Mass (g)		Mole (mmol)	
		EDA	MAB	EDA	MAB
HBPAMAM 17.1	1: 1.10	2.63	7.31	43.75	47.30
HBPAMAM 17.2	1: 1.15	2.63	7.62	43.75	49.45
HBPAMAM 17.3	1: 1.20	2.63	7.95	43.75	51.60
HBPAMAM 17.4	1:1.25	2.63	8.28	43.75	53.75
HBPAMAM 17.5	1: 1.30	2.63	8.62	43.75	56.00
HBPAMAM 17.6	1: 1.35	2.63	8.94	43.75	58.05
HBPAMAM 17.7	1: 1.40	2.63	9.28	43.75	60.02
HBPAMAM 17.8	1: 1.45	2.63	9.61	43.75	62.35
MBPAMAM 17.9	1: 1.50	2.63	10.11	43.75	64.50
MBPAMAM17.10	1:2	2.63	13.26	43.75	86
MBPAMAM17.11	1:3	2.63	20.10	43.75	129
MBPAMAM17.12	1:4	2.63	26.55	43.75	172

Table. Synthesis of sample procedures of HBPAMAM used different molar ratio

9.13. Converting of HBPAMAM-NH2 17 to HBPAMAM-OMe

In three 100 mL round bottom flasks, HPAMAM 17.3, HPAMAM 17.5 and HPAMAM 17.6 were each added 1 g to 20 ml of methanol. Then 5ml of methyl acrylate was added dropwise to the HBPs solutions. Methanol was recovered by rotary evaporation. All products were obtained as light-yellow oil. The ^{1}H NMR data summarised in the table below.

^{1}H NMR (δH ppm)	Sample code		
	HBPAMAM 17.3	**HBPAMAM 17.5**	**HBPAMAM 17.6**
-COOCH3-	(s, ~3.66)	(s, ~3.65)	(s, ~3.65)
-NCH$_2$CH$_2$CO-	(t, ~2.78)	(t, ~2.73)	(t, 2.76)
-NCH$_2$CH$_2$CO-	(t, ~2.48)	(t, ~2.47)	(t, ~2.49)
- NCH$_2$CH$_2$N-	(s, ~2.53)	(s, ~2.52)	(s, ~2.51)

9.14. General Procedure for encapsulation of Ibuprofen/ ZnTDHPP within dendrimers and hyperbranched polymers

An excess of Ibuprofen/Zn TDHPP in methanol (10 mL) was added to each system. The solutions were physically mixed, and the solvent was removed by rotary evaporation. The precipitates were then formed in a phosphate buffer (10 mL). Each sample was vacuum filtered to remove solid residues before UV-VIS spectroscopy was used for analysis.

9.14.1. Encapsulation of ibuprofen by HBPAMAM-NH2 17.3

Two concentrations of 0.05 and 0.75 g were dissolved in 100 mL methanol to give concentrations 0.005 mg/mL and 0.075 mg/mL.

9.14.2. preparation procedure for encapsulation of ibuprofen using HBPAMAM-NH$_2$ 17.3 in different concentrations

Four concentrations (0.1, 0.2, 0.4 and 0.6 g) were prepared of HBPAMAM was diluted in four (100 ml) volumetric flasks to made different concentrations (0.01, 0.02, 0.004, 0.06 mg/mL).

9.14.3. Preparation procedures for dynamic light scattering (DLS) study of HBPAMAM-NH2 17.3

Four concentrations of HBPAMAM-NH$_2$ **1** (0.1, 0.2 ,0.4, and 0.6 g) were dissolved in 100 mL PBS pH 7.4 to obtain concentrations of (0.01, 0.02, 0.04, 0.06 mg/mL). Then analysed by DLS instrument at 25 ^{0}C. The DLS measurements were typically made in triplicate.

9.14.4. Preparation procedures of encapsulation of Zn TDHPP using HBPAMAM-NH$_2$ 17.3

HBPAMAM-NH$_2$ 17.3 stock solutions were prepared by dissolved (0.05, 0.1, 0.4 g) to give concentration 0.005, 0.01 and 0.04 mg/mL, respectively.

9.14.5. Preparation procedures of encapsulation of Ibuprofen using aromatic (Ar-HBPAMAM-OH 23)

Preparation stock 0.32 mg/mL and 0.70 mg/mL in 100 ml methanol
0.0325 g and 0.070 g of HBP were dissolved in 100 mL

9.14.6. Preparation solutions for G3/ HBPAMAM-NH2 in 100 ml methanol

In 100 ml volumetric flasks, 0.032 g of G3/ HBPAMAM-NH$_2$ were added to make concentration 0.32 mg/mL.

9.14.7. Preparation solutions for G2/ HBPAMAM-NH2 in 100 ml methanol

In 100 ml volumetric flasks, 0.014 g of G2/ HBPAMAM-NH$_2$ were added to make concentration 0.14 mg/mL.

9.14.8. Preparation solution of G3.0-OH/ Ar-HBPAMAM-OH

In 100 ml volumetric flasks, 0.032 g of G3.0-OH or **Ar-HBPAMAM-OH** were dissolved in 100 mL methanol to make a concentration of 0.32 mg/mL.

9.14.9. Preparation Procedures for encapsulation of Zn TDHPP using G2 and HBPAMAM-NH$_2$

The solutions of 0.005mg/mL G2 or HBPAMAM-NH2 were prepared in 100 ml methanol to make a concentration of 0.05mg/mL.

10. References

1   M. Melo, R. Nunes, B. Sarmento and J. das Neves, Rectal administration of nanosystems: from drug delivery to diagnostics, *Mater. Today Chem.*, 2018, **10**, 128–141.

2   A. D. Bangham and R. W. Horne, Negative Staining ofPhospholipids and their Structural Modification by Surface-active Agents as observed in the Electron Microscope, *J. Mol. Biol.*, 1964, **8**, 660–668, IN2–IN10.

3   A. D. Bangham, M. M. Standish and J. C. Watkins, Diffusion of Univalent Ions across the Lamellae of Swollen Phospholipids, *J. Mol. Biol.*, 1965, **13**, 238–252, IN26–IN27.

4   K. P. Hillery, Anya M, *Drug Delivery Fundamentals and Applications, Second Edition Edited ByAnya Hillery, Kinam Park*, Taylor & Francis Group, Saint Louis University - Madrid Campus, Madrid, Spain. Purdue University, West Lafayette, IN, USA, 2nd Editio., 2016.

5   G. Birrenbach and P. P. Speiser, Polymerized Micelles and Their Use as Adjuvants in Immunology, *J. Pharm. Sci.*, 1976, **65**, 1763–1766.

6   P. S. P. Couvreur, P. Tulkenst, M. Roland, A. Trouet, NANOCAPSULES: A NEW TYPE OF LYSOSOMOTROPIC CARRIER, *North-holl. Publ. Co. - Amsterdam*, 1977, **84**, 0–3.

7   K. Park, Drug delivery of the future : Chasing the invisible gorilla, *J. Control. Release*, 2016, **240**, 2–8.

8   M. Ye, S. Kim and K. Park, Issues in long-term protein delivery using biodegradable microparticles, *J. Control. Release*, 2010, **146**, 241–260.

9   K. Park, Controlled drug delivery systems : Past forward and future back, *J. Control. Release*, 2014, **190**, 3–8.

10   Y. Zhang, H. F. Chan and K. W. Leong, Advanced materials and processing for drug delivery: The past and the future, *Adv. Drug Deliv. Rev.*, 2013, **65**, 104–120.

11   N. P. Truong, M. R. Whittaker, C. W. Mak and T. P. Davis, The importance of nanoparticle shape in cancer drug delivery, 2015, 129–142.

12   P. Kolhe, E. Misra, R. M. Kannan, S. Kannan and M. Lieh-Lai, Drug complexation, in vitro release and cellular entry of dendrimers and hyperbranched polymers, *Int. J. Pharm.*, 2003, **259**, 143–160.

13   Z. Zhao, A. Ukidve, J. Kim and S. Mitragotri, Targeting Strategies for Tissue-Specific Drug Delivery, *Cell*, 2020, **181**, 151–167.

14   A. K. Patri, I. J. Majoros and J. R. Baker, Dendritic polymer macromolecular carriers for drug delivery, *Curr. Opin. Chem. Biol.*, 2002, **6**, 466–471.

15   S. R. Mudshinge, A. B. Deore, S. Patil and C. M. Bhalgat, Nanoparticles: Emerging carriers for drug delivery, *Saudi Pharm. J.*, 2011, **19**, 129–141.

16   M. M. and K. Asare-Addo, A mini-review of nanocarriers in drug delivery systems, *Br. J. Pharm.*, 2002, 124–128.

17   A. M. Jhaveri and V. P. Torchilin, Multifunctional polymeric micelles for delivery of drugs and siRNA, *Front. Pharmacol.*, 2014, **5 APR**, 1–26.

18   A. Z. Wang, R. Langer and O. C. Farokhzad, Nanoparticle delivery of cancer drugs, *Annu. Rev. Med.*, 2012, **63**, 185–198.

19   R. R. Sawant, A. M. Jhaveri and V. P. Torchilin, Immunomicelles for advancing personalized therapy, *Adv. Drug Deliv. Rev.*, 2012, **64**, 1436–1446.

20   E. Biazar, Majdi, M. Zafari, M. Avar, S. Aminifard, D. Zaeifi, Ai, Jafarpour, Montazeri

and Gh, Nanotoxicology and nanoparticle safety in biomedical designs, *Int. J. Nanomedicine*, 2011, 1117.

21   A. Elsaesser and C. V. Howard, Toxicology of nanoparticles, *Adv. Drug Deliv. Rev.*, 2012, **64**, 129–137.

22   E. Masoudipour, S. Kashanian and N. Maleki, A targeted drug delivery system based on dopamine functionalized nano graphene oxide, *Chem. Phys. Lett.*, 2017, **668**, 56–63.

23   K. B. Sutradhar and L. Amin, Nanoemulsions: Increasing possibilities in drug delivery, *Eur. J. Nanomedicine*, 2013, **5**, 97–110.

24   R. Duncan and R. Gaspar, Nanomedicine (s) under the Microscope, 2011, 2101–2141.

25   A. Schroeder, D. A. Heller, M. M. Winslow, J. E. Dahlman, G. W. Pratt, R. Langer, T. Jacks and D. G. Anderson, Treating metastatic cancer with nanotechnology, *Nat. Rev. Cancer*, 2012, **12**, 39–50.

26   M. Kenchegowda, M. Rahamathulla, U. Hani, M. Y. Begum, S. Guruswamy, R. A. M. Osmani, M. P. Gowrav, S. Alshehri, M. M. Ghoneim, A. Alshlowi and D. V. Gowda, Smart Nanocarriers as an Emerging Platform for Cancer Therapy: A Review, *Molecules*, , DOI:10.3390/molecules27010146.

27   Y. Malam, M. Loizidou and A. M. Seifalian, Liposomes and nanoparticles: nanosized vehicles for drug delivery in cancer, *Trends Pharmacol. Sci.*, 2009, **30**, 592–599.

28   S. Bayda, M. Adeel, T. Tuccinardi, M. Cordani and F. Rizzolio, The History of Nanoscience and Nanotechnology : From Chemical – Physical Applications to Nanomedicine, 1–15.

29   P. Chaubey, M. Momin and S. Sawarkar, Signi fi cance of Ligand-Anchored Polymers for Drug Targeting in the Treatment of Colonic Disorders, 2020, **10**, 1–14.

30   J. Wanigasekara and C. Witharana, Applications of nanotechnology in drug delivery and design - an insight, *Curr. Trends Biotechnol. Pharm.*, 2016, **10**, 78–91.

31   A. Z. Wilczewska, K. Niemirowicz, K. H. Markiewicz and H. Car, Nanoparticles as drug delivery systems, *Pharmacol. Reports*, 2012, **64**, 1020–1037.

32   A. Vila, A. Sánchez, M. Tobío, P. Calvo and M. J. Alonso, Design of biodegradable particles for protein delivery, *J. Control. Release*, 2002, **78**, 15–24.

33   E. Pérez-Herrero and A. Fernández-Medarde, Advanced targeted therapies in cancer: Drug nanocarriers, the future of chemotherapy, *Eur. J. Pharm. Biopharm.*, 2015, **93**, 52–79.

34   R. Duncan and L. Izzo, Dendrimer biocompatibility and toxicity, *Adv. Drug Deliv. Rev.*, 2005, **57**, 2215–2237.

35   A. W. Bosman, H. M. Janssen and E. W. Meijer, About Dendrimers: Structure, Physical Properties, and Applications, *Chem. Rev.*, 1999, **99**, 1665–1688.

36   J. Voskuhl, U. Kauscher, M. Gruener, H. Frisch, B. Wibbeling, C. A. Strassert and B. J. Ravoo, A soft supramolecular carrier with enhanced singlet oxygen photosensitizing properties, *Soft Matter*, 2013, **9**, 2453–2457.

37   C. Dufès, Dendrimer-Based Drug Delivery Systems: From Theory to Practice . Edited by Yiyun Cheng , *ChemMedChem*, 2013, **8**, 336–336.

38   D. A. Tomalia, J. B. Christensen and U. Boas, Dendrimers, Dendrons, and Dendritic Polymers, *Dendrimers, Dendrons, Dendritic Polym.*, , DOI:10.1017/cbo9781139048859.

39   A. Morgado, F. Najera, A. Lagunas, J. Samitier, Y. Vida and E. Perez-Inestrosa, Slightly congested amino terminal dendrimers. The synthesis of amide-based stable structures

on a large scale, *Polym. Chem.*, 2021, **12**, 5168–5177.

40 D. A. Tomalia, H. Baker, J. Dewald, M. Hall, G. Kallos, S. Martin, J. Roeck, J. Ryder and P. Smith, A New Class of Polymers : Starburst-Dendritic, *Polym. J.*, 1985, **17**, 117–132.

41 Craig J. Hawker and J. M. J. Fréchet, Preparation of Polymers with Controlled Molecular Architecture. A New Convergent Approach to Dendritic Macromolecules, *Am. Chem. Soc.*, 1970, **42Vol.112**, 7638–7647.

42 Z. Lyu, L. Ding, A. Y. T. Huang, C. L. Kao and L. Peng, Poly(amidoamine)dendrimers: covalent and supramolecular synthesis, *Mater. Today Chem.*, 2019, **13**, 34–48.

43 K. Bacha, C. Chemotti, J. Mbakidi and M. Deleu, Dendrimers : Synthesis , Encapsulation Applications and Specific Interaction with the Stratum Corneum — A Review, 2023, 343–370.

44 V. Gupta and S. K. Nayak, Dendrimers: A review on synthetic approaches, *J. Appl. Pharm. Sci.*, 2015, **5**, 117–122.

45 R. Y. Sathe and P. V Bharatam, Drug-dendrimer complexes and conjugates : Detailed furtherance through theory and experiments, *Adv. Colloid Interface Sci.*, 2022, **303**, 102639.

46 X. Montané, A. Bajek, K. Roszkowski, J. M. Montornés, M. Giamberini, S. Roszkowski, O. Kowalczyk, R. Garcia-Valls and B. Tylkowski, Encapsulation for cancer therapy, *Molecules*, 2020, **25**, 1–25.

47 W. D. Jang, K. M. Kamruzzaman Selim, C. H. Lee and I. K. Kang, Bioinspired application of dendrimers: From bio-mimicry to biomedical applications, *Prog. Polym. Sci.*, 2009, **34**, 1–23.

48   J. F. G. A. Jansen, E. M. M. De Brabander-Van Den Berg and E. W. Meijer, Encapsulation of guest molecules into a dendritic box, *Science (80-.).*, 1994, **266**, 1226–1229.

49   C. J. Hawker, K. L. Wooley and J. M. J. Fréchet, Unimolecular micelles and globular amphiphiles: Dendritic macromolecules as novel recyclable solubilization agents, *J. Chem. Soc. Perkin Trans. 1*, 1993, 1287–1297.

50   C. Kojima, K. Kono, K. Maruyama and T. Takagishi, Synthesis of polyamidoamine dendrimers having poly(ethylene glycol) grafts and their ability to encapsulate anticancer drugs, *Bioconjug. Chem.*, 2000, **11**, 910–917.

51   U. Boas, S. H. M. Söntjens, K. J. Jensen, J. B. Christensen and E. W. Meijer, New dendrimer - Peptide host - Guest complexes: Towards dendrimers as peptide carriers, *ChemBioChem*, 2002, **3**, 433–439.

52   A. K. Patri, J. F. Kukowska-Latallo and J. R. Baker, Targeted drug delivery with dendrimers: Comparison of the release kinetics of covalently conjugated drug and non-covalent drug inclusion complex, *Adv. Drug Deliv. Rev.*, 2005, **57**, 2203–2214.

53   R. N. Prajapati, R. K. Tekade, U. Gupta, V. Gajbhiye and N. K. Jain, Dendimer-Mediated Solubilization, Formulation Development and, 2009, 742–745.

54   R. D. N Malik, EG Evagorou, Dendrimer-platinate: a novel approach to cancer chemotherapy., *Anticancer. Drugs*, 1999, **10(8)**, 767–776.

55   L. M. Kaminskas, V. M. McLeod, B. D. Kelly, G. Sberna, B. J. Boyd, M. Williamson, D. J. Owen and C. J. H. Porter, A comparison of changes to doxorubicin pharmacokinetics, antitumor activity, and toxicity mediated by PEGylated dendrimer and PEGylated liposome drug delivery systems, *Nanomedicine Nanotechnology, Biol.*

Med., 2012, **8**, 103–111.

56   G. Pasut, S. Scaramuzza, O. Schiavon, R. Mendichi and F. M. Veronese, PEG-epirubicin conjugates with high drug loading, *J. Bioact. Compat. Polym.*, 2005, **20**, 213–230.

57   D. Soto-Castro, J. A. Cruz-Morales, M. T. R. Apan and P. Guadarrama, Solubilization and anticancer-activity enhancement of Methotrexate by novel dendrimeric nanodevices synthesized in one-step reaction, *Bioorg. Chem.*, 2012, **41**–**42**, 13–21.

58   Z. Zhou, A. D'Emanuele and D. Attwood, Solubility enhancement of paclitaxel using a linear-dendritic block copolymer, *Int. J. Pharm.*, 2013, **452**, 173–179.

59   N. Malik, R. Wiwattanapatapee, R. Klopsch, K. Lorenz, H. Frey, J. W. Weener, E. W. Meijer, W. Paulus and R. Duncan, Erratum: Dendrimers: Relationship between structure and biocompatibility in vitro, and preliminary studies on the biodistribution of 125I-labelled polyamidoamine dendrimers in vivo (Journal of Controlled Release 65 (2000) (133-148), *J. Control. Release*, 2000, **68**, 299–302.

60   W. Wijagkanalan, S. Kawakami and M. Hashida, Designing dendrimers for drug delivery and imaging: Pharmacokinetic considerations, *Pharm. Res.*, 2011, **28**, 1500–1519.

61   A. Zeeshan, M. Farhan and A. Siddiqui, Nanomedicine and drug delivery : a mini review, , DOI:10.1007/s40089-014-0094-7.

62   A. Santos, F. Veiga and A. Figueiras, *Dendrimers as pharmaceutical excipients: Synthesis, properties, toxicity and biomedical applications*, 2020, vol. 13.

63   Y. Kim, E. J. Park and D. H. Na, Recent progress in dendrimer-based nanomedicine development, *Arch. Pharm. Res.*, 2018, **41**, 571–582.

64   B. Surekha, N. Sreenu, S. Kumar, A. V. P. Kumar, R. Shukla and P. Kesharwani,

Colloids and Surfaces B: Biointerfaces PAMAM dendrimer as a talented multifunctional biomimetic nanocarrier for cancer diagnosis and therapy, *Colloids Surfaces B Biointerfaces*, 2021, **204**, 111837.

65   H. Yang, Targeted nanosystems : Advances in targeted dendrimers for cancer therapy, *Nanomedicine Nanotechnology, Biol. Med.*, 2016, **12**, 309–316.

66   D. He, H. Lin, Y. Yu, L. Shi and J. Tu, Precisely Defined Polymers for Efficient Gene Delivery, *Top. Curr. Chem.*, 2018, **376**, 1–17.

67   K. Wang, Y. Tu, W. Yao, Q. Zong, X. Xiao, R. Yang, X. Jiang and Y. Yuan, Size-Switchable Nanoparticles with Self-Destructive and Tumor Penetration Characteristics for Site-Speci fi c Phototherapy of Cancer, , DOI:10.1021/acsami.9b21525.

68   Y. Gao, J. Wang, M. Chai, X. Li, Y. Deng, Q. Jin and J. Ji, Size and Charge Adaptive Clustered Nanoparticles Targeting the Bio fi lm Microenvironment for Chronic Lung Infection Management, , DOI:10.1021/acsnano.0c00269.

69   S. Barua and S. Mitragotri, Challenges associated with penetration of nanoparticles across cell and tissue barriers: A review of current status and future prospects, *Nano Today*, 2014, **9**, 223–243.

70   X. Zhang, Z. Zhang, X. Xu, Y. Li, Y. Li and Y. Jian, Bioinspired Therapeutic Dendrimers as Efficient Peptide Drugs Based on Supramolecular Interactions for Tumor Inhibition **, 2015, 4289–4294.

71   M. Kaurav, S. Ruhi, H. A. Al-goshae, A. K. Jeppu, D. Ramachandran, R. K. Sahu, A. K. Sarkar, J. Khan and A. A. Ikbal, Dendrimer : An update on recent developments and future opportunities for the brain tumors diagnosis and treatment, 2023, 1–20.

72   F. Abedi-gaballu, G. Dehghan, M. Ghaffari, R. Yekta, S. Abbaspour-ravasjani, B.

Baradaran, J. Ezzati, N. Dolatabadi, M. R. Hamblin and M. G. Hospital, PAMAM dendrimers as efficient drug and gene delivery nanosystems for cancer therapy, 2019, 177–190.

73   I. Ekladious, Y. L. Colson and M. W. Grinstaff, Polymer – drug conjugate therapeutics : advances , insights and prospects, *Nat. Rev. Drug Discov.*, , DOI:10.1038/s41573-018-0005-0.

74   P. Chytil, P. Cernoch, L. Starovoytova, M. Pechar and K. Ulbrich, Biodegradable star HPMA polymer conjugates of doxorubicin for passive tumor targeting European Journal of Pharmaceutical Sciences Biodegradable star HPMA polymer conjugates of doxorubicin for passive tumor targeting ˇ, , DOI:10.1016/j.ejps.2011.03.001.

75   W. She, N. Li, K. Luo, C. Guo, G. Wang, Y. Geng and Z. Gu, Biomaterials Dendronized heparin À doxorubicin conjugate based nanoparticle as pH-responsive drug delivery system for cancer therapy, *Biomaterials*, 2013, **34**, 2252–2264.

76   A. Janaszewska, J. Lazniewska, P. Trzepiński, M. Marcinkowska and B. Klajnert-Maculewicz, Cytotoxicity of dendrimers, *Biomolecules*, 2019, **9**, 1–23.

77   A. Behera and S. Padhi, Passive and active targeting strategies for the delivery of the camptothecin anticancer drug: a review, *Environ. Chem. Lett.*, 2020, **18**, 1557–1567.

78   M. M. Gottesman, T. Fojo and S. E. Bates, MULTIDRUG RESISTANCE IN CANCER : ROLE OF ATP-DEPENDENT TRANSPORTERS, 2002, **2**, 48–58.

79   J. Ban, S. Li, Q. Zhan, X. Li, H. Xing, N. Chen, L. Long and X. Hou, PMPC Modified PAMAM Dendrimer Enhances Brain Tumor-Targeted Drug Delivery, 2021, **2000392**, 1–13.

80   A. C. Rinkenauer, S. Schubert, A. Traeger and U. S. Schubert, The influence of polymer

architecture on in vitro pDNA transfection, *J. Mater. Chem. B*, 2015, **3**, 7477–7493.

81   K. Ulbrich, K. Holá, V. Šubr, A. Bakandritsos, J. Tuček and R. Zbořil, Targeted Drug Delivery with Polymers and Magnetic Nanoparticles: Covalent and Noncovalent Approaches, Release Control, and Clinical Studies, *Chem. Rev.*, 2016, **116**, 5338–5431.

82   A. B. Cook and S. Perrier, Branched and Dendritic Polymer Architectures: Functional Nanomaterials for Therapeutic Delivery, *Adv. Funct. Mater.*, 2020, **30**, 1–24.

83   Y. Ma, Q. Mou, D. Wang, X. Zhu and D. Yan, Dendritic polymers for theranostics, *Theranostics*, 2016, **6**, 930–947.

84   B. Begines, T. Ortiz, M. Pérez-Aranda, G. Martínez, M. Merinero, F. Argüelles-Arias and A. Alcudia, Polymeric nanoparticles for drug delivery: Recent developments and future prospects, *Nanomaterials*, 2020, **10**, 1–41.

85   A. Braunová, P. Chytil, R. Laga, Š. Milada, D. Machová and J. Parnica, Polymer nanomedicines based on micelle-forming amphiphilic or water- soluble polymer-doxorubicin conjugates : Comparative study of in vitro and in vivo properties related to the polymer carrier structure , composition , and hydrodynamic properties ☆, 2020, **321**, 718–733.

86   H. Wu, T. Yin, K. Li, R. Wang, Y. Chen and L. Jing, Encapsulation property of hyperbranched polyglycerols as prospective drug delivery systems, 2018, 300–306.

87   W. Wang, J. Ma, F. Jin and J. Liao, Hyperbranched polymer drug delivery treatment for lung metastasis of salivary adenoid cystic carcinoma in nude mice, 2017, 3105–3111.

88   A. S. Picco, B. Yameen, W. Knoll, M. R. Ceolín and O. Azzaroni, Journal of Colloid and Interface Science Temperature-driven self-assembly of self-limiting uniform supraparticles from non-uniform unimolecular micelles q, 2016, **471**, 71–75.

89   A. Kavand, N. Anton, T. Vandamme, C. A. Serra and D. Chan-Seng, *J. Control. Release*, 2020, 321, 285–311.

90   P. Kolhe, J. Khandare, O. Pillai, S. Kannan, M. Lieh-Lai and R. Kannan, Hyperbranched polymer-drug conjugates with high drug payload for enhanced cellular delivery, *Pharm. Res.*, 2004, **21**, 2185–2195.

91   C. Mugabe, Y. Matsui, A. I. So, M. E. Gleave, M. Heller, M. Zeisser-Labouèbe, L. Heller, I. Chafeeva, D. E. Brooks and H. M. Burt, In vitro and in vivo evaluation of intravesical docetaxel loaded hydrophobically derivatized hyperbranched polyglycerols in an orthotopic model of bladder cancer, *Biomacromolecules*, 2011, **12**, 949–960.

92   L. Ye, K. Letchford, M. Heller, R. Liggins, D. Guan, J. N. Kizhakkedathu, D. E. Brooks, J. K. Jackson and H. M. Burt, Synthesis and characterization of carboxylic acid conjugated, hydrophobically derivatized, hyperbranched polyglycerols as nanoparticulate drug carriers for cisplatin, *Biomacromolecules*, 2011, **12**, 145–155.

93   T. Ooya, J. Lee and K. Park, Effects of ethylene glycol-based graft, star-shaped, and dendritic polymers on solubilization and controlled release of paclitaxel, *J. Control. Release*, 2003, **93**, 121–127.

94   C. Gao and D. Yan, Hyperbranched polymers: From synthesis to applications, *Prog. Polym. Sci.*, 2004, **29**, 183–275.

95   F. Moret and E. Reddi, photosensitizers used in photodynamic therapy (PDT) Strategies for optimizing the delivery to tumors of macrocyclic photosensitizers used in photodynamic therapy (PDT), , DOI:10.1142/S1088424617300014.

96   R. R. Allison and K. Moghissi, Photodynamic therapy (PDT): PDT mechanisms, *Clin. Endosc.*, 2013, **46**, 24–29.

97   W. Wu, X. Shao, J. Zhao and M. Wu, Controllable Photodynamic Therapy Implemented by Regulating Singlet Oxygen Efficiency, *Adv. Sci.*, , DOI:10.1002/advs.201700113.

98   J. M. Ang, I. Bin Riaz, M. U. Kamal, G. Paragh and N. C. Zeitouni, Photodiagnosis and Photodynamic Therapy Photodynamic therapy and pain : A systematic review, 2017, **19**, 308–344.

99   G. Gunaydin, M. E. Gedik and S. Ayan, Photodynamic Therapy — Current Limitations and Novel Approaches, 2021, **9**, 1–25.

100   G. Maria, F. Calixto, J. Bernegossi and L. M. De Freitas, Nanotechnology-Based Drug Delivery Systems for Photodynamic Therapy of Cancer : A Review, , DOI:10.3390/molecules21030342.

101   S. G. Zheng, M. A. Rajora, J. W. H. Lou and G. Zheng, As featured in : Advancing porphyrin ' s biomedical utility via supramolecular chemistry, , DOI:10.1039/c7cs00525c.

102   N. Tsolekile and S. Nelana, Porphyrin as Diagnostic and Therapeutic Agent.

103   S. Shao, V. Rajendiran and J. F. Lovell, Metalloporphyrin nanoparticles: Coordinating diverse theranostic functions, *Coord. Chem. Rev.*, 2019, **379**, 99–120.

104   R. Boscencu, R. P. Socoteanu, G. Manda, N. Radulea, M. Anastasescu, A. Gama, I. F. Machado and L. F. V. Ferreira, Dyes and Pigments New A 3 B porphyrins as potential candidates for theranostic . Synthesis and photochemical behaviour, *Dye. Pigment.*, 2019, **160**, 410–417.

105   L. Bolzonello, M. Albertini, E. Collini and M. Di Valentin, Delocalized triplet state in porphyrin J-aggregates revealed by EPR spectroscopy †, 2017, 27173–27177.

106   P. Kubát, K. Lang and Z. Zelinger, Interaction of porphyrins with PAMAM dendrimers

in aqueous solution, *J. Mol. Liq.*, 2007, **131**–**132**, 200–205.

107   Z. Cheng, M. Li, R. Dey and Y. Chen, Nanomaterials for cancer therapy: current progress and perspectives, *J. Hematol. Oncol.*, 2021, **14**, 1–27.

108   R. Hourani and A. Kakkar, Advances in the elegance of chemistry in designing dendrimers, *Macromol. Rapid Commun.*, 2010, **31**, 947–974.

109   S. Choudhary, L. Gupta, S. Rani, K. Dave and U. Gupta, Impact of dendrimers on solubility of hydrophobic drug molecules, *Front. Pharmacol.*, 2017, **8**, 1–23.

110   P. Kesharwani, K. Jain and N. K. Jain, Dendrimer as nanocarrier for drug delivery, *Prog. Polym. Sci.*, 2014, **39**, 268–307.

111   J. Haensler and F. C. Szoka, Polyamidoamine Cascade Polymers Mediate Efficient Transfection of Cells in Culture, *Bioconjug. Chem.*, 1993, **4**, 372–379.

112   S. Shamsudin, T. Synthesis and D. Application, The Synthesis and Characterisation of Dendritic Macromolecules for Drug Delivery Application Suriani Shamsudin PhD Thesis.

113   D. A. Tomalia, A. M. Naylor and W. A. Goddard, Starburst Dendrimers: Molecular-Level Control of Size, Shape, Surface Chemistry, Topology, and Flexibility from Atoms to Macroscopic Matter, *Angew. Chemie Int. Ed. English*, 1990, **29**, 138–175.

114   I. Tanis and K. Karatasos, Association of a weakly acidic anti-inflammatory drug (ibuprofen) with a poly(amidoamine) dendrimer as studied by molecular dynamics Simulations, *J. Phys. Chem. B*, 2009, **113**, 10984–10993.

115   F. Aboshnaf, The Synthesis and Application of Dendritic Polymer for Photodynamic Therapy.

116   O. Perumal, J. Khandare, P. Kolhe, S. Kannan, M. Lieh-Lai and R. M. Kannan, Effects of branching architecture and linker on the activity of hyperbranched polymer-drug conjugates, *Bioconjug. Chem.*, 2009, **20**, 842–846.

117   N. Desai, Challenges in development of nanoparticle-based therapeutics, *AAPS J.*, 2012, **14**, 282–295.

118   L. J. Twyman, A. E. Beezer, R. Esfand, M. J. Hardy and J. C. Mitchell, The synthesis of water soluble dendrimers, and their application as possible drug delivery systems, *Tetrahedron Lett.*, 1999, **40**, 1743–1746.

119   A. R. Menjoge, R. M. Kannan and D. A. Tomalia, Dendrimer-based drug and imaging conjugates: design considerations for nanomedical applications, *Drug Discov. Today*, 2010, **15**, 171–185.

120   F. Aulenta, W. Hayes and S. Rannard, Dendrimers: A new class of nanoscopic containers and delivery devices, *Eur. Polym. J.*, 2003, **39**, 1741–1771.

121   T. Mavromoustakos and A. G. Tzakos, *Supramolecules in Drug Discovery and Drug Delivery*, 2021, vol. 2207.

122   U. Gupta, S. K. D. Dwivedi, H. K. Bid, R. Konwar and N. K. Jain, Ligand anchored dendrimers based nanoconstructs for effective targeting to cancer cells, *Int. J. Pharm.*, 2010, **393**, 186–197.

123   S. H. Medina and M. E. H. El-Sayed, Dendrimers as carriers for delivery of chemotherapeutic agents, *Chem. Rev.*, 2009, **109**, 3141–3157.

124   J. Patel, B. Basu, A. Dharamsi, K. Garala and M. Raval, Solubility of aceclofenac in polyamidoamine dendrimer solutions, *Int. J. Pharm. Investig.*, 2011, **1**, 135.

125   C. Yiyun, X. Tongwen and F. Rongqiang, Polyamidoamine dendrimers used as

solubility enhancers of ketoprofen, *Eur. J. Med. Chem.*, 2005, **40**, 1390–1393.

126   A. D'Emanuele, R. Jevprasesphant, J. Penny and D. Attwood, The use of a dendrimer-propranolol prodrug to bypass efflux transporters and enhance oral bioavailability, *J. Control. Release*, 2004, **95**, 447–453.

127   A. Hamidi, S. Sharifi, S. Davaran, S. Ghasemi, Y. Omidi and M. R. Rashidi, Novel aldehyde-terminated dendrimers; Synthesis and cytotoxicity assay, *BioImpacts*, 2012, **2**, 97–103.

128   P. Danheiser, W. R. Roush, M. A. Adam, D. J. Harris, G. R. Newkome, Z. Yaolc, G. R. Baker and V. K. Gupta, very weak (soft) nucleophiles and because the trajectory of reagent approach to the carbonyl is constrained to a considerably smaller value than in biomolecular carbonyl these conclusions are in progress and will be reported in grants from the National , 2004, 2003–2004.

129   A. E. Beezer, A. S. H. King, I. K. Martin, J. C. Mitchel, L. J. Twyman and C. F. Wain, Dendrimers as potential drug carriers; encapsulation of acidic hydrophobes within water soluble PAMAM derivatives, *Tetrahedron*, 2003, **59**, 3873–3880.

130   R. Kharwade, S. More, A. Warokar, P. Agrawal and N. Mahajan, Starburst pamam dendrimers: Synthetic approaches, surface modifications, and biomedical applications, *Arab. J. Chem.*, 2020, **13**, 6009–6039.

131   X. Shi, I. Bányai, M. T. Islam, W. Lesniak, D. Z. Davis, J. R. Baker and L. P. Balogh, Generational, skeletal and substitutional diversities in generation one poly(amidoamine) dendrimers, *Polymer (Guildf).*, 2005, **46**, 3022–3034.

132   L. P. Tolić, G. A. Anderson, R. D. Smith, H. M. Brothers, R. Spindler and D. A. Tomalia, Electrospray ionization Fourier transform ion cyclotron resonance mass spectrometric

characterization of high molecular mass Starburst^{TM} dendrimers, *Int. J. Mass Spectrom. Ion Process.*, 1997, **165–166**, 405–418.

133   R. Giordanengo, M. Mazarin, J. Wu, L. Peng and L. Charles, Propagation of structural deviations of poly(amidoamine) fan-shape dendrimers (generations 0-3) characterized by MALDI and electrospray mass spectrometry, *Int. J. Mass Spectrom.*, 2007, **266**, 62– 75.

134   L. Scheetz, K. S. Park, Q. Li, P. R. Lowenstein, M. G. Castro, A. Schwendeman and J. J. Moon, Engineering patient-specific cancer immunotherapies, *Nat. Biomed. Eng.*, , DOI:10.1038/s41551-019-0436-x.

135   H. Han, The effect of nanoparticle size on in vivo pharmacokinetics and cellular interaction, 2016, **11**, 673–692.

136   J. Nanobiotechnol, C. Zhang, Y. Cheng, D. Liu, M. Liu, H. Cui, B. Zhang and Q. Mei, Mitochondria - targeted cyclosporin A delivery system to treat myocardial ischemia reperfusion injury of rats, *J. Nanobiotechnology*, 2019, 1–16.

137   K. M. Hocking and B. C. Evans, Nanotechnology Enabled Modulation of Signaling Pathways Affects Physiologic Responses in Intact Vascular Tissue, 2019, **25**, 416–426.

138   J. Jose and R. N. Charyulu, Prolonged drug delivery system of an antifungal drug by association with polyamidoamine dendrimers, 2016, 123–127.

139   R. Giovannetti, The Use of Spectrophotometry UV-Vis for the Study of Porphyrins, *Macro To Nano Spectrosc.*, , DOI:10.5772/38797.

140   A. Gupta, S. Dubey and M. Mishra, Unique Structures, Properties and Applications of Dendrimers, *J. Drug Deliv. Ther.*, 2018, **8**, 328–339.

141   J. Chen, E. S. Garcia and S. C. Zimmerman, Intramolecularly Cross-Linked Polymers:

From Structure to Function with Applications as Artificial Antibodies and Artificial Enzymes, *Acc. Chem. Res.*, 2020, **53**, 1244–1256.

142 E. Burakowska, S. C. Zimmerman and R. Haag, Photoresponsive crosslinked hyperbranched polyglycerols as smart nanocarriers for guest binding and controlled release, *Small*, 2009, **5**, 2199–2204.

143 Y. Zheng, S. Li, Z. Weng and C. Gao, Hyperbranched polymers: advances from synthesis to applications, *Chem. Soc. Rev.*, 2015, **44**, 4091–4130.

144 D. Chang, Y. Ma, X. Xu, J. Xie and S. Ju, Stimuli-Responsive Polymeric Nanoplatforms for Cancer Therapy, *Front. Bioeng. Biotechnol.*, 2021, **9**, 1–26.

145 A. M. Caminade, D. Yan and D. K. Smith, Dendrimers and hyperbranched polymers, *Chem. Soc. Rev.*, 2015, **44**, 3870–3873.

146 S. Lee, Y. Eom, J. Park, J. Lee and S. Y. Kim, Micro-hydrogel Particles Consisting of Hyperbranched Polyamidoamine for the Removal of Heavy Metal Ions from Water, *Sci. Rep.*, 2017, **7**, 1–9.

147 L. J. Twyman, A. S. H. King, J. Burnett and I. K. Martin, Synthesis of aromatic hyperbranched PAMAM polymers, *Tetrahedron Lett.*, 2004, **45**, 433–435.

148 K. Paulsen, D. Frasco and T. F. Scientific, Qualitative and quantitative analysis of the polymerization of PS- b -P t BA block copolymer using picoSpin 80 NMR, 2017, 5.

149 Y. Chen, L. Wang, H. Yu, R. Sun and G. Jing, Stimuli-responsive HBPS- g - PDMAEMA and its application as nanocarrier in loading hydrophobic molecules, 2016, 939–949.

150 O. Bourrier, J. Butlin, R. Hourani and A. K. Kakkar, Aggregation of 3 , 5- dihydroxybenzyl alcohol based dendrimers and hyperbranched polymers , and

encapsulation of DR1 in such dendritic aggregates, *Inorganica Chim. Acta*, 2004, **357**, 3836–3846.

151 T. Transport and T. O. F. Pamam, TRANSEPITHELIAL TRANSPORT AND TOXICITY OF PAMAM DENDRIMERS : IMPLICATIONS FOR ORAL DRUG DELIVERY, 2013, **64**, 571–588.

152 A. S. H. King, I. K. Martin and L. J. Twyman, Synthesis and aggregation of amine-cored polyamidoamine dendrons synthesised without invoking a protection / deprotection strategy, 2006, **807**, 798–807.